NONLINEAR ULTRASONICS FOR POLYMER QUALITY MONITORING

NONLINEAR ULTRASONICS FOR IN-LINE QUALITY MONITORING OF POLYMER PROCESSING METHODS

By Felipe P. C. Gomes, B. Eng.

A Thesis Submitted to the School of Graduate Studies in Partial Fulfilment of the Requirements for the Degree Doctor of Philosophy

McMaster University DOCTOR OF PHILOSOPHY (2018) Hamilton, Ontario (Chemical Engineering)

TITLE: Nonlinear Ultrasonics for In-line Quality Monitoring of Polymer Processing Methods

AUTHOR: Felipe P. C. Gomes, B.Eng. (Universidade Federal do Rio Grande do Norte)

SUPERVISOR: Professor Dr. Michael R. Thompson

NUMBER OF PAGES: xviii, 165

Lay Abstract

We have been using ultrasonic devices to investigate different things from medical diagnosis of prenatal development to nondestructive exploration of small rocks brought from the Moon. This study takes the ultrasonic testing to the challenge of characterizing plastics. Using information from the propagation of these inaudible sound waves, we can explore the entire structure and observe structural changes that can lead to defects or failures. With the help of computer-based data processing, we investigate these complex signals creating tools for more efficient manufacturing and safer products like water and fuel storage tanks.

Abstract

Ultrasonic testing is a nondestructive structural characterization technique with limited examples of application for polymeric products due to the high signal attenuation in this class of materials. Recent developments in this thesis on ultrasonics have focused on a guided waves test method and used nonlinear analysis of harmonic frequencies to characterize polyethylene, a semi-crystalline polymer. This sensor technology was demonstrated in the detection of initial plastic deformation and to monitor solvent swelling. Frequency regions of low signal attenuation and a nonlinear ultrasonic parameter using amplitude ratio of harmonic peaks were used to classify different crystalline morphologies, controlled by thermal treatment. With an established connection between the ultrasonic spectrum signal and the internal structure of polyethylene, a quality monitoring tool was developed and applied to a batch rotational molding process. Multiple traditional quality measurements were correlated with the ultrasonic signal using multivariate statistical analysis. Finally, an in-line statistical approach for quality classification and an on-line process monitoring using dynamic process modeling were validated. The results presented in this study demonstrate the relevancy of incorporation of the ultrasonic sensor technology to promote advanced manufacturing practices for the polymer manufacturing industry.

Acknowledgements

I would like to recall several contributions that helped this thesis to be developed. First, the finantial support from the Brazilian federal government through the National Council for Scientific and Technological Development (CNPq) for the Doctorate Science Without Borders Scholarship. I hope that the output from this work and several others from the same program can enlighten the future of science, technology and education in Brazil.

I would like to thank my supervisor, Dr. Michael Thompson, for all his trust throughout these years. His example of guidance, patience and correctness will always be a north for my development as a researcher. And I will always be greatful for the opportunities given to explore and learn in research, leadership and teaching.

Another important contribution comes from the members of the supervisory committee. Dr. Prashant Mhaskar who patiently supported the work from the beguinning, but had an enourmous impact when we had the chance to connect our research goals and explore new experimental challenges toguether. Dr. Samir Ziada (*in memoriam*), his kind and gentle words will never be forgotten and his encoragement that motivated me to face the most difficult barriers for this thesis. And, I would like to thank Dr. Stephen Vheldius, for his openess and confidence to support the conclusion of my work.

I would like to mention the importance of colleagues, professors and friends at the university. Trevor, Abhinav, Ahmed and Guoqing for the collaraboration in different projects. Wing Hei, Sam, Kristi, and Heera, to name a few of the colleages in the research group. Elizabeth for the imporant initial guidance in lab. All professors from the Chemical Engineering department that were the support for my educational

development and the instructors in the MacPhearson Institute for their important contribution for teaching development. Vida, Fei, Nicola, Kelli and many other friends from the office. Brazilians, Canadians and international friends that I have made over these years, but some special thanks to Debora, Harold, Gabi, Nina, Karina, Nil, Matt, Chiara and Emily.

And last but not less important, I would like to thank those that were in physical distance but never far from their support. Silvana, Zezo, Andre and Renan for their long friendship. And very special thanks for those always close to my heart and feelings, *mainha* Ione and *padrinhos* Ivete and Manuel, and my lovely, patient and supportive parter Jaqueline.

Contents

List of Figures

List of Tables

Declaration of Academic Achievement

In accordance with the guidelines for the preparation of a doctoral thesis set forth by the McMaster University School of Graduate Studies, this work has been prepared as a sandwich thesis. The majority of the work described in this thesis was conducted, interpreted, and written by the author of this thesis. The work was done in consultation with and under the supervision of Dr. Michael Thompson who also revised the drafts to the final versions. An outline of the contributions of authors, other than myself and my supervisorare indicated at the opening statement of each chapter.

Chapter 1

Introduction

The focus of manufacturing research and development for the early years of the twenty-first century has been the adoption of new tools and procedures to create more integrated and flexible production lines. 'Quantity' has lost its standing as the main industrial objective, giving way to concepts like product personalization, use of sustainable resources, and cradle-to-grave waste management. All of these new responsibilities create production challenges in managing so much variability and maintaining final product quality.

In the search for solutions to current challenges, there has been one common mantra for the manufacturing industry: gathering more data. In an era of informational development, new technologies are seeking to connect more 'things'. This change in paradigm has been called by some as the fourth industrial revolution. But outside the branding dispute, the goal for an advanced manufacturing environment is to integrate process and product sensors with data management technologies to support the new demands of the market.

With a need for more information from every part produced and with more computing power available to process data, multivariate nondestructive sensors have been an attractive alternative adopted for in-line monitoring in the manufacturing industry. Spectroscopic methods (such as infrared, UV-Vis, X-ray, acoustic, ultrasonic and others) that use the propagation of electromagnetic or mechanical waves are common examples. However, with increasing complexity in data, more difficulties emerge in connecting actual product properties and a mechanistic description of the process. High cost and demand for a highly skilled operation are barriers that create a gap in the development and adoption of these sensors for the factory floor.

Each manufacturer also faces the task of selecting and adapting a sensor that fits to its product peculiarities. In the case of polymer processing industry, the limitations on sensor performance are caused by its complex structures of plastic products that

are generally thermal and acoustic insulators. Another challenge is to select between local characterization, that may not be representative of the whole part properties, or bulk characterization, that might be limited due to physical constraints.

Based on the current scenario for polymer manufacturing, two objectives were proposed for exploration in this research. The first part of this thesis focused on the development of ultrasonic sensor technology for the characterization of a semi-crystalline polymer. And the second part explored statistical strategies to combine process data and multivariate analysis of the ultrasonic signal for product quality monitoring. Thus, the overall goal is to demonstrate conditions for a new monitoring tool designed for polymeric products with promotion of an efficient quality control, based on a nondestructive sensor technology.

In order to provide a background to the concepts applied in the manuscripts and lay out the current state for the research in the areas related to this thesis, Chapter 2 provides a historical progression on the ultrasonic sensor technology focused on plastic characterization until recent years and the challenges of characterizing semi-crystalline polymers. Then, a presentation of the rotational molding process, a batch polymer manufacturing technique selected to be the application for process integration with the ultrasonic sensor as its main monitoring tool. Lastly, the chapter includes a short introduction to multivariate statistical tools for data processing and interpretation.

Part I of the main research work combines two published research papers, Chapters 3 and 4, that apply ultrasonic characterization to polyethylene samples. Both papers focused on the correlation of microstructural modifications of the semi-crystalline morphology to features of the multivariate frequency spectrum for propagated ultrasonic signals through molded parts. In Chapter 3, polyethylene samples with different crystalline content were plastically deformed and tested with the propagation of ultrasonic guided waves. Cyclic strain-controlled deformation showed that specific

frequency regions had lower signal attenuation and could be used to follow the evolving microstructure corresponding to the initial stage of plastic deformation. Considering the findings and methodology developed in the first manuscript, Chapter 4 follows the crystalline morphology of the polyethylene samples as controlled by thermal treatment. Results demonstrated that the proposed characterization technique using a nonlinear ultrasonic descriptor based on an acoustic parameter corresponding to the amplitude ratio of frequency harmonic peaks, was correlated with the progression of inter-crystalline residual stresses caused by either plastic deformation or solvent swelling.

The advances demonstrated in Part I of the research provided evidence that multivariate frequency analysis of the ultrasonic signal could be related to structural features of a semi-crystalline polymer part. In Part II, this multivariate sensor technology was applied to the monitoring of a batch manufacturing process to evaluate the final product quality; a process whose industrial reliance on destructive test methods has left it with noted part consistency issues. The manuscript presented in Chapter 5 shows a correlation of the ultrasonic signal with two different quality features of rotational molded parts that would traditionally be assessed using impact testing. Residual internal air bubbles from powder sintering and thermo-oxidative degradation from prolonged exposure to heat have a direct impact in mechanical properties of the molded polyethylene part which can be evaluated using the multivariate ultrasonic signal by calibrated statistical models. Improved approaches for quality monitoring tools applied to the rotational molding process were demonstrated in Chapter 6. In this manuscript, different from than in the previous chapter, the focus was on the use of available historical data from the process and the nondestructive ultrasonic test to create both in-line and on-line statistical strategies to classify final parts based on different categorical groups. These proposed methods showed the potential

implementation of ultrasonic technology in an advanced manufacturing scenario with intelligent analytical tools that can be improved with increasing data availability (i.e. machine learning).

In addition to the results obtained and described on the main body of this thesis, collaboration projects have sought different applications of the developed technique for further validation or progression on the main contributions. Chapter 7 combines excerpts of findings from three draft manuscripts that use the ultrasonic technique to focus on the quality characterization of semi-crystalline parts. The first study is a continuation of the Chapter 6 with the application of a model predictive control strategy to achieved desired quality products from the batch rotational molding process. The second and third projects used directly the methodology developed in Chapter 4 to monitor structural changes using the nonlinear ultrasonic parameter, applied to the plasticization effect of biodiesel on polyethylene and plastic deformation of thermally treated poly(lactic acid).

The final chapter of this thesis focuses on the overall impact of the contributions and the future impact of these areas for the improvement of polymer processing, nondestructive characterization and advanced manufacturing.

Chapter 2

Literature Review

In this chapter the three main areas related to the research are presented with the definition of basic concepts and recent important publications that influenced the findings presented in the subsequent chapters.

2.1 Ultrasonic testing for semi-crystalline polymeric materials

Characterization using ultrasonic technique relies on the interaction of mechanical waves with the material being evaluated. Traditional acoustic measurements for describing polymeric materials are the calculated ultrasonic velocity and signal attenuation per unit distance of propagation[1]. These two effects consider a pure elastic propagation of planar waves through the solid part, following Equations 2.1 and 2.2.

$$\frac{\delta^2 u_x}{\delta t^2} = c^2 \frac{\delta^2 u_x}{\delta x^2} \quad \text{for} \quad c = \sqrt{\frac{E}{\rho}} \tag{2.1}$$

$$A = A_0 e^{-\alpha x} \tag{2.2}$$

where u is displacement (strain), x is the unidirectional spacial variable, t is the temporal variable, c is the speed of sound at the medium, E is the Young's modulus, ρ is the density, A0 is the initial signal amplitude, A is the attenuated signal amplitude, and α is the attenuation coefficient (per unit length).

In order to measure these properties and calculate these parameters, a common approach is to use pulse-echo tests with samples of known dimensions[2]. Based on the signal reflected over the thickness of the sample, the time difference between pulses can be used to identify the speed of sound and the amplitude difference to

calculated attenuation (schematic presented in Figure 2.1). Polymeric materials have a distinctly higher attenuation compared to metals and ceramics that propagate mechanical waves better[3]. An increase in degree of crystallinity is associated with further signal attenuation[4]. Good coupling between the transducer and the surface of the sample, and amplification of the received signal are often required to allow the use of this technique with polymers.

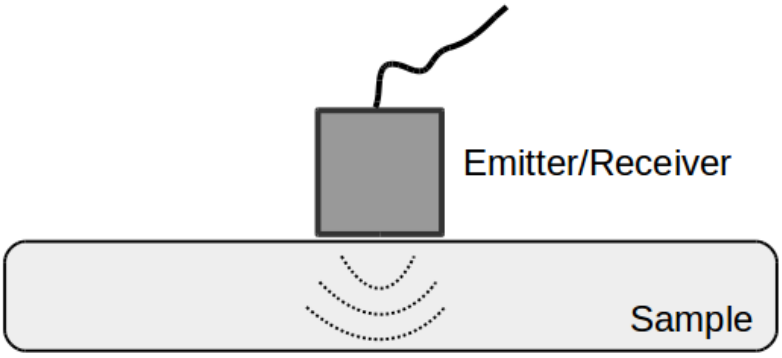

Figure 2.1: Schematic of Pulse-echo ultrasonic test

An alternative to the pulse-echo test is guided wave propagation, where two transducers are required, one acting as an emitter of the ultrasonic wave and a second positioned in a different spot as a passive receiver of the propagated wave (see schematic in Figure 2.2). This method relies on the principles of planar waves, also called plate waves, which considers the propagation of ultrasonic waves over longer distances, due to an amplified effect caused by reflection of the geometrical boundaries[5]. However, signal amplification for these waves is frequency dependent. Thus, identification of guided waves modes that have lower attenuation based on the sample geometry and characteristics can help to increase the signal propagation and efficiency of the test[6]. Equations for the dispersion curves are used to identify the modes (See equations 2.3-2.5). For semi-crystalline polymers, application of ultrasonic guided waves has

advantages over traditional pulse-echo tests due to the fact that these are materials with high attenuation and it allows for the exploration of larger areas.

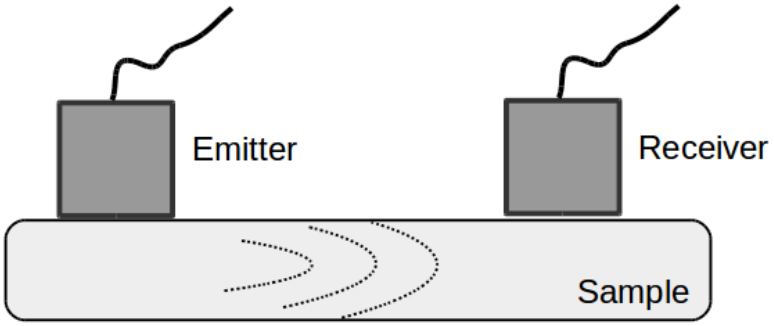

Figure 2.2: Schematic of ultrasonic guided waves test

$$\frac{tan(qh)}{tan(ph)} = \frac{-4k^2pq}{(q^2-k^2)^2} \quad \text{(for symmetric modes)} \tag{2.3}$$

$$\frac{tan(qh)}{tan(ph)} = \frac{(q^2-k^2)^2}{-4k^2pq} \quad \text{(for antisymmetric modes)} \tag{2.4}$$

$$p^2 = \frac{w^2}{c_L^2} - k^2 \quad \text{and} \quad q^2 = \frac{w^2}{c_T^2} - k^2 \tag{2.5}$$

where w is the circular frequency, k is the wavenumber, h is the plate thickness, c_L is the longitudinal velocity, and c_T is the transverse velocity.

High signal attenuation of ultrasonic waves by semi-crystalline polymers is related to the viscoelastic nature of these materials[7]. Ultrasonic propagation can be affected by significant differences in elastic properties between internal regions and by the mismatch of stress transmitter elements (i.e. internal defects)[8]. Thus, a new area of

ultrasonic characterization has focused on the study of nonlinear propagation. The introduction of a nonlinear elastic parameter, shown in Equation 2.6, compared to the elastic wave equation shown in Equation 2.1, shows how there can be a significant change in wave propagation, observable in the frequency domain with the formation of harmonic signals[9].

$$\frac{\delta^2 u_x}{\delta t^2} = c^2(1 + \beta\frac{\delta u_x}{\delta x})\frac{\delta^2 u_x}{\delta x^2} \tag{2.6}$$

where β is the nonlinear parameter. An increase in internal stresses and defects has been reported to cause the appearance of higher harmonic peaks in several materials[10] but has not been previously reported in semi-crystalline polymers.

Previous ultrasonic characterization studies for polyethylene have first shown the variation of attenuation with frequency[4], traditional ultrasonic testing strategies applied for polymer blends[11–14] and composites[15,16]. Recent studies have also investigated the characterization by acoustic emission during destructive plastic deformation[17,18].

2.2 Rotational molding process

Rotational molding is a batch process that produces hollow parts based on the deposition, sintering and solidification of polymer powders on the walls of metallic molds. Although the full batch cycle can be divided into six different stages (initial powder heating, adhesion, melting, sintering, solidification and cooling), see schematic in Figure 2.3, final part quality is most directly affected by two different processes: sintering and degradation.

During the melting stage as powder particles gradually transition to a viscous melt, air is trapped into voids located in the geometric spaces. The number and size of

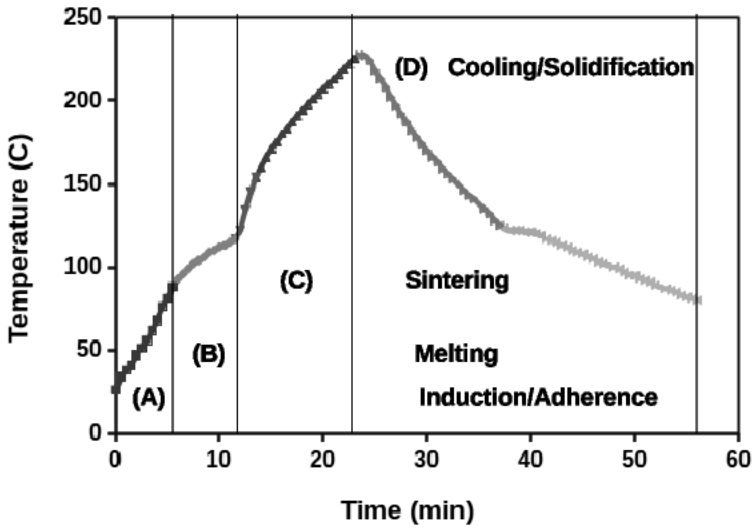

Figure 2.3: Rotational molding batch cycle

the initially formed bubbles is highly influenced by the particle size distribution of the polymer powder[19]. With increasing heat being provided to the system the initial concentration of bubbles tends to reduce through coalescence and air diffusion[20]. This densification or sintering process has a significant effect on the mechanical strength of the final part and optimal quality can only be achieved with minimal residual air bubbles[21].

In parallel to the sintering process, the high temperatures and the exposure to the air inside of the metallic mold also promotes the formation of radicals that lead to thermo-oxidative degradation. Above a certain threshold, the concentration of stabilizers (antioxidants) originally added to the polymeric compounding manufacturer to prevent this phenomena will decrease more rapidly[22]. For polyethylene molded parts, this thermo-oxidative reaction can lead to cross-linking, changes in color, emission of volatile compounds and in severe cases a reduction of mechanical properties due to brittleness[23].

2.3 Multivariate statistical analysis and batch process monitoring

Statistical data processing and analysis from multivariate signals, such as the frequency spectrum of an ultrasonic guided wave, are necessary to extract information contained. Due to the complexity of the interaction between a polymeric structure and the propagated ultrasonic waves, the selection of frequencies to correlate with final product qualities is not a trivial task. Orthogonal projections using principal component analysis have been applied to reduce the dimensions of these multivariate spaces without loss of important data[24]. A common calibration technique applied to multivariate sensor technology is the projection to latent spaces (PLS) that correlates the measured spectra to other standard test values[25], a schematic is demonstrated in Figure 2.4.

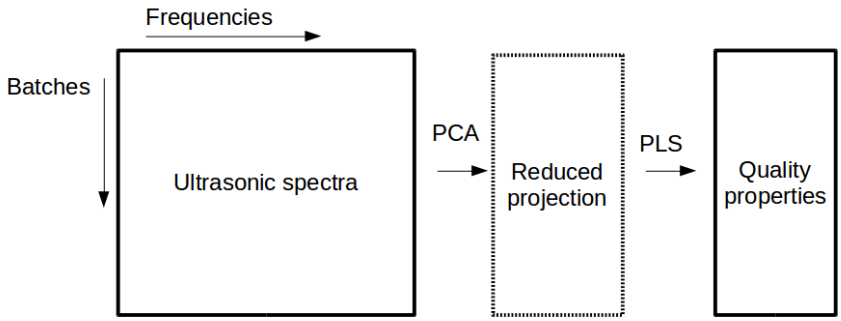

Figure 2.4: Schematic of PLS

A supervisory system based on advanced manufacturing tools should help understand the dynamics of the process through its observed variables and correlate them to the final quality properties. A PLS approach can also be applied to correlate observation from on-line batch process variables with the final quality. However, these batches are usually non-uniform, thus, time alignment of each batch vector is required

to form a calibration matrix[26]. A recent alternative to this problem has been explored with the use of a subspace identification technique with the alignment of the batch data into Hankel matrices. Each batch is organized in a square matrix with fix number of rows, then each sub-matrix is concatenated to an overall Hankel matrix aligned horizontally, thus, only the number of rows should match, allowing for batches with different lengths to be matched[27]. Then, these aligned matrices of the observed and controlled variables on the batch can be used to identify the system matrices by ordinary least squares.

Multivariate sensor analysis for process on-line and in-line monitoring have been previously analyzed for continuous polymer processing techniques, focused on the traditional extrusion[28–33] and injection molding processes[34–39].

Bibliography

[1] Vikram K. Kinra and Vasudevan R. Iyer. Ultrasonic measurement of the thickness, phase velocity, density or attenuation of a thin-viscoelastic plate. Part II: the inverse problem. *Ultrasonics*, 33(2):111–122, 1995.

[2] B. Zhao, O.A. Basir, and G.S. Mittal. Estimation of ultrasound attenuation and dispersion using short time Fourier transform. *Ultrasonics*, 43(5):375–381, mar 2005.

[3] A. Bernard, M. J. S. Lowe, and M. Deschamps. Guided waves energy velocity in absorbing and non-absorbing plates. *The Journal of the Acoustical Society of America*, 110(1):186–196, jul 2001.

[4] Keiichiro Adachi, Gilroy Harrison, John Lamb, Alastair M. North, and Richard A.

Pethrick. High frequency ultrasonic studies of polyethylene. *Polymer*, 22(8): 1032–1039, 1981.

[5] Mira Mitra and S Gopalakrishnan. Guided wave based structural health monitoring: A review. *Smart Materials and Structures*, 25(5):053001, 2016.

[6] Mihai V Predoi, Michel Castaings, and Ludovic Moreau. Influence of material viscoelasticity on the scattering of guided waves by defects. *The Journal of the Acoustical Society of America*, 124(5):2883–2894, nov 2008.

[7] B. Hosten and M. Castaings. Comments on the ultrasonic estimation of the viscoelastic properties of anisotropic materials. *Composites Part A: Applied Science and Manufacturing*, 39(6):1054–1058, jun 2008.

[8] Kyung-young Jhang. Nonlinear ultrasonic techniques for nondestructive assessment of micro damage in material: A review. *International Journal of Precision Engineering and Manufacturing*, 10(1):123–135, jan 2009.

[9] Claudio Nucera and Francesco Lanza. Higher-Harmonic Generation Analysis in Complex Waveguides via a Nonlinear Semianalytical Finite Element Algorithm. 2012, 2012.

[10] Vamshi Krishna Chillara and Cliff J Lissenden. Review of nonlinear ultrasonic guided wave nondestructive evaluation: theory, numerics, and experiments. *Optical Engineering*, 55(1):011002, aug 2015.

[11] R. Gendron, J. Tatibouët, J. Guèvremont, M. M. Dumoulin, and L. Piché. Ultrasonic behavior of polymer blends. *Polymer Engineering & Science*, 35(1): 79–91, jan 1995.

[12] T.H. Nayfeh, N.H. Abu-Zahra, W.M. Fedek, and A.A. Salem. Ultrasound Measurement of Two-Filler Concentrations in Polypropylene Compounds. Part 1: Static Calibration. *The International Journal of Advanced Manufacturing Technology*, 20(4):313–318, aug 2002.

[13] Claude Verdier and Monique Piau. Analysis of the morphology of polymer blends using ultrasound. *Journal of Physics D: Applied Physics*, 29(6):1454–1461, jun 1996.

[14] Shan Wang, Congmei Lin, Huimin Sun, Fan Chen, Jiang Li, and Shaoyun Guo. Ultrasonic characterization of phase morphology of high density polyethylene/polyamide 6 blend melts. *Polymer Engineering & Science*, 52(2):338–345, feb 2012.

[15] M. Castaings, B. Hosten, and T. Kundu. Inversion of ultrasonic, plane-wave transmission data in composite plates to infer viscoelastic material properties. *NDT & E International*, 33(6):377–392, sep 2000.

[16] M. J. Jenkins, P. J. Hine, J. N. Hay, and I. M. Ward. Mechanical and acoustic frequency responses in flat hot-compacted polyethylene and polypropylene panels. *Journal of Applied Polymer Science*, 99(5):2789–2796, 2006.

[17] N. Casiez, S. Deschanel, T. Monnier, and O. Lame. Ultrasonic in situ investigation of the initiation of Polyethylene's plastic deformation during tensile tests. *Polymer*, 123(25):258–266, aug 2017.

[18] F.P.C. Gomes, A Bovell, G.P. Balamurugan, M.R. Thompson, and K.G. Dunn. Evaluating the influence of contacting fluids on polyethylene using acoustic emissions analysis. *Polymer Testing*, 39:61–69, oct 2014.

[19] M. Kontopoulou and J. Vlachopoulos. Bubble dissolution in molten polymers and its role in rotational molding. *Polymer Engineering & Science*, 39(7):1189–1198, jul 1999.

[20] A. G. Spence and R. J. Crawford. The effect of processing variables on the formation and removal of bubbles in rotationally molded products. *Polymer Engineering & Science*, 36(7):993–1009, apr 1996.

[21] M. J. Oliveira, M. C. Cramez, and R. J. Crawford. Structure-properties relationships in rotationally moulded polyethylene. *Journal of Materials Science*, 31(9):2227–2240, 1996.

[22] M.C Cramez, M.J Oliveira, and R.J Crawford. Optimisation of rotational moulding of polyethylene by predicting antioxidant consumption. *Polymer Degradation and Stability*, 75(2):321–327, jan 2002.

[23] Maria Clara Cramez, Maria Jovita Oliveira, Stoyko Fakirov, Robert James Crawford, Anton Atanassov Apostolov, and Marina Krumova. Rotationally molded polyethylene: Structural characterization by x-ray and microhardness measurements. *Advances in Polymer Technology*, 20(2):116–124, 2001.

[24] Svante Wold, Kim Esbensen, and Paul Geladi. Principal component analysis. *Chemometrics and Intelligent Laboratory Systems*, 2(1-3):37–52, aug 1987.

[25] Richard G. Brereton. Pattern recognition in chemometrics. *Chemometrics and Intelligent Laboratory Systems*, 149:90–96, dec 2015.

[26] Theodora Kourti and John F. MacGregor. Process analysis, monitoring and diagnosis, using multivariate projection methods. *Chemometrics and Intelligent Laboratory Systems*, 28(1):3–21, apr 1995.

[27] Abhinav Garg, Brandon Corbett, Prashant Mhaskar, Gangshi Hu, and Jesus Flores-Cerrillo. Subspace-based model identification of a hydrogen plant startup dynamics. *Computers & Chemical Engineering*, 106:183–190, nov 2017.

[28] P.D. Coates, S.E. Barnes, M.G. Sibley, E.C. Brown, H.G.M. Edwards, and I.J. Scowen. In-process vibrational spectroscopy and ultrasound measurements in polymer melt extrusion. *Polymer*, 44(19):5937–5949, sep 2003.

[29] Dieter Fischer, Jan Müller, Sven Kummer, and Bernd Kretzschmar. Real Time Monitoring of Morphologic and Mechanical Properties of Polymer Nanocomposites During Extrusion by near Infrared and Ultrasonic Spectroscopy. *Macromolecular Symposia*, 305(1):10–17, jul 2011.

[30] D. R. Françla, C.-K. Jen, K T Nguyen, and R Gendron. Ultrasonic in-line monitoring of polymer extrusion. *Polymer Engineering & Science*, 40(1):82–94, jan 2000.

[31] Ryan Gosselin, Denis Rodrigue, and Carl Duchesne. A hyperspectral imaging sensor for on-line quality control of extruded polymer composite products. *Computers & Chemical Engineering*, 35(2):296–306, feb 2011.

[32] Dongbiao Wang and Kyonsuku Min. In-line monitoring and analysis of polymer melting behavior in an intermeshing counter-rotating twin-screw extruder by ultrasound waves. *Polymer Engineering & Science*, 45(7):998–1010, jul 2005.

[33] Ke Wang, Feng Chen, Zhongming Li, and Qiang Fu. Control of the hierarchical structure of polymer articles via "structuring" processing. *Progress in Polymer Science*, 39(5):891–920, 2014.

[34] Chin-Chi Cheng, Yuu Ono, and Cheng-Kuei Jen. Real-time diagnosis of co-injection molding using ultrasound. *Polymer Engineering & Science*, 47(9): 1491–1500, sep 2007.

[35] Bobing He, Xiaoqing Zhang, Qin Zhang, and Qiang Fu. Real-time ultrasonic monitoring of the injection-molding process. *Journal of Applied Polymer Science*, 107(1):94–101, jan 2008.

[36] Francesca Lionetto and Alfonso Maffezzoli. Polymer characterization by ultrasonic wave propagation. *Advances in Polymer Technology*, 27(2):63–73, feb 2009.

[37] W. Michaeli and C. Starke. Ultrasonic investigations of the thermoplastics injection moulding process. *Polymer Testing*, 24(2):205–209, apr 2005.

[38] F. Yacoub and J. F. MacGregor. Analysis and optimization of a polyurethane reaction injection molding (RIM) process using multivariate projection methods. *Chemometrics and Intelligent Laboratory Systems*, 65(1):17–33, 2003.

[39] Yi Yang, Bo Yang, Shengqiang Zhu, and Xi Chen. Online quality optimization of the injection molding process via digital image processing and model-free optimization. *Journal of Materials Processing Technology*, 226:85–98, dec 2015.

Part I

Nolinear Ultrasonics

Chapter 3

Analysis of Mullins Effect in Polyethylene Using Ultrasonic Guided Waves

Analysis of Mullins Effect in Polyethylene Using Ultrasonic Guided Waves

F. P. C. Gomes[1], M.R. Thompson[1]

[1]Department of Chemical Engineering, CAPPA-D/MMRI

McMaster University, Hamilton, Ontario, Canada

Published manuscript at Polymer Testing

DOI: 10.1016/j.polymertesting.2017.04.020

Author contributions:

The main author of this research paper, F.P.C. Gomes, was responsible for the design of the experimental setup with the selection of transducers and testing conditions; coding of the algorithm to process the acquired signals; execution of experiments; analyses of the obtained data and writing of the reported document. M.R. Thompson was responsible for supervision of the design and experiments, and review of the reported document.

Main scientific contributions

- Use of ultrasonic guided waves test for detection of initial plastic deformation in polyethylene.
- Demonstration of irreversible cyclic process at early stages of plastic deformation (Mullins effect) for polyethylene.

ABSTRACT

Small strain deformations below yielding can cause plastic deformation in semicrystalline polymers by a process similar to what is described for filled rubber-like materials

known as the Mullins effect. Inter-lamellae chains contribute predominantly in deformations at this level, and the residual plastic strain can be attributed to permanent damage to the tie chains, affecting the long-term mechanical resistance of a molded part. With little detectable alteration of the polymer crystallinity at this early onset of plastic deformation, the primary characterization method applied to date is cyclic tensile loading, which provides information of stress-softening by monitoring the unloading path or relaxed stress behavior. An alternative method for monitoring the development of Mullins effect is proposed that can examine a molded part by using selected modes based on ultrasonic guided waves analysis. The technique was examined to determine if it could follow this effect induced by cyclic strain-controlled tensile deformations since it does not require sample preparation and could ultimately be applied while a part was in-service. Results for different polyethylene grades agree in trend with relaxed stress values over four cycles for tests of increasing applied tensile strain, demonstrated by an increase in the attenuation of ultrasonic guided waves. The correlation reveals a good promise in applying this method to structural health monitoring of plastic parts, while in use, to follow the initiation and progress of early service damage.

Key-words: Ultrasonics; Mullins effect; Plastic deformation; Semicrystalline.

3.1 Introduction

Polyethylene (PE) will undergo non-linear elastoplastic deformation under tensile load before reaching its maximum stress. Although the yield point is a clear transition onto plastic deformation, the initiation of permanent damage can occur well before this transition[1]. Even small strains have been demonstrated to be capable of producing rearrangement of the semi-crystalline structure, affecting long-term mechanical

properties[2]. The stress-strain response of semi-crystalline polymers at small strains below yield corresponds to deformations of the inter-lamellae amorphous phase[3]. The separation of crystallites promotes the stretching and rupture of bridging chains that interconnect crystallites, resulting in permanent plastic damage[4]. Macroscopically, in cyclic mechanical testing, it is possible to observe this damage characteristic of the Mullins effect, mainly recognized by an observable strain-softening along the unloading path of the stress-strain curve and a non-recoverable residual strain after only the first cycle[5]. This effect is a result of the rupture of connection points (tie chains) in the crystalline network, being dependent on the history of maximum stretching and is a key characteristic to understanding the resistance of materials to crystalline slip that leads to yielding[6]. Based on this subtle damage, the Mullins effect is considered to reflect properties that are intrinsically correlated with long-term mechanical stability of parts molded with semicrystalline polymers. Since the primary method of assessing the Mullins effect is strain-controlled cycling mechanical testing, which requires detailed data recording, sample preparation and interpretation of stress-strain curves, the development of alternative techniques is currently sought by companies concerned with aging behaviors of their products, either for use in quality assessment or monitoring a part while in service.

Macroscopic, characteristic changes such as significant permanent variation of dimensions or sample discoloration can be visually observed but only after major plastic deformation beyond yield point of a semicrystalline polymer[7]. Considering microscopic structural observations, current experimental methods used in the detection of plastic deformation include small-angle X-Ray scattering (SAXS)[8], near-infrared spectroscopy (NIRS)[9], and Raman spectroscopy[10]. Such methods experience difficulties in detecting plastic flow initiation at early stages of deformation as they depend on the presence of cavitation or significant crystal deformation and orientation, that are only

present closer to yield[11]. The non-crystalline phase of PE has a significantly greater role in dislocations during viscoelastic deformation due to its lower bulk modulus[12]. Therefore, in order to promote early detection of plastic deformation it is essential to develop practical methods capable of characterizing changes in the interconnectivity of crystallites and non-crystalline phase mobility. However, current methods that have demonstrated successful results such as atomic force microscopy (AFM) [4] and nuclear magnetic resonance spectroscopy (NMR)[13] require highly specialized sample preparation and testing procedures, restricting their practical application in industry.

Ultrasonic techniques are non-destructive characterization methods that analyze the manner by which sound waves are altered upon propagating through a medium to reveal micro-structural details, such as information related with thermo-mechanical and morphological properties. Important contributions from Nitta and collaborators have demonstrated the effectiveness of ultrasonic methods using parameters of bulk wave velocity and signal attenuation to analyze the plastic deformation of semi-crystalline homopolymers and polymer blends under oscillatory and uniaxial tensile deformation[14–16]. Increases in ultrasonic velocity and attenuation were correlated with orientation of crystallites and the occurrence of cavitation due to large strain deformation. The dispersive nature of semi-crystalline polymers requires a spectroscopic analysis of the ultrasonic signal since attenuation for such materials is frequency dependent[17]. Recent improvements to materials characterization have been achieved with the use of ultrasonic guided waves, a method that presents advantages to characterization of highly attenuative materials. The interference phenomenon of reflective waves on plate walls allows propagation over longer distances, combined with the analysis of dispersive properties of semicrystalline polymers providing features of bulk macroscopic properties of the investigated sample[18,19].

Therefore, this paper will focus on demonstrating the use of ultrasonic guided

waves to analyze plastic deformation at its early stages in different polyethylenes (high density, linear low density and bimodal). The novelty of the study is showing that parametric descriptors of the ultrasonic signal are correlated with the initiation of plastic deformation when using small strain-controlled tensile deformation testing to detect Mullins effect. Demonstrating the practicability of ultrasonic techniques to the observation of inter-lamellae alteration of semi-crystalline polymers undergoing plastic deformation is an important advance to the development of a suitable characterization methods under Industry 4.0, and can be later exploited as non-destructive evaluation for in-line process monitoring or in-field early failure detection.

3.2 Materials and Methods

3.2.1 Materials

Four commercial grades of polyethylene were supplied by Imperial Oil Ltd (Sarnia, ON). Table 3.1 provides a summary of the grades, listing their corresponding density, melt index (MFI; measured according to ASTM D1238) and environmental stress cracking resistance (ESCR; measured according to ASTM D1693A) which were determined by the supplier for this work, and includes PE Grade numbers which will be used to reference these samples in this study. The grades varied from homopolymer high density (HD) to linear low density (LL) polyethylene, with different degrees of hexene used as copolymer. A bimodal grade (HD.B) is included in the study with intermediate values in terms of density and ESCR. All samples were prepared as plaques by compression molding the resin for 5 minutes at 190oC and then quenched using water-cooled plates. Rectangular test specimens of approximately 20 mm (width) x 180 mm (length) x 3 mm (thickness) dimensions were cut from the 180 mm x 180

Table 3.1: List of PE grade studied and selected properties

Grade	Type	Density (kg/m3)	MFI (g/10min)	ESCR (hours)
HD1	Homopolymer	965	8.8	2
HD.B	Bimodal	956	0.3	775
HD2	Copolymer (Hexene)	943	2.1	554
LL	Copolymer (Hexene)	933	5	>1008

mm plaques.

3.2.2 Mechanical Characterization

Strain-controlled tensile testing was performed using a 10 kN benchtop Model 3366 Universal Mechanical Testing System (UMTS, Instron Corporation; Norwood, MA). The rectangular samples were pulled longitudinally with a strain rate of 1.4x10-3 s-1. Young's modulus was calculated from the stress-strain data to represent specimen stiffness. Two tests were performed: a varying strain test and a cyclic test. Every test was stopped at a specific strain, above the proportionality limit but before the yield point, at which time the specimen was held at that fixed displacement to observe its relaxation stress for an additional 20 minutes. For the varying strain test, samples were tested for elastoplastic deformation at strain values of 0.5, 1, 2, 4 and 8%. For the cyclic strain-controlled test, each sample was submitted to four consecutive cycles of a fixed value of 2% strain followed by relaxation with intervals of 20 minutes, and in between each cycle the sample was removed for ultrasonic measurements. In each cycle, three points of the cross-section of the sample were measured with a caliper for thickness and width dimensions. The tensile tests were performed at ambient room temperature. Reported experimental variability was based on a 95% confidence interval from three repeats for each grade.

3.2.3 Ultrasonic test

Pulse transmission testing to produce ultrasonic guided waves within the specimens was performed using a Panametrics NDT C604 (2.25 MHz-1.0") ultrasonic transducer as an emitter and a Physical Acoustics F30α as a broadband receiver sensor.. The emitter and sensor were positioned on opposite faces of the rectangular shaped samples at 85 mm distance from their center points, using Dow Corning high vacuum grease as a coupling agent. Excitation of the undeformed and strained samples after being taken from the UMTS was done with a square wave pulse of controlled frequency produced with an Agilent 33210A waveform generator. The received signal was amplified using a Physical Acoustic 2/4/6c amplifier set to +60dB. Acquisition was done at a sampling rate of 4MHz using a National Instruments Corporation 10 MHz 12-bit 4-channel data acquisition card and a LabVIEWTM (National Instruments Corporation) software environment to create separate files for each pulse registering an amplitude over a threshold of 0.06 mV.

Each test consisted of creating 25 pulses of different emitted frequencies (f) varying from 360 to 600 kHz at a step size of 10 kHz; for all polyethylenes with the specific geometry tested, signals above 600 kHz showed modes with low signal-to-noise ratio due to high attenuation, whereas for modes below 350 kHz, the identification of dispersion modes was affected by overlapping waves. The selected frequency range of the study had been previously demonstrated as relevant to characterizing the deformation mechanism of polyethylenes in acoustic emission tests[20,21]. The dispersion profile used to analyze the ultrasonic modes was generated by plotting the frequency spectrum of normalized signal amplitude, calculated as the area under the amplitude-frequency curve integrated between f-2.5 kHz to f+2.5 kHz and divided by the total spectrum area, compiling all 25 detected spectra. To quantify the changes in microstructure of the strained

polyethylene samples as a result of plastic deformation, the change in ultrasonic signal was reported in terms of attenuation ratio, which was defined as the amplitude after deformation over the undeformed sample maximum peak amplitude. Tests were performed at ambient room temperature. Experimental variability was based on a 95% confidence interval from three test repeats for each grade.

3.2.4 Crystalline characterization by Differential Scanning Calorimetry

The crystallinity of each grade of polyethylene was determined using Differential Scanning Calorimetry (DSC). The DSC characterization was done with a TA Instruments Q200 instrument over a temperature range of 15-180°C at a 10°C/min ramp rate under nitrogen gas flow. All tested sample specimens weigthed between 7-8 mg. The percent crystallinity was calculated using the measured melting endotherm relative to a theoretical heat of fusion for 100% crystalline polyethylene (293 J/g,[22]).

3.3 Results and discussion

3.3.1 Influence of small strain deformation on mechanical and acoustic properties of polyethylene

Table 3.2 shows how the mechanical properties of different polyethylene grades changed after four cycles of the cyclic strain-controlled deformation at 2%, values are compared against a control group of samples from the same grade that were not subjected to any deformation before the tensile test. While some bulk properties like Young's modulus and yield stress remained statistically unchanged, other properties that are more related with elastoplastic resistance to deformation presented a significant

change. A reduction in the strain at yield can be explained by the residual plastic strain due to maximum deformation history. Similarly, a reduction in tangent modulus can be connected with the strain softening process. Both properties indicate a significant reduction occurred over the course of the test based on the cumulative strain applied, as evidence of the structural damage related to the Mullins effect; the sensitive mechanical properties, shown in Table 3.2 to be demonstrating elastoplastic damage cannot be collected per cycle since it requires strain beyond the yielding limit which is not consistent with our test procedure. This is a deficiency of the approach, in that it requires yielding to monitor, and hence why reported studies[23,24] have relied upon recording the unloading strain path per cycle as a mean to highlight the progressive damage relatable to the Mullins effect. Since this study could not simultaneously monitor the unloading strain and remove the sample between cycles for acoustic testing, we have chosen to assess the cumulative structural changes being caused by small strain plastic deformation via observing stress relaxation behavior instead. Figure 3.1 shows stress-relaxation curves for different PE grades in four successive strain-controlled cyclic tensile tests at 2%. Values were normalized based on the stress reading at the initial time of the relaxation test. Comparison of the curves indicates different levels of relaxation time for the different crystalline content of these PE grades, which was quantified in Table 3.2. Although, a small deviation is noticeable between curves of the same grade for cycles past the first applied deformation, the variation was not considered significant. Changes in stress relaxation have been demonstrated as indicative of the resistance of crystalline network to plastic flow, and hence was felt to correlate with the same principles related to the Mullins effect[6]. Therefore, this mechanical characterization method should be useful as an alternative to calculation of energy dissipation using the stress softening of the unloading path in cyclic tests[25], a method that has been reported as not to follow closely the behavior observed in

Table 3.2: Tensile mechanical properties of polyethylene samples from undeformed control group and after four cycles of viscoelastic deformation at 2% strain

	Young's Modulus (MPa)		Yield Stress (MPa)		Strain (%) at Yield		Tangent Modulus (MPa)		Cryst. by DSC (%)
Grade	Control	Deformed	Control	Deformed	Control	Deformed	Control	Deformed	Control
HD1	1138 ± 11	1192 ± 90	25.6 ± 0.1	25.8 ± 0.1	11.5 ± 0.2	9.9 ± 0.4	129.2 ± 0.9	111.0 ± 1.7	82
HD.B	906 ± 67	914 ± 24	22.5 ± 0.3	23.2 ± 0.2	13.0 ± 0.5	11.2 ± 0.3	126.6 ± 3.5	116.3 ± 1.7	72
HD2	625 ± 24	628 ± 20	17.2 ± 0.1	17.4 ± 0.1	15.7 ± 0.4	14.0 ± 0.4	105.5 ± 6.4	96.9 ± 0.7	58
LL	573 ± 17	584 ± 19	16.1 ± 0.1	16.1 ± 0.1	16.7 ± 0.2	14.9 ± 0.2	97.9 ± 1.0	93.7 ± 2.8	51

some rubber-like materials that exhibit Mullins effect[24].

A significant change in the ultrasonic wave signal is observed in both time domain and frequency domain when contrasting results before and after one and four cycles of strain-controlled deformation at 2%, as demonstrated in Figure 3.2. The figure shows the detected signal in both time and frequency domain. There was an increase in attenuation specifically at the frequency of the emitted pulse (450 kHz), denoting an increase in wave dispersion within the sample. Ultrasonic attenuation of polyethylene is expected to increase as a consequence of increased plastic deformation[15]. An increase in attenuation of ultrasonic guided waves can be associated with decoupling between partial longitudinal and shear waves, reflecting the higher magnitude of attenuation of bulk shear waves in comparison with bulk longitudinal waves[26]. This can mean that the proportion of taut tie chains and mobile amorphous chains in the non-crystalline phase affected the manner that stresses were propagated through the crystalline network, changing attenuation and dispersion of the ultrasonic waves. Tie chains also play an important role on the viscoplastic properties controlling the stress-strain relationship in the pre-yield deformation region[27].

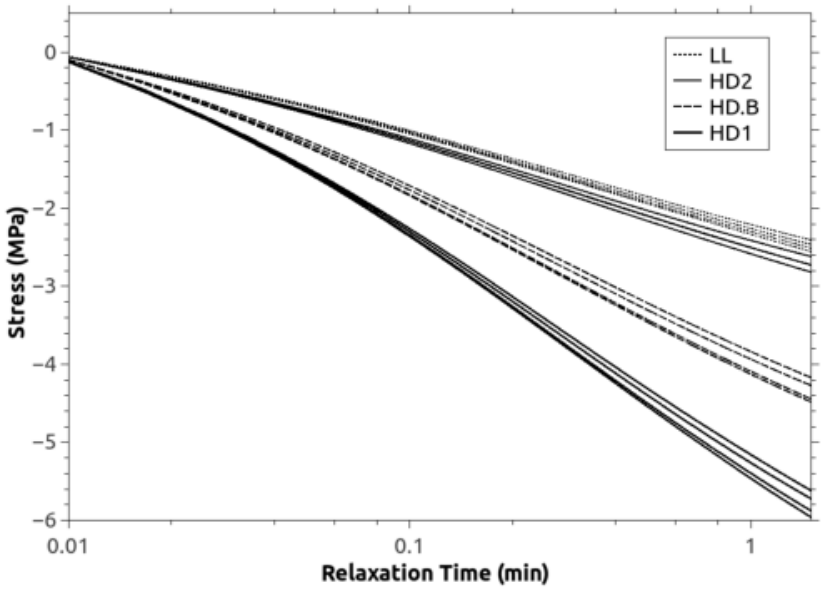

Figure 3.1: Stress relaxation curves of PE samples for four cycles of tensile deformation at 2% strain

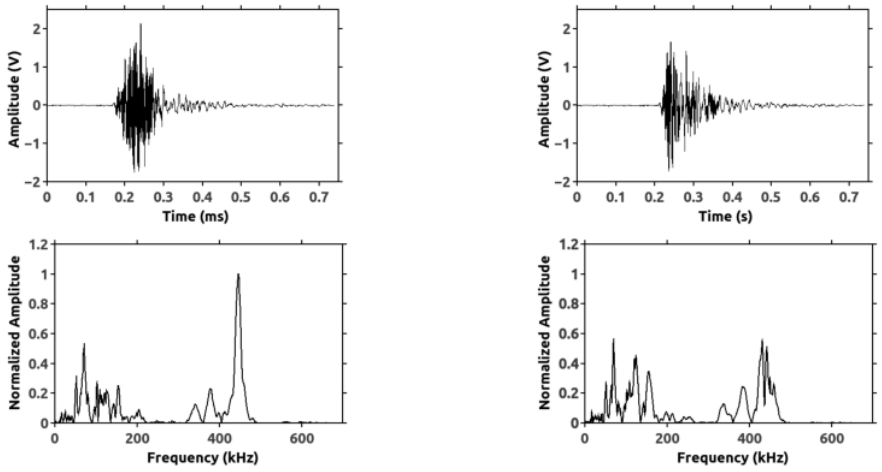

(a) Plot A (b) Plot B

Figure 3.2: Time-domain signal (top) and FFT spectra (bottom) of HD2 sample undeformed (A) and after strain-controlled deformation (B). Emitted signal frequency of 450 kHz

3.3.2 Identification of dispersion modes for optimal ultrasonic analysis with guided waves

As seen above, the changes in structure on account of the Mullins effect are small, at least in the beginning and so, achieving highest sensitivity of the characterization methods is critical. For semi-crystalline polymers, likely polyethylene, where there is a considerable heterogeneity in the crystal structures to disperse the sound wave, attenuation tends to be frequency dependent[28]. Therefore, identification of suitable frequencies for characterization will improve the efficiency of the method by reducing the effects of highly attenuated signals and increase the reliability in terms of signal-to-noise ratio. Figure 3.3 shows normalized spectra for samples of HD2 grade before and after a strain-controlled deformation to 2% strain. Additionally, a comparison of the peak signal is shown along with a theoretically calculated dispersion curve using the method of potentials to solve the Rayleigh-Lamb frequency equations for symmetric and antisymmetric modes. Chan and Cawley[26] have demonstrated the relevancy of asymptotic shear modes in polymeric materials, identifying the frequency range where phase velocity converges momentarily for the bulk longitudinal velocity ideal for testing, providing minimum attenuation. By analyzing the dispersion curves and spectral response of the different polyethylene grades, different modes were identified as candidates for characterization, specifically, the sixth antisymmetric mode (A6) for the grade HD1, the seventh symmetric mode (S7) for grades HD.B and HD2 and the eighth antisymmetric mode (A8) for grade LL. The frequency spectrum analysis to calculate the attenuation ratio between undeformed and strained samples was based on the peak amplitude from the selected dispersion modes. Different authors have demonstrated the relevance of ultrasonic guided waves to help understand the complexity of wave propagation in viscoelastic media and how to identify specific

modes suitable for non-destructive evaluation[26,29–31]. As a result, this approach was considered most suitable for improving the sensitivity of the analysis of the Mullins effect in our polyethylene samples.

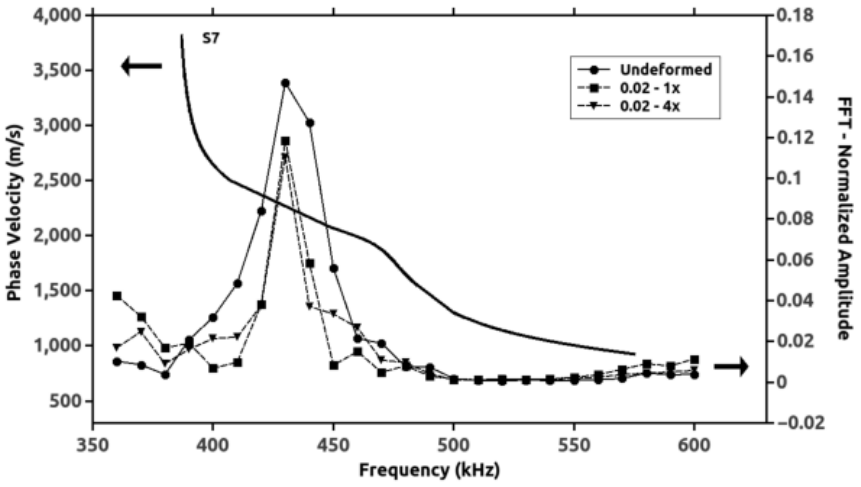

Figure 3.3: Dispersion curve of ultrasonic guided wave mode S7 and FFT spectra for HD2 sample before and after strain controlled deformation

3.3.3 Analysis of Mullins effect with cyclic tensile testing

The analysis of cyclic deformation testing is commonly used in order to observe the Mullins effect, with expected stress softening and residual plastic strain dependent on the maximum strain applied. Therefore, it is expected that the mentioned structural damage cannot increase with successive cycles if done at the same level of deformation. Similar trends in cyclic deformation at 2% strain were observed among all polyethylene grades, with each showing a decrease in the attenuation ratio with increasing cycles, as shown in Figure 3.4. A major decrease in attenuation ratio occurred with the first cycle whereas for further cycles, the ratio value remained constant within the uncertainty of the measurement, matching the trend seen with the reduction in strain at yield. There are however differences seen among the PE grades, with higher attenuation for

grades of higher degree of crystallinity. Accordingly, the same pattern was observed in relaxed stress values from the stress relaxation data of the cyclically deformed samples, as demonstrated in Figure 3.5. Differences are noted between the relaxed stresses of the different PE grades but they occurred for the first cycle, with only constant values reported for successive cycles. These observations are in agreement with the description of the Mullins effect, reported for filled rubber-like materials[23]. The stress softening consequence of the Mullins effect can be explained in semicrystalline polymers by the disruption of tie chains (i.e. rupture, desorption, pull-out from connected crystalline lammela) and the resultant increase in contributions from the amorphous-confined chains in the inter-lamellae regions on the measurement of bulk modulus[32]. Therefore, monitoring the Mullins effect through measurement of ultrasonic attenuation in a plastic part, while in service, could provide valuable information about the historical maximum deformation that was applied, thus indicating possible permanent structural changes caused by early plastic deformation.

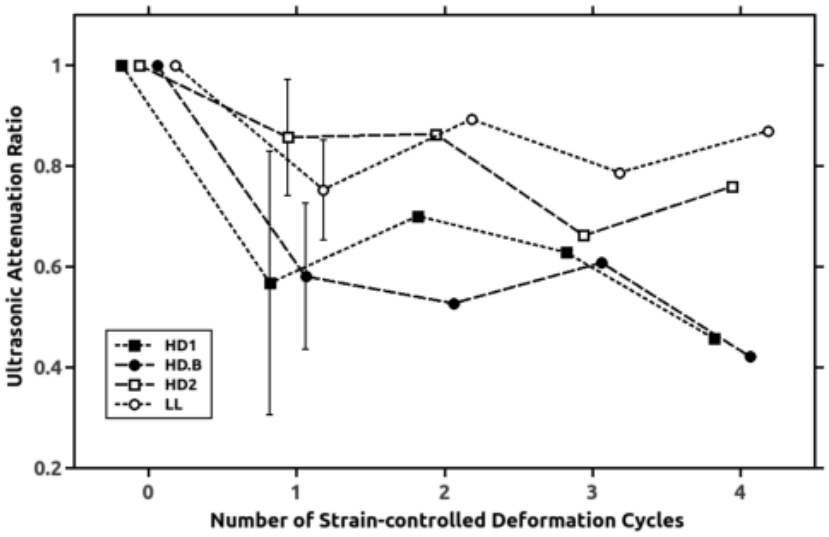

Figure 3.4: Attenuation ratio of different polyethylene grades after one and four successive strain-controlled deformation cycles

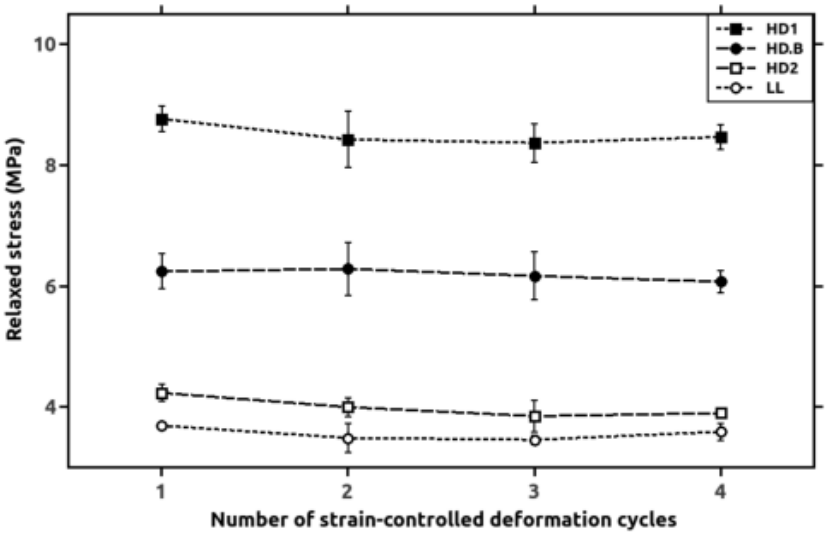

Figure 3.5: Relaxed stress for different polyethylene grades after one and four successive strain-controlled deformation cycles

3.3.4 Analysis of ultrasonic attenuation ratio with increasing small strain deformation

The study develops upon the analysis of Mullins effect through cyclic tensile strain test to investigate the range of small strain deformations where the onset of plastic initiation will occur. By increasing the fixed strain of the strain-controlled deformation test, a significant increase in the attenuation, therefore, a decrease in attenuation ratio and increase in relaxed stresses are expected; in all cases, the strain did not exceed the yield limit of the polymer, though at 8% it was quite close. Figure 3.6 shows the rising relaxed stress values while Figure 3.7 shows the ultrasonic results, with increasing maximum strain being applied to samples of different PE grades. Although the same trend is observed for all PE grades in terms of relaxed stresses, it is possible to observe differences when comparing the curves of the ultrasonic attenuation ratio. Grades HD1 and HD.B with their higher degree of crystallinity showed a faster decrease in the

attenuation ratio for small strain values, though constant in attenuation after the first cycle. Conversely, for lower crystallinity grades, such as HD2, a slower attenuation increase with increasing strain was found, or no significant change was observed as for the case of the LL grade. A larger separation of crystalline lamellae due to higher strains will increase the probability of rupture and pull-out of tie chains that interconnect the crystalline structure. The relevance of this statement is to show the applicability of the proposed method using ultrasonic guided waves for small strains, before reaching yield, is in agreement with changes in properties observed from the mechanical tests. Therefore, macroscopic effects, that could only be studied by the stress-strain profile before, can now be monitored by the attenuation of specific ultrasonic guided wave modes. This proposed method also provides a way to monitor structural changes, like the disruption of links of the elastic network structure, as result of plastic deformation close to the onset of initiation.

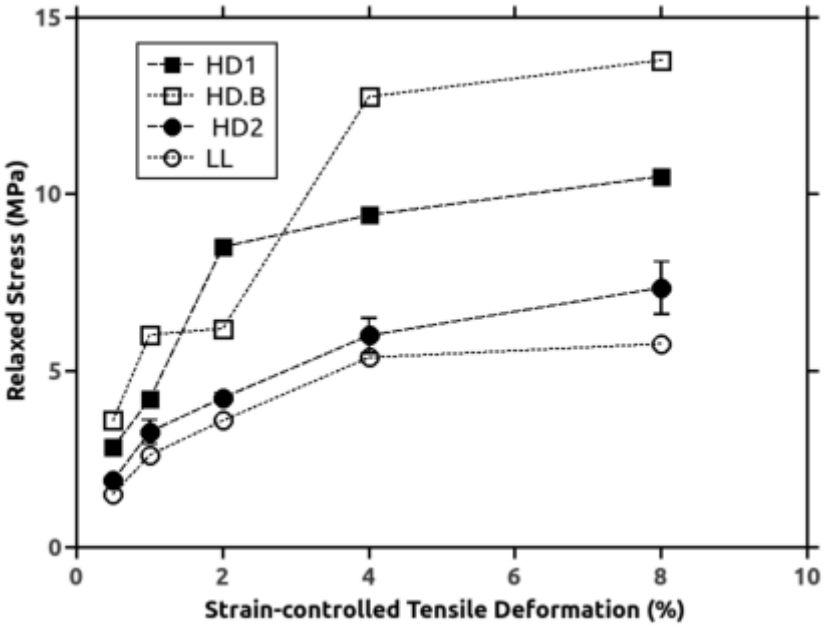

Figure 3.6: Profile of relaxed stress for PE samples with different maximum strain deformation

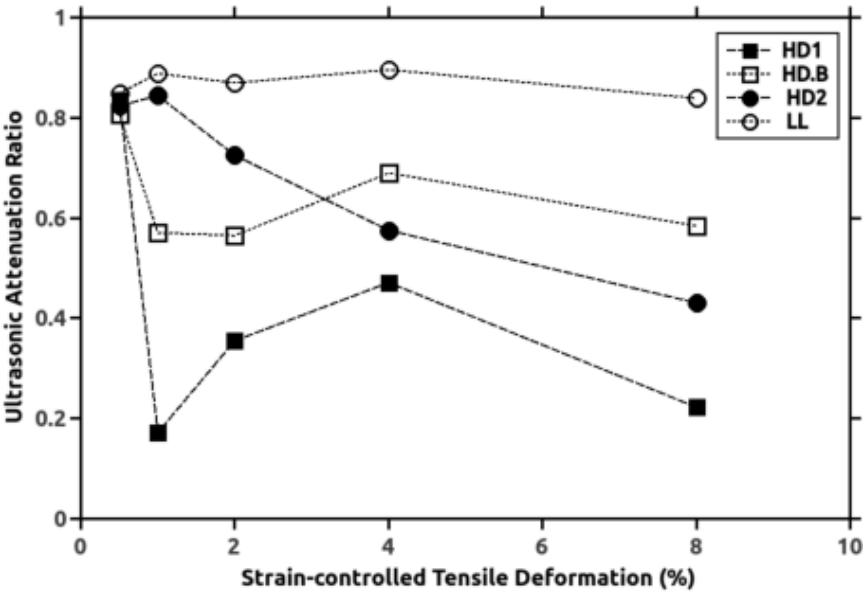

Figure 3.7: Profile of relaxed stress for PE samples with different maximum strain deformation

3.4 Conclusion

Results presented in this paper support the use of ultrasonic guided waves as an alternative method to observe the Mullins effect in cyclic strain-controlled tests. Attenuation of selected ultrasonic modes was correlated with historical maximum strain applied for different polyethylene grades. Most of the reduction in amplitude occurred after the fixed strain was reached for the first cycle, with no significant change in successive deformations to approximately the same strain; this response is evidence supportive that the study is observing the Mullins effect in PE. Changing responses from stress relaxation data were used to show damage mechanically. Attenuation was shown to increase between 20-80% with increasing strain for different PE grades, following in trend with relaxed stress values. The promising use of this ultrasonic

method to monitor damage indicative of long term service life will help us to develop ways to evaluate the failure behavior of semicrystalline polymer in operation, as well as point to important aspects in the processing of formed parts that will be predictive of long-term mechanical resistance.

Acknowledgments

The authors wish to acknowledge the funding support of this work by Imperial Oil Ltd. They want to especially thank Ron Cooke and Mark Woolston for their technical guidance and supply of the polyethylene samples used in the study. And to Conselho Nacional de Desenvolvimento Científico e Tecnológico (CNPq) - Brazil for the PhD Science without Borders Scholarship.

Bibliography

[1] Stanislav Patlazhan and Yves Remond. Structural mechanics of semicrystalline polymers prior to the yield point: A review. *Journal of Materials Science*, 47(19): 6749–6767, 2012.

[2] P.-Y. Ben Jar. Effect of tensile loading history on mechanical properties for polyethylene. *Polymer Engineering & Science*, 55(9):2002–2010, sep 2015.

[3] Koh Hei Nitta. A molecular theory of stress-strain relationship of spherulitic materials. *Computational and Theoretical Polymer Science*, 9(1):19–26, 1999.

[4] F. Detrez, S. Cantournet, and R. Seguela. Plasticity/damage coupling in semicrystalline polymers prior to yielding: Micromechanisms and damage law identification. *Polymer*, 52(9):1998–2008, apr 2011.

[5] A D Drozdov. Mullins' effect in semicrystalline polymers experiments.pdf. *International Journal of Solids and Structures*, 46(18-19):3336–3345, 2009.

[6] Ming Wang, Jiabin Shen, Jiang Li, and Shaoyun Guo. Network alteration theory on Mullins effect in semicrystalline polymers. *Polymer International*, 64(1): 105–112, 2015.

[7] D. Tscharnuter, M. Jerabek, Z. Major, and G. Pinter. Irreversible deformation of isotactic polypropylene in the pre-yield regime. *European Polymer Journal*, 47 (5):989–996, may 2011.

[8] Andrzej Pawlak, Andrzej Galeski, and Artur Rozanski. Cavitation during deformation of semicrystalline polymers. *Progress in Polymer Science*, 39(5): 921–958, 2014.

[9] M Mizushima, T Kawamura, K Takahashi, and K Nitta. In situ near-infrared spectroscopic studies of the structural changes of polyethylene during melting. *Polymer Journal*, 44(2):162–166, 2012.

[10] Takumitsu Kida, Tatsuya Oku, Yusuke Hiejima, and Koh-hei Nitta. Deformation mechanism of high-density polyethylene probed by in situ Raman spectroscopy. *Polymer*, 58:88–95, feb 2015.

[11] Bijin Xiong, O. Lame, J. M. Chenal, C. Rochas, R. Seguela, and G. Vigier. Temperature-Microstructure Mapping of the Initiation of the Plastic Deformation Processes in Polyethylene via In Situ WAXS and SAXS. *Macromolecules*, 48(15): 5267–5275, 2015.

[12] Artur Rozanski and Andrzej Galeski. Plastic yielding of semicrystalline polymers affected by amorphous phase. *International Journal of Plasticity*, 41:14–29, feb 2013.

[13] V.M. Litvinov and L. Kurelec. Remarkably high mobility of some chain segments in the amorphous phase of strained HDPE. *Polymer*, 55(2):620–625, jan 2014.

[14] Akira Tanaka, K Nitta, and S Onogi. Ultrasonic velocity and attenuation of polymeric solids under oscillatory deformation: Apparatus and preliminary results. *Polymer Engineering and Science*, 29(16):1124–1130, aug 1989.

[15] Akira Tanaka and Koh-hei Nitta. Ultrasonic velocity and attenuation of polymeric solids under oscillatory deformation. II: High density and linear low density polyethylene and their blends. *Polymer Engineering and Science*, 31(8):571–576, apr 1991.

[16] Masayuki Yamagushi and Koh-Hei Nitta. Optical and Acoustical Investigation for Plastic Deformation of Isotatic Polypropylene/Ethylene-1-Hexene Copolymer Blends. *Polymer Engineering & Science*, 39(5):833–840, 1999.

[17] D. Zellouf, Y. Jayet, N. Saint-Pierre, J. Tatibouet, and J. C. Baboux. Ultrasonic Spectroscopy in Polymeric Materials. Application of the Kramers–Kronig Relations. *Journal of Applied Physics*, 80(5):2728–2732, 1996.

[18] B. Hosten and M. Castaings. Comments on the ultrasonic estimation of the viscoelastic properties of anisotropic materials. *Composites Part A: Applied Science and Manufacturing*, 39(6):1054–1058, jun 2008.

[19] S. F. Chabira, M. Sebaa, R. Huchon, and B. De Jeso. The changing anisotropy character of weathered low-density polyethylene films recognized by quasi-static and ultrasonic mechanical testing. *Polymer Degradation and Stability*, 91(8): 1887–1895, 2006.

[20] F.P.C. Gomes, A Bovell, G.P. Balamurugan, M.R. Thompson, and K.G. Dunn. Evaluating the influence of contacting fluids on polyethylene using acoustic emissions analysis. *Polymer Testing*, 39:61–69, oct 2014.

[21] N. Casiez, S. Deschanel, T. Monnier, and O. Lame. Acoustic emission from the initiation of plastic deformation of Polyethylenes during tensile tests. *Polymer*, 55(25):6561–6568, dec 2014.

[22] Bernhard Wunderlich. *Macromolecular physics, volume 3—crystal melting*, volume 18. dec 1980.

[23] Julie Diani, Bruno Fayolle, and Pierre Gilormini. A review on the Mullins effect. *European Polymer Journal*, 45(3):601–612, 2009.

[24] A. D. Drozdov, R. Klitkou, and J. Dec Christiansen. Multi-cycle deformation of semicrystalline polymers: Observations and constitutive modeling. *Mechanics Research Communications*, 48:70–75, 2013.

[25] Y. Pan and Z. Zhong. Modeling the Mullins effect of rubber-like materials. *International Journal of Damage Mechanics*, 0(0):1–16, 2016.

[26] C W Chan and P Cawley. Lamb waves in highly attenuative plastic plates. *Journal of the Acoustical Society of America*, 104(2):874–881, 1998.

[27] Koh-hei Nitta and Naoto Yamaguchi. Influence of Morphological Factors on Tensile Properties in the Pre-yield Region of Isotactic Polypropylenes. *Polymer Journal*, 38(2):122–131, feb 2006.

[28] Junru Wu. Effects of nonlinear interaction on measurements of frequency-dependent attenuation coefficients. *The Journal of the Acoustical Society of America*, 99(6):3380, 1996.

[29] Vikram K. Kinra and Vasudevan R. Iyer. Ultrasonic measurement of the thickness, phase velocity, density or attenuation of a thin-viscoelastic plate. Part II: the inverse problem. *Ultrasonics*, 33(2):111–122, 1995.

[30] A. Bernard, M. J. S. Lowe, and M. Deschamps. Guided waves energy velocity in absorbing and non-absorbing plates. *The Journal of the Acoustical Society of America*, 110(1):186–196, jul 2001.

[31] Ivan Bartoli, Alessandro Marzani, Francesco Lanza di Scalea, and Erasmo Viola. Modeling wave propagation in damped waveguides of arbitrary cross-section. *Journal of Sound and Vibration*, 295(3-5):685–707, 2006.

[32] Richard J Gaylord and Richard J Gaylord. The Confined Chain Approach to the Deformation Behavior of Bulk Polymers. 19(14), 1979.

Chapter 4

Effects of Annealing and Swelling to Initial Plastic Deformation of Polyethylene probed by Nonlinear Ultrasonic Guided Waves

Effects of Annealing and Swelling to Initial Plastic Deformation of Polyethylene probed by Nonlinear Ultrasonic Guided Waves

F.P.C. Gomes[1], W.T.J. West[1], M.R. Thompson[1]

[1]Department of Chemical Engineering, CAPPA-D/MMRI

McMaster University, Hamilton, Ontario, Canada

Published manuscript at Polymer (Guildf)

DOI: 10.1016/j.polymer.2017.10.041

Author contribution:

The first author of this research paper, F.P.C. Gomes, was responsible for the design and execution of the experiments; processing of the acquired data and writing of the reported document for peer-review and publication. The second author, W.T.J. West, contributed with the design of the test apparatus and method to evaluate the long-term stress cracking resistance. The author M. R. Thompson was responsible for supervision of the experiments and revision of the manuscript.

Main scientific contributions of the paper:

- Demonstrated the calculation and use of a nonlinear ultrasonic parameter (ultrasonic ratio) correlating with the extent of plastic deformation.
- Application of the nonlinear ultrasonic parameter to observe the progression in solvent swelling.
- Connect how variations of semi-crystalline structural morphological (due to thermal treatment) affected the initial plastic deformation by observing changes in the nonlinear ultrasonic parameter.

- Calculate a parametric descriptor using ultrasonic spectral data to monitor the evolution of internal structural stresses,

ABSTRACT

Identification of precursor events related to incipient plastic deformation in polyethylene parts using a nondestructive technique is investigated in this study. A pair of ultrasonic transducers mounted on the surface of a test sample were used to propagate ultrasonic pulses of varying frequency while progressively small flexural deformations below yielding were applied. The evolution of higher order harmonics was observed in association with increasing micro-structural modification. Three different polyethylene grades were molded using different thermal treatments. Results showed that different crystalline networks could be correlated to different mechanisms of plastic deformation that were observed by a defined ultrasonic parameter under proposed method. Variation of the ultrasonic parameter was similarly observed with the residual stresses associated with solvent swelling, as studied by penetration of toluene into the bimodal and copolymer grades. Results and discussion presented in this study connect this non-destructive characterization method with mechanisms of incipient plastic deformation in polyethylene.

Key-words: Nonlinear Ultrasonics, Plastic deformation, Polyethylene.

4.1 Introduction

Understanding the mechanisms of plastic deformation is essential for prediction of long-term sustained service of polyethylene (PE) parts. Initiation of yielding corresponds to a non-linear response to deformation prior to permanent structural damage, which is directly associated with the concentration of internal stresses causing crystalline dislocation[1]. Heterogeneous crystalline lattice formation is an essential physical

element providing the strength resistance and unique plasticity of semi-crystalline polymers compared to amorphous polymers[2]. Although the degree of crystallinity is an important parameter influencing this early stage of plastic deformation for PE, another important factor controlling crystalline dislocation is the morphology of its interlamellae crystalline regions[3,4]. These regions are comprised of stress transmitters across the crystal lamellae boundaries known as tie chains, that are associated with the mobility of the macromolecular network and are known to control structural changes arising during these early stages of deformation[5–7]. Processing history, particularly the associated crystallization kinetics, for a semi-crystalline polymer directly impact the density of these tie chains, which in turn significantly influences the slow crack resistance of formed parts[8–10]. The inter-crystalline region can also be affected by penetration of low molecular weight contacting fluids, which can similarly promote internal stresses[11]. Therefore, connecting mechanical and environmental stresses through characteristics of the inter-crystalline network is important to predict the plasticity and long-term performance of PE parts.

Above the proportionality limits of elasticity, internal microstructural damage leads to an accumulation of residual stresses attributable to crystal shear, lamellae separation/cavitation and/or crystal stretching[12]. Currently, a limited number of characterization methods can be applied to observe structural changes at the onset of plastic deformation. Local strain deformation can be observed at the microscopic level through the long period of crystals using in situ small angle X-ray scattering (SAXS)[3,13]. Orientation by plastic deformation is demonstrated by in situ Raman spectroscopy[14] and small angle neutron scattering (SANS)[15]. Mobility of different semi-crystalline domains can be measured using nuclear magnetic resonance spectroscopy (NMR)[16]. Permanent damage due to crystalline fragmentation has been visualized by atomic force microscopy (AFM)[17]. Additionally, the energy from cavitation and

crystal damage can be recorded using acoustic sensors[18]. Although, these methods are effective in the investigation of some elements of initial plastic deformation, they provide micro to meso-scale analysis of local events, which has a limited applicability to predict macroscale events that occur in the long-term service of these parts[19]. From a practical perspective, none of the current experimental methods can characterize the bulk plasticity of PE samples.

Conversely, characterization methods based on ultrasonic guided waves are promising non-destructive alternatives that can be used for damage monitoring in bulk samples[20]. The non-destructive qualities and capacity to assess the bulk nature of materials by such methods lend themselves well to inclusion as sensing technology in advanced manufacturing platforms[21]. Recent evidence has shown the application of such methods to observe post-yielding lamellae to fribrillar transformation[22] and strain-softening after small cyclic deformation[23] for PE samples using tensile tests. The complexity of the propagated signal often requires further processing and spectroscopic analysis. A promising spectroscopic characterization is the use of detected variations in the amplitude of higher harmonics, also referred to as nonlinear ultrasonic evaluation[24]. The use of nonlinear ultrasonic guided waves methods to follow the degree of plastic deformation has been demonstrated in metals[25–28], which are comparatively homogeneous in their structure, but also to detect localized damages in composites[29]. The suitability of the nonlinear ultrasonic approach has yet to be experimentally demonstrated with semicrystalline polymers, being only previously described theoretically for a second harmonic resonance[30] and for linear elastic regime[31,32]. Based on the elements demonstrated, this paper presents the use of nonlinear ultrasonic guided waves to evaluate incipient plastic behavior in modified polyethylene samples before yielding and assess the influence of their crystallization history or solvent swelling in the performance of prepared parts.

4.2 Materials and Methods

4.2.1 Materials

Three different grades of polyethylene were supplied in pellet form by Imperial Oil Ltd. (Sarnia, ON). These grades included a reference homopolymer (HO) grade with density of 965 kg/m3 and melt flow index (MFI) of 8.8 g/10min and two modified grades, namely: a hexene copolymer grade with bimodal molecular weight distribution (BM), density of 956 kg/m3 and MFI of 0.3 g/10 min; and, a hexene copolymer (CO) grade with density of 933 kg/m3 and MFI of 5 g/10 min. Detailed information related to the concentration of hexene was not provided. Reported data on density and MFI were measured and provided by the supplier.

4.2.2 Specimen Preparation

Samples of each polyethylene grade were compression molded into 180 mm x 180 mm x 3.2 mm thick plaques using a laboratory Carver press with heated platens. Pellets in a mold were initially heated to 145 ^{o}C for five minutes and then increased to 170 ^{o}C for additional five minutes, with gradually increasing pressure up to 10 MPa across the two stages of heating. With the polymer fully melted and compressed, two different thermal treatments were applied, namely: i) rapid quenching (Q), where the mold was water cooled at a rate of approximately 72 ^{o}C/min till reaching 80 ^{o}C, while maintaining pressure; or ii) annealing (A), where the platen temperature was reduced to 100 ^{o}C at the same previous cooling rate and then kept constant while the sample was held at pressure for one hour. After each treatment, the sample plaque was removed from the mold and allowed to further cool in ambient air. Flexural specimens with dimensions of 180mm (length) x 20mm (width) x 3.2mm (thickness) were cut

from the plaques. Tensile samples with Type IV dimensions accordingly with ASTM D638-14 were prepared in a split mold using the same melting and thermal treatment procedures described above.

For studies involving solvent physical swelling, flexural and tensile specimens of each sample were immersed in toluene (laboratory grade, Caledon Laboratories) for 15 and 48hrs at room temperature. After removal, samples were kept in the fume-hood for 30 minutes and wiped cleaned with paper tower to remove any excess of the chemical from the surface before testing. Weight of each sample was measured before immersion and after removal from the fume-hood using a Mettler Toledo analytical balance (model AE200).

4.2.3 Tensile and Flexural tests

Mechanical characterization of the samples was done with a Model 3366 benchtop universal mechanical testing system (Instron Corporation) at room temperature and a relative humidity of 35%. Under tensile deformation, appropriate specimens were constantly strained to failure at a crosshead speed of 100 mm/min. Studies on flexural deformation were performed using a three-point method with a 65 mm support span. Specimens were progressively deformed to different degrees of strain (0.5, 1, 1.5 and 2%) in a step-wise manner at a crosshead speed of 2 mm/min. After being strained to one of these conditions, a specimen was allowed to relax with the return of the crosshead to its original position and ultrasonic testing was then performed while still in place before continuing to the next strain state.

4.2.4 Ultrasonic test

With a specimen positioned for three-point flexural testing, two ultrasonic transducers were coupled to its surface using high vacuum grease (Dow Corning), each at a distance of 35 mm from the center where the crosshead tip would press to deflect. A 150 kHz resonant transducer (Physical Acoustics) was used as the signal emitter and a 350 kHz broadband sensor (Physical Acoustics) as the receiver. The signal was induced using a waveform generator (Agilent) to create a 10-cycles pulse, with each pulse at a predefined yet different frequency varying from 135 to 165 kHz by steps of 1 kHz. The received signal was recorded using a data acquisition system (National Instruments) with 4 MHz acquisition rate. Amplitude of time-domain events is reported in decibels (dB) converting the maximum recorded level using a reference threshold of 0.06 V. Each event was converted to frequency domain using fast Fourier transformation, totaling 31 spectra being collected per strain condition. The collected data was analyzed using code programmed in Python language to calculate an 'ultrasonic parameter' that was based on the ratio of the third harmonic amplitude (A3) to the amplitude at the emitted frequency (A1). In order to allow the comparison between samples with different attenuation, results reported in this study follow the progress of the ultrasonic parameter using the amplitude ratio normalized based on the parameter value for the same sample before the first step in flexural strain was applied. The selection of the frequency range for the higher harmonics was based on previously identified guided wave modes that were suitable to characterization due to their low attenuation[23].

4.2.5 Differential Scanning Calorimetry (DSC)

DSC tests were performed in a TA Instruments (model Q200) to analyze the melting peak of crystals from samples with different thermal histories. Samples of

approximately 8 mg were cut from molded plaques for flexural samples, and tested in a hermetically sealed Tzero pans. With a heat ramp rate of 10 oC/min, heat flow was recorded between 23 oC and 180 oC. The environmental chamber was kept with a constant nitrogen gas flow of approximately 50 ml/min. The content of crystals was calculated based on the enthalpy of the melting endotherm relative to an enthalpy of 290 J/g for purely crystalline PE[33].

4.2.6 Modified Bent Strip test

For the long-term characterization of the PE samples, a modified bent strip test, adapted from the ASTM D1693 was performed. Strips with 115mm (length) x 20mm (width) x 3.2mm (thickness) were simultaneously bent into a U-shape with a 15.88mm radius and notched (0.5mm deep) with an in-house developed rig. The U-bent sample was mounted in a custom-made retaining device against an affixed 0.1 kN force sensor, allowing compression forces to be recorded over the test time. This test was capable of providing detailed information about the progression of slow crack growth. Analysis was made based on the crack growth time which is defined as the difference between the time of crack initiation (defined as the point of inflexion of the force after full stress relaxation) and the time of fracture.

4.3 Results

Over the two following sections, characterization of PE properties is given for the different grades with different thermal processing histories (Section 4.3.1). These results based on traditional destructive tests serve as reference to correlate with the proposed nonlinear ultrasonic results in Section 4.3.2. Complementary observations of the ultrasonic method are presented in Section 4.3.3 with varied swelling states based

on exposure of PE to toluene. Discussion is presented in Section 4.4.

4.3.1 Effects of Annealing on PE properties

Figure 4.1 shows the DSC thermograms of samples prepared from different grades and thermal histories. The PE grades are indicated based on their unique structural characteristic: homopolymer (HO), bimodal molecular weight distribution (BM), and copolymer (CO). A general increase in the endothermic peak, from 8 to 12 J/g can be observed in the annealed (A) samples compared to the quenched (Q), pointing to a higher degree of crystallinity in the former cases. The transition exhibited a single, though wider, peak in the thermograms of both annealed BM and HO samples compared to their respective quenched conditions, demonstrating the effect of prolonged crystallization time to promote growth of the lamellae thickness[34]. In contrast, the thermogram of annealed CO presented a noticeable secondary crystallization peak at 105 oC located closer to the annealing temperature, in addition to its peak transition temperature at 130 oC. This form of shoulder in the transition profile might be an indication of the organization of smaller crystals from mobile chains that were "frozen" in the amorphous phase in the quenching process. This effect can happen in parallel to the lamellae thickening of the main crystallization peak[35].

The effects of thermal history on crystallinity and mechanical properties for the different resin grades are presented in Table 4.1, assuming that samples from the same PE grade processed at similar thermal treatments present closely related properties. Elastic properties, namely flexural modulus and yield stress, can be direct correlated with changes in the total crystal content, with both increasing for the annealed sample versus quenched samples from all grades. Crystallinity increased between 2 and 7 % from quenched versus annealed samples, while flexural modulus increased between

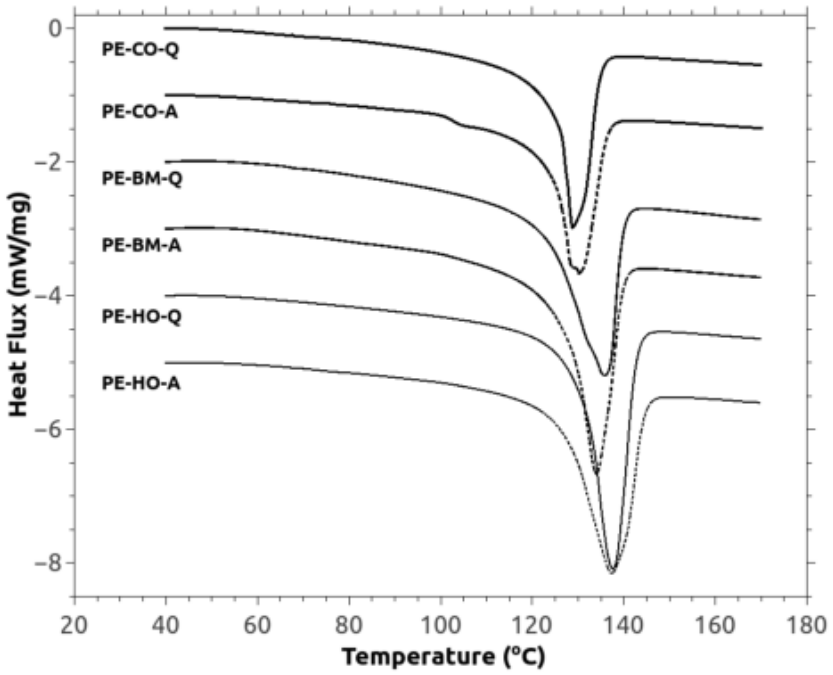

Figure 4.1: DSC curves of PE samples for different thermal treatments

4 and 10%, respectively. Properties knowingly related to the plastic behavior of semi-crystalline polymers showed some divergent results among the three resins. A reduction in elongation at break was observed for annealed HO and BM compared to quenching. Reduction in plasticity caused by annealing also affected crack propagation, as results in Table 4.1 show a small reduction in crack growth time for HO and a significant decrease for BM. The lower resistance to crack propagation of an annealed specimen can be related to modifications in tie chain conformation, with progressively straightening reported as being inversely proportional to the lamellae thickness[7]. Conversely, annealed CO showed a general increase in plasticity based on strain at break values. Secondary crystallization seen by DSC in the CO samples might have created a reinforcement of the macromolecular network, responsible for increasing its yield stress and enhancing its plasticity[34]. Other short-term mechanical properties

Table 4.1: DSC and mechanical characterization results for PE grades with different thermal history

Material	Crystallinity – DSC (%)	Flexural Modulus (MPa)	Tensile - Yield Stress (MPa)	Tensile – Elongation at break (%)	Slow Crack Growth Time (h)*
PE-HO-Q	75.4 ± 1.0	1265 ± 100	29.8 ± 0.3	17 ± 2.0	3.9
PE-HO-A	77.0 ± 1.1	1343 ± 129	27.1 ± 1.0	4 ± 1.7	3.1
PE-BM-Q	75.7 ± 1.0	1086 ± 61	25.4 ± 0.9	60 ± 37	73
PE-BM-A	77.5 ± 1.1	1143 ± 86	28.2 ± 1.0	24 ± 6.1	38
PE-CO-Q	56.6 ± 0.8	749 ± 16	18.2 ± 0.2	197 ± 4.3	47
PE-CO-A	61.1 ± 0.9	674 ± 77	22.0 ± 0.5	255 ± 42	57

*Standard deviation for these results was not determined

that could only be observed for CO samples under tensile load, and not for HO or BM, were natural draw ratio (NDR) and strain hardening (SH). The CO samples demonstrated a significant increase from quenched (NDR = 1.86, SH =10.6 MPa) to annealed (NDR = 2, SH = 14.4 MPa) samples for both properties. Both properties are expected to correlate with concentration of tie chains[36]. Therefore, these results presented corroborate the earlier observation by DSC of secondary crystallization, in this case having a dominant effect on the plasticity of CO samples compared to any changes in tie chain conformation.

4.3.2 Nonlinear Ultrasonics

Traditional ultrasonic characterization relies on information drawn from the amplitude or travel time of an ultrasonic signal in the time domain. Figure 4.2 demonstrates how maximum recorded amplitude from each polyethylene grade of differing thermal histories is correlated with flexural modulus. As the modulus decreases with declining crystal content, attenuation of the ultrasonic signal increases. This is a reliable

non-destructive estimation of the density and stiffness of the crystalline structure prior to incipient plastic deformation. However, no information can be drawn on the plastic behavior of these samples from such analysis. No significant differences between annealed and quenched samples are observed by this manner of characterization. Another similar measurement that is directly correlated with the elastic properties is the ultrasonic sound velocity, which also requires the precise measurement and control of the sample thickness. Therefore, a new approach is proposed to characterize the initial plastic deformation using nonlinear ultrasonic guided waves.

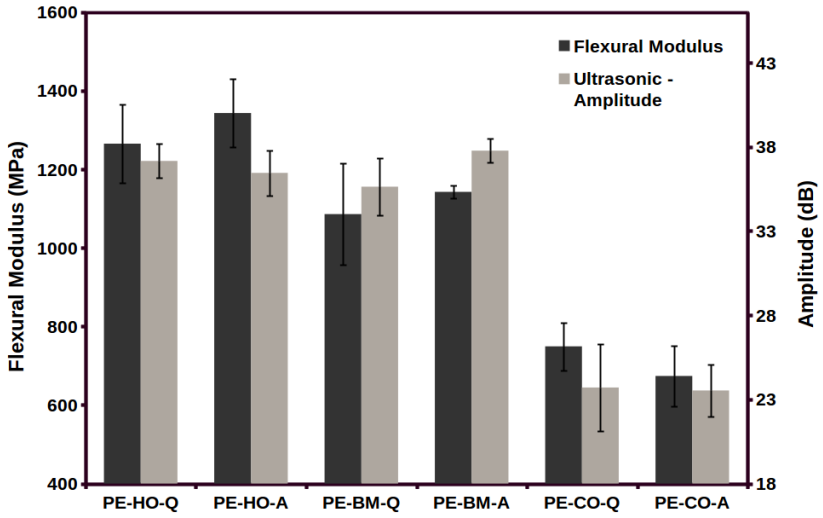

Figure 4.2: Flexural modulus and ultrasonic signal amplitude of PE samples with different thermal treatments

Figure 4.3 shows how the amplitude of the third harmonic (A3) grew with increased flexural deformation in the elasto-plastic region well before yielding (expected at 5 to 6 %). Observations of these harmonics are only possible due to nonlinearities in the structure of the material, thus this distinguishes the analysis from the traditional ultrasonic methods[24]. The amplitude ratio between the third harmonic (A3) and the input frequency or primary wave (A1), referred to as the ultrasonic parameter, is proposed to be used as an analytical descriptor of structural changes without interference

of attenuation of the ultrasonic signal. Figure 4.4 highlights the strong correlation found between the nonlinear ultrasonic parameter and increasing flexural deformation of the PE specimen, most notable beyond the purely elastic limits (highlighted by the included dashed line). The initiation of plastic behavior in the deforming specimen affects its crystalline network by creating residual stresses[12]. Higher harmonics are directly coupled with structural anisotropy induced by permanent spatial deformations[37]. A noticeable peak is already present in the original spectrum for the processed sample before flexural deformation, possibly an indication of inherent anisotropy, which then increases with induced deformation. Similar evidence relating a variation in ultrasonic spectrum with increasing plastic deformation was previously demonstrated to PE samples after applied tensile stresses below yielding[23].

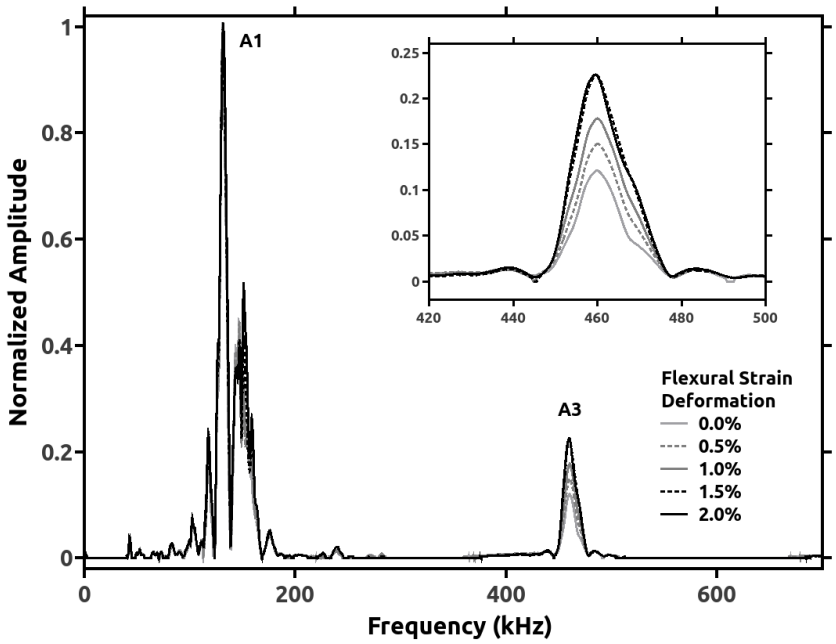

Figure 4.3: Normalized ultrasonic frequency spectra for increasing flexural deformation in PE-BM-Q sample showing variation of third harmonic amplitude (A3) correlated with input frequency (A1)

Plots (a-c) in Figure 4.5 show the profile of the ultrasonic parameter with increasing

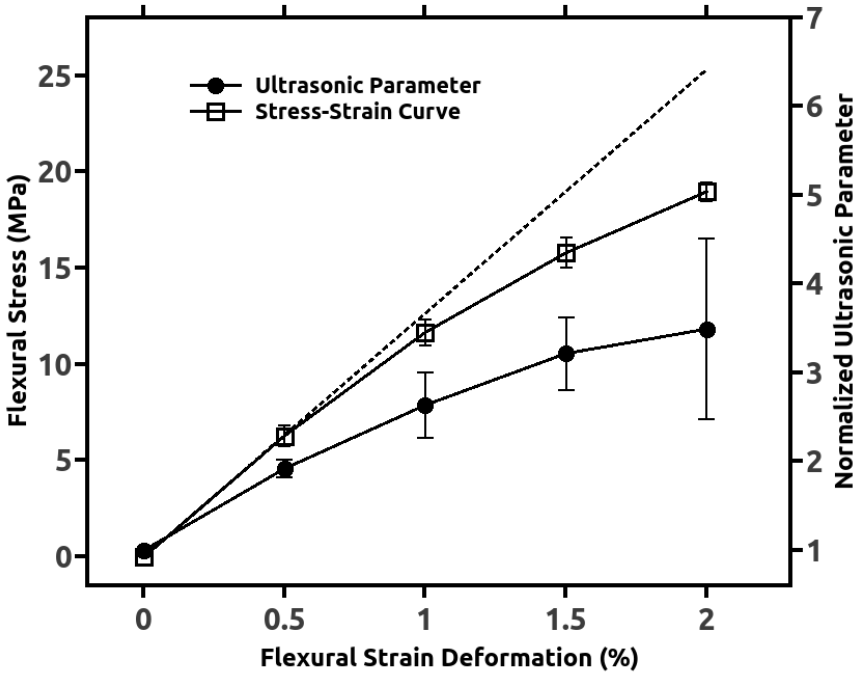

Figure 4.4: Evolution of nonlinear ultrasonic parameter with increasing flexural deformation in PE-BM-Q samples (dashed and solid lines were included for visual reference only)

flexural deformation for samples with different thermal history. Samples with higher crystal content yet same quenched thermal treatment showed significantly higher values of the ultrasonic parameter with increasing deformation. Negligible change for the normalized ultrasonic parameter was observed for the annealed cases of both HO and BM, seen in plots (a,b), whereas their quenched cases showed a progressive increase with deformation. For CO, plot (c) shows the annealed sample produced the same lack of variation in the parameter seen with the other two resins, while the quenched sample increasingly exhibited a decrease in ultrasonic parameter value as deformation increased.

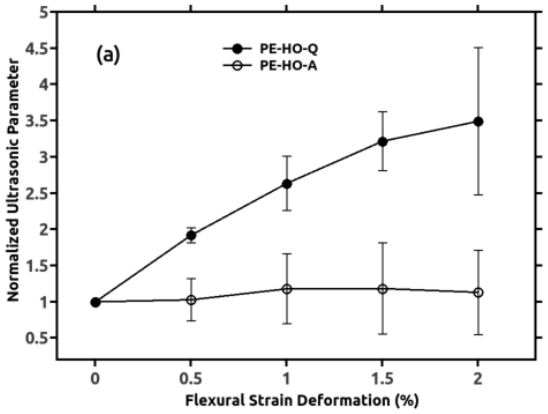

(a) Plot A

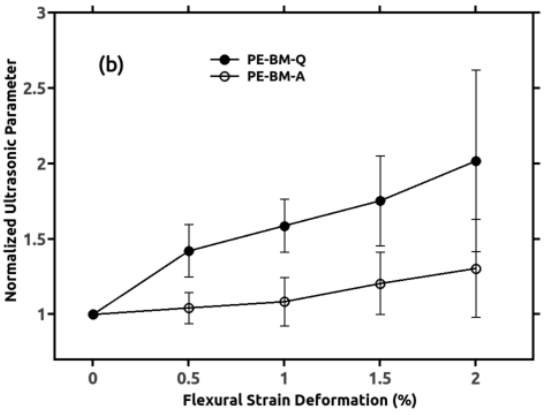

(b) Plot B

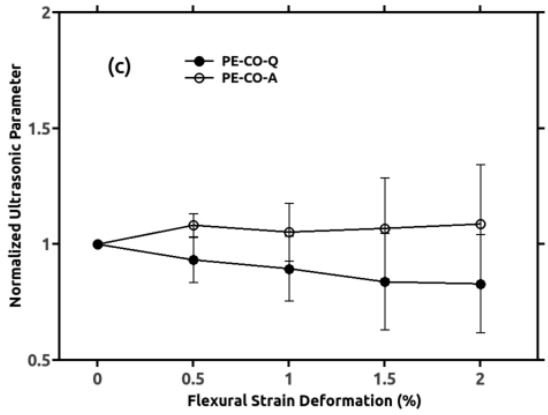

(c) Plot C

Figure 4.5: Profile of nonlinear ultrasonic parameter with increasing flexural deformation for homopolymer (a), bimodal (b) and copolymer (c) PE with different thermal treatments

4.3.3 Effects of Swelling on PE properties

Effects of solvent swelling on incipient plastic behavior were examined with quenched BM and CO samples, which exhibited similar chemistries yet vastly different crystallinity. The changes in mechanical properties from long term immersion in toluene are reported in Table 4.2.These two polyethylene grades are manufactured to enhance environmental stress cracking resistance, making them commercially interesting to study for exposure to solvents. A significant decrease is observed in the flexural modulus of both grades due to toluene penetration. This effect seen under flexural deformation is plotted in Figure 4.6 for BM, which demonstrates a direct relation between declining modulus and the time allowed for penetration of toluene; the same trend was seen for CO and as a result, not shown in the figure. Although significant reduction of mechanical elastic properties was reported, no significant reduction in crystallinity was directly related to solvent swelling was observed in DSC tests for samples after 48 hours of contact with toluene. The absorption rate was significantly different with BM samples presenting an increase in weight of 2.1 % (+/− 0.1) after 15 hours and 4.2 % (+/− 0.1) after 48 hours of soaking; meanwhile CO samples had a higher weight gain with 3.1% (+/− 0.2) after 15 hours and 6.0 % (+/− 0.3) after 48 hours in contact with toluene. CO samples after 48 hours of contact with the fluid showed a significant increase in strain at break, demonstrating an expected plasticization effect of toluene[38]. Conversely, BM samples demonstrated an opposite effect, with a decrease in elongation before break, which was considered to similarly indicate a decrease in plasticity.

Plots (a, b) in Figure 4.7 demonstrate how the signal amplitude (in the time domain) and ultrasonic parameter were affected by swelling for the quenched BM and CO samples. Attenuation of the average ultrasonic signal can be correlated with

Table 4.2: Mechanical characterization for PE samples after solvent physical swelling

Material	Flexural Modulus (MPa)	Tensile - Yield Stress (MPa)	Tensile – Elongation at break (%)
PE-BM-Q	1142 ± 85	25.4 ± 0.9	60 ± 37
PE-BM-TL48	617 ± 124	25.6 ± 0.3	35 ± 5
PE-CO-Q	749 ± 16	18.2 ± 0.2	197 ± 4
PE-CO-TL48	407 ± 23	18.9 ± 0.4	228 ± 32

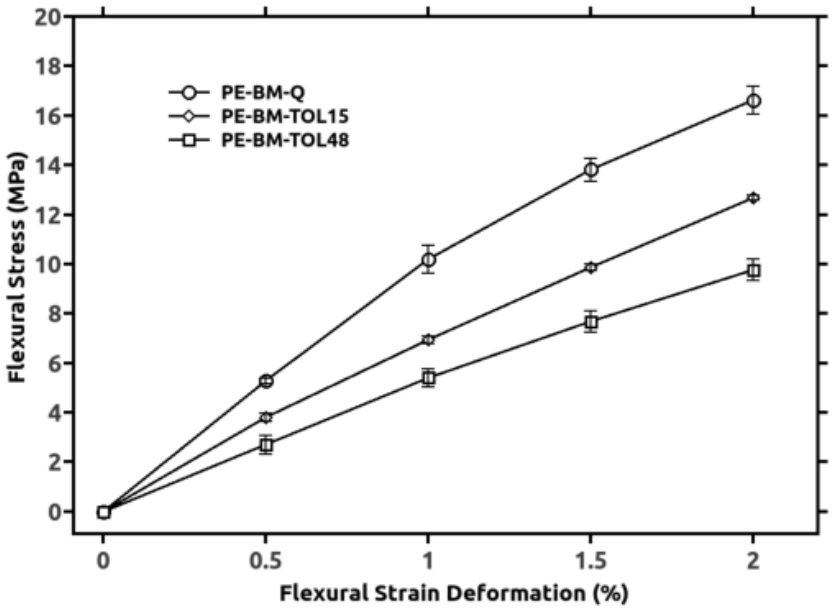

Figure 4.6: Flexural stress-strain curves for bimodal (BM) PE samples with increasing swelling time

the effect of toluene to decrease elastic modulus, as shown in Table 2. However, the ultrasonic parameter, which is based on the nonlinear interaction with the structure of a material, did not follow the same trend. The harmonic amplitude ratio remained insignificantly changed for BM, while progressively increased for CO based on contact time with the fluid.

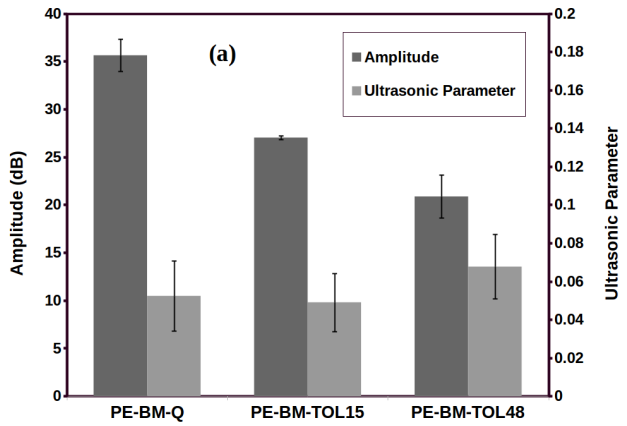

(a) Plot A

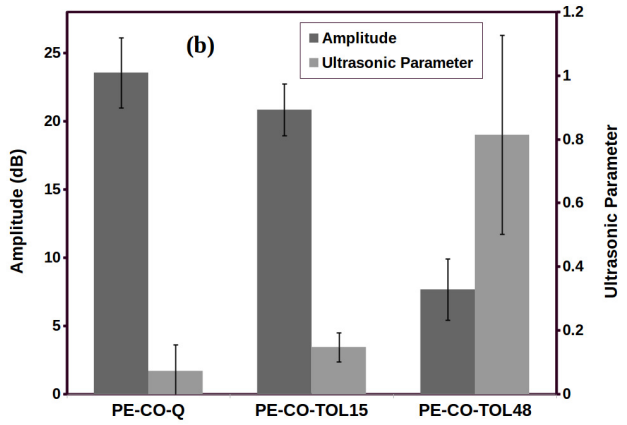

(b) Plot B

Figure 4.7: Nonlinear ultrasonic parameter and the time domain signal amplitude for (a) bimodal and (b) copolymer PE with increasing time immersed in toluene

4.4 Discussion

Results presented in the previous sections showed a distinctive elastic and plastic behavior among the PE samples studied. The three grades of polyethylene were chosen to highlight how the introduced ultrasonic technique can distinguish changing morphological details in the inter-crystalline region, often best detected by mechanical characterizations, that are related to incipient yielding and affected by annealing or swelling. The primary assumption of this study is that propagation of ultrasonic

waves in PE will be dispersive and differ from a perfect elastic body. Therefore, our proposed approach focuses on the non-linear interaction of ultrasonic vibrations with the discontinuities of a semicrystalline network responsible for generating a signal with a frequency different than the original wave introduced[39]. Reliance on linear equations, such as Hooke's law, can only be applied to describe the bulk wave interaction through velocity and attenuation with major structural events, namely, cavitation and fibrillar transition[22,40,41]. The introduced nonlinear ultrasonic method is believed to be sensitive to more minute microstructure events that modify the crystalline network at incipient plastic deformation, by observation of the evolution of anharmonicity in PE samples with increasing stresses below the yield point.

Between quenched samples with differing crystal content it was observed that higher crystallinity promote a larger variation of the ultrasonic parameter for the same level of deformation. From Figure 5, while quenched HO and BM grades showed an increase of 2 to 3 times in the ultrasonic parameter after 2% of flexural strain was applied, CO quenched samples, with significantly lower crystallinity, demonstrated an actual decrease in the ultrasonic parameter from its baseline value for the same deformation level. There is a direct relation between the crystalline structure and differentiation of bulk PE from an ideal oscillator to small deformations[42]. However, comparison of ultrasonic parameter results from annealed to quenched samples showed that there is no direct correlation between the generation of harmonics and the degree of crystallinity. Noticeably, contributions to anharmonicity are not related to the size of PE crystals themselves, but on their interaction through the non-crystalline regions.

Three different mechanisms are normally used to explain initiation of plastic deformation: cavitation, elongation and shear[43]. For the PE grades tested under flexural load below yielding, no cavitation should be expected[44] leaving two competing crystallographic mechanisms to be considered, homogeneous crystal slip and heterogeneous

lamellae stack separation. Both events occur in the vicinity of a inter-crystalline interface. In such cases, the conformation of tie chains plays a very important role in balancing between these two mechanisms. A reduction in plasticity is demonstrated through the significant reduction in elongation at break and slow crack growth time for annealed cases of HO and BM, reported in Table 4.1. The decline in these properties by annealing indicated a change in the conformation of tie chains resulting from increasing lamellae thickness[35], which in part will favor interlamellae crystal slip during early stages of plastic deformation. From a bulk to meso-scale perspective, a higher concentration of crystal slips represents a homogeneous rearrangement of the macromolecular network for the same level of internal stresses[45], in this case induced by flexural deformation. Analysis of the ultrasonic parameter showed that samples with theoretically more homogeneous inter-crystalline dislocations caused by mechanical deformation presented little to no effect in the anharmonicity of the PE structure, while samples with expected higher concentration of heterogeneous intra-lamellae separation, ie. quenched HO and BM, showed an increase in the amplitude of higher harmonics. Nonlinear ultrasonic wave propagation can be correlated to microstructural asymmetries and discontinuities[26], thus relating the observed increase in ultrasonic parameter with plastic deformation through intralamellae separation that is expected to be prominent in crystals aligned to the applied force[13]. Conversely, it was the quenched samples rather than annealed case for CO that exhibited reduced slow crack growth time and elongation at break as well as produced significant attenuation of the higher harmonics, pointing to extensive occurrence of crystal slip in the former. The annealed CO samples showed the same resistance to variation of the ultrasonic parameter as the other resins, which can be correlated with the reportedly hindering of the interlamellae slipping by secondary crystallization[46].

To complement the observations made by mechanical deformation, swelling results

were presented as additional evidence on how the proposed ultrasonic test can be used to follow progressive changes in microstructure of polyethylene. Increased contact time of the samples with toluene showed a significant weight gain and reduction in the elastic modulus on both CO and BM samples. Penetration of compatible low molecular weight agents is expected to promote swelling of the amorphous phase, which induces internal stresses within the interlamellae region[47]. Thus, observations of an increase in the ultrasonic parameter with exposure time to toluene might be interpreted as an indication of the level of penetration of the fluid, creating a localized stress concentration in the interlamellar region of crystallites closely located to the exposed surface. This swelling is only located in the amorphous phase and does not affect the crystallographic interpretation of the plastic deformation modes previously described, but the resultant residual stresses can be compared to the localized stresses associated with heterogeneous dislocations in the highly crystalline quenched samples after incipient plastic deformation. A higher penetration rate was observed for CO samples, possibly due to their lower crystal content resulting in greater vulnerability to swelling[48]. And the stability presented by the BM can also be explained by the barrier effect of tie chains to diffusion of low molecular weight molecules[49]. This is unlikely to be the exclusive reason with some consideration given to the possibility of a 'skin effect' due to differences in cooling rate from the outside to the core of each sample, that can lead to relative differences in crystalline morphology and hence differences in solvent penetration between the two polymers. These results highlight the potential of using the ultrasonic parameter to monitor diffusion of low molecular weight components over exposure time in polyethylene parts in use.

Based on the evidence shown in this study, nonlinear ultrasonics seems to be a relevant non-destructive method to characterize stress-induced micro-structural modifications of a crystalline network. Initial results demonstrated by this technique

indicate a potential to follow localized stresses concentrated in the intralamellae region related to incipient plastic deformation or in the interlamellae region caused by penetration of low molecular weight component, as summarized in Figure 4.8. Understanding early processes of plastic deformation can help predict the kinetic control over the propagation of dislocations in the later stages[50]. Further theoretical analysis and modeling can also help understand the capabilities of this method to quantify and predict the long-term plastic behavior of tested samples in operating conditions[51]. However, it is also important to highlight that propagation of the ultrasonic guided waves in the bulk material is affected by several characteristic properties. Thus, the path to a practical application of this technique requires the isolation of the micro-structural phenomena from other macroscopic changes that might affect the signal, such as reducing dimensional and surface changes.

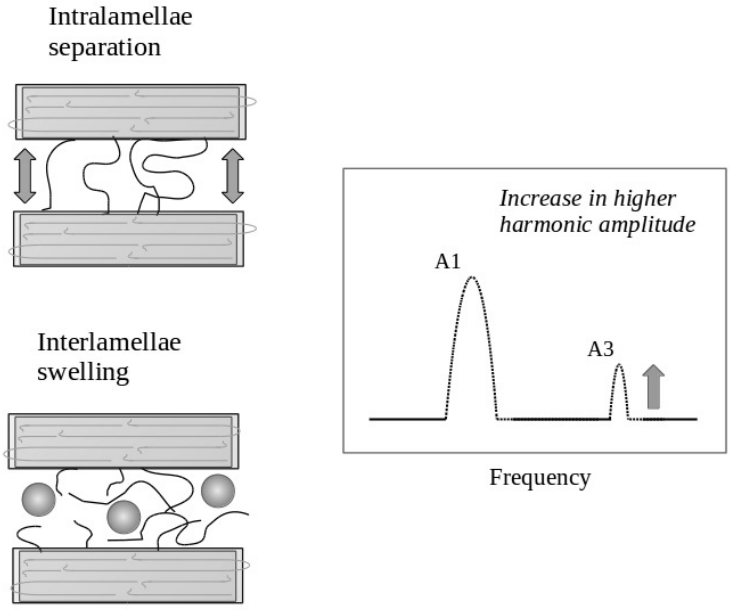

Figure 4.8: Schematic of the correlation between plastic deformation and swelling of PE samples with increase in higher harmonic amplitude of ultrasonic guided waves

4.5 Conclusions

Plasticity of PE samples with different thermal history and after solvent swelling was evaluated using traditional destructive methods and a proposed non-destructive alternative using ultrasonics. A nonlinear ultrasonic parameter, based on the the amplitude ratio of the third harmonic and the input frequency, was correlated with increased localized stresses due to crystalline plane dislocations and low molecular weight swelling of the amorphous phase. Results showed that the proposed method was able to monitor microstructural changes in crystalline network during incipient plastically deformed PE samples from different grades and thermal history. Variation of the ultrasonic parameter with increasing flexural deformation was significantly higher for samples with higher crystallinity and fast cooling rate history.

Annealed samples for HO and BM grades showed a reduction in plasticity, observed from traditional destructive short-term and long-term tests and also through a significant reduction in the variation of the ultrasonic parameter. Changes can be linked to a significant restriction in conformation of tie chains due to thermal treatment. Secondary crystallization observed in annealed CO samples caused an opposite effect, with a hindering effect comparing results from quenched CO samples. A second application of the proposed method involving the observation of the ultrasonic parameter with sorption of toluene, showed that BM samples demonstrated a lower variation of the ultrasonic parameter over CO samples subjected to the same contact time, highlighting different barrier properties due to crystalline morphology and plasticity.

Different from the traditional ultrasonic testing that can mostly be linked with variations of elastic properties or dimensional changes for PE samples, this proposed approach based can provide important quantification of the contribution of different semicrystalline morphologies to the resistance to plastic deformation. With further

research and development this method can become an important nondestructive technique for characterization of PE.

Acknowledgments

Special thanks for Ron Cooke and Mark Woolston for the technical support and material. Also the funding support by Imperial Oil Ltd and Conselho Nacional de Desenvolvimento Científico e Tecnológico (CNPq) - Brazil through the Science Without Borders Scholarship Program.

Bibliography

[1] L Lin and A. S. Argon. Structure and plastic deformation of polyethylene. *Journal of Materials Science*, 29(2):294–323, 1994.

[2] George Z Voyiadjis, Amir Shojaei, and Navid Mozaffari. Strain gradient plasticity for amorphous and crystalline polymers with application to micro- and nano-scale deformation analysis. *Polymer*, 55(16):4182–4198, 2014.

[3] C. Millot, R. Séguéla, O. Lame, L.-A. Fillot, C. Rochas, and P. Sotta. Tensile Deformation of Bulk Polyamide 6 in the Preyield Strain Range. Micro–Macro Strain Relationships via in Situ SAXS and WAXS. *Macromolecules*, 50(4): 1541–1553, feb 2017.

[4] Koh-hei Nitta and Naoto Yamaguchi. Influence of Morphological Factors on Tensile Properties in the Pre-yield Region of Isotactic Polypropylenes. *Polymer Journal*, 38(2):122–131, feb 2006.

[5] J. Cazenave, R. Seguela, B. Sixou, and Y. Germain. Short-term mechanical and structural approaches for the evaluation of polyethylene stress crack resistance. *Polymer*, 47(11):3904–3914, may 2006.

[6] L. Kurelec, M. Teeuwen, H. Schoffeleers, and R. Deblieck. Strain hardening modulus as a measure of environmental stress crack resistance of high density polyethylene. *Polymer*, 46(17):6369–6379, aug 2005.

[7] Bijin Xiong, O. Lame, J. M. Chenal, C. Rochas, R. Seguela, and G. Vigier. Temperature-Microstructure Mapping of the Initiation of the Plastic Deformation Processes in Polyethylene via In Situ WAXS and SAXS. *Macromolecules*, 48(15): 5267–5275, 2015.

[8] J. J. Lear and P. H. Geil. Slow Crack Growth and Molecular Mobility in Commercial Gas Pipe Resins. *International Journal of Polymeric Materials*, 15 (3-4):147–170, dec 1991.

[9] Bernard A G Schrauwen, Roel P M Janssen, Leon E. Govaert, and Han E H Meijer. Intrinsic deformation behavior of semicrystalline polymers. *Macromolecules*, 37 (16):6069–6078, 2004.

[10] A. Sharif, N. Mohammadi, and S. R. Ghaffarian. Model prediction of the ESCR of semicrystalline polyethylene: Effects of melt cooling rate. *Journal of Applied Polymer Science*, 112(6):3249–3256, jun 2009.

[11] Artur Krajenta, Artur Rozanski, and Rafał Idczak. Morphology and properties alterations in cavitating and non-cavitating high density polyethylene. *Polymer*, 103:353–364, oct 2016.

[12] R Hiss, S Hobeika, C Lynn, and G Strobl. Network Stretching, Slip Processes, and Fragmentation of Crystallites during Uniaxial Drawing of Polyethylene and Related Copolymers. A Comparative Study. *Macromolecules*, 32(13):4390–4403, jun 1999.

[13] Bijin Xiong, Olivier Lame, Jean-Marc Chenal, Cyrille Rochas, Roland Seguela, and Gerard Vigier. In-situ SAXS study of the mesoscale deformation of polyethylene in the pre-yield strain domain: Influence of microstructure and temperature. *Polymer*, 55(5):1223–1227, mar 2014.

[14] Takumitsu Kida, Tatsuya Oku, Yusuke Hiejima, and Koh-hei Nitta. Deformation mechanism of high-density polyethylene probed by in situ Raman spectroscopy. *Polymer*, 58:88–95, feb 2015.

[15] Carlos R. López-Barrón, Yiming Zeng, Jonathan J. Schaefer, Aaron P. R. Eberle, Timothy P. Lodge, and Frank S. Bates. Molecular Alignment in Polyethylene during Cold Drawing Using In-Situ SANS and Raman Spectroscopy. *Macromolecules*, 50(9):3627–3636, may 2017.

[16] V.M. Litvinov and L. Kurelec. Remarkably high mobility of some chain segments in the amorphous phase of strained HDPE. *Polymer*, 55(2):620–625, jan 2014.

[17] F. Detrez, S. Cantournet, and R. Seguela. Plasticity/damage coupling in semi-crystalline polymers prior to yielding: Micromechanisms and damage law identification. *Polymer*, 52(9):1998–2008, apr 2011.

[18] N. Casiez, S. Deschanel, T. Monnier, and O. Lame. Acoustic emission from the initiation of plastic deformation of Polyethylenes during tensile tests. *Polymer*, 55(25):6561–6568, dec 2014.

[19] Hossein Sepiani, Maria Anna Polak, and Alexander Penlidis. Modeling short- and long-term time-dependent nonlinear behavior of polyethylene ARTICLE HISTORY. *Mechanics of Advanced Materials and Structures*, 0(0):1–11, 2017.

[20] Mira Mitra and S Gopalakrishnan. Guided wave based structural health monitoring: A review. *Smart Materials and Structures*, 25(5):053001, 2016.

[21] Behzad Esmaeilian, Sara Behdad, and Ben Wang. The evolution and future of manufacturing: A review. *Journal of Manufacturing Systems*, 39:79–100, apr 2016.

[22] N. Casiez, S. Deschanel, T. Monnier, and O. Lame. Ultrasonic in situ investigation of the initiation of Polyethylene's plastic deformation during tensile tests. *Polymer*, 123(25):258–266, aug 2017.

[23] F.P.C. Gomes and M.R. Thompson. Analysis of Mullins effect in polyethylene using ultrasonic guided waves. *Polymer Testing*, 60:351–356, jul 2017.

[24] Vamshi Krishna Chillara, Baiyang Ren, and Cliff J Lissenden. Guided wave mode selection for inhomogeneous elastic waveguides using frequency domain finite element approach. *Ultrasonics*, 67(December):1–13, 2015.

[25] Mingxi Deng and Junfeng Pei. Assessment of accumulated fatigue damage in solid plates using nonlinear Lamb wave approach. *Applied Physics Letters*, 90 (12):121902, mar 2007.

[26] C. J. Lissenden, Y. Liu, G. W. Choi, and X. Yao. Effect of Localized Microstructure Evolution on Higher Harmonic Generation of Guided Waves. *Journal of Nondestructive Evaluation*, 33(2):178–186, jun 2014.

[27] C Pruell, J.-Y. Kim, J Qu, and L.J. Jacobs. A nonlinear-guided wave technique for evaluating plasticity-driven material damage in a metal plate. *NDT & E International*, 42(3):199–203, apr 2009.

[28] Yanxun Xiang, Mingxi Deng, and Fu-Zhen Xuan. Creep damage characterization using nonlinear ultrasonic guided wave method: A mesoscale model. *Journal of Applied Physics*, 115(4):044914, jan 2014.

[29] Natalie Rauter and Rolf Lammering. Impact Damage Detection in Composite Structures Considering Nonlinear Lamb Wave Propagation. *Mechanics of Advanced Materials and Structures*, 22(1-2):44–51, jan 2015.

[30] Claudio Nucera and Francesco Lanza. Modeling of Nonlinear Guided Waves and Applications to Structural Health Monitoring. *Journal of Computing in Civil Engineering*, 29(4):1–15, jul 2015.

[31] Ivan Bartoli, Alessandro Marzani, Francesco Lanza di Scalea, and Erasmo Viola. Modeling wave propagation in damped waveguides of arbitrary cross-section. *Journal of Sound and Vibration*, 295(3-5):685–707, 2006.

[32] A. Bernard, M. J. S. Lowe, and M. Deschamps. Guided waves energy velocity in absorbing and non-absorbing plates. *The Journal of the Acoustical Society of America*, 110(1):186–196, jul 2001.

[33] Roger S. Porter. Macromolecular physics, volume 3—crystal melting, Bernhard Wunderlich, Academic Press, New York, 1980, 363 pp. *Journal of Polymer Science: Polymer Letters Edition*, 18(12):824–824, dec 1980.

[34] Sylvie Castagnet and David Girard. Sensitivity of damage to microstructure evolution occurring during long-term high-temperature annealing in a semi-crystalline polymer. *Journal of Materials Science*, 42(18):7850–7860, jul 2007.

[35] J. J. Strebel and A. Moet. The effects of annealing on fatigue crack propagation

in polyethylene. *Journal of Polymer Science Part B: Polymer Physics*, 33(13): 1969–1984, sep 1995.

[36] Roland Séguéla. On the Natural Draw Ratio of Semi-Crystalline Polymers: Review of the Mechanical, Physical and Molecular Aspects. *Macromolecular Materials and Engineering*, 292(3):235–244, mar 2007.

[37] Vamshi Krishna Chillara and Cliff J Lissenden. On some aspects of material behavior relating microstructure and ultrasonic higher harmonic generation. *International Journal of Engineering Science*, 94:59–70, sep 2015.

[38] F.P.C. Gomes, A Bovell, G.P. Balamurugan, M.R. Thompson, and K.G. Dunn. Evaluating the influence of contacting fluids on polyethylene using acoustic emissions analysis. *Polymer Testing*, 39:61–69, oct 2014.

[39] C J Lissenden, Y Liu, and J L Rose. Use of non-linear ultrasonic guided waves for early damage detection. *Insight - Non-Destructive Testing and Condition Monitoring*, 57(4):206–211, apr 2015.

[40] K.H. Nitta and A. Tanaka. Ultrasonic velocity and attenuation of polymeric solids under oscillatory deformation. III: Drawn films of high density and linear low density polyethylene and their blends. *Polymer Engineering & Science*, 31 (13):1–4, 1991.

[41] Yi Zhang, P.-Y. Ben Jar, Kim-Cuong T. Nguyen, and Lawrence H. Le. Characterization of ductile damage in polyethylene plate using ultrasonic testing. *Polymer Testing*, 62:51–60, sep 2017.

[42] K Nitta, K Suzuki, and A Tanaka. Comparison of tensile properties in the pre-yield

region of metallocene-catalyzed and Ziegler-Natta-catalyzed linear polyethylenes. *Journal of Materials Science*, 35:2719–2727, 2000.

[43] Stanislav Patlazhan and Yves Remond. Structural mechanics of semicrystalline polymers prior to the yield point: A review. *Journal of Materials Science*, 47(19): 6749–6767, 2012.

[44] Andrzej Pawlak, Andrzej Galeski, and Artur Rozanski. Cavitation during deformation of semicrystalline polymers. *Progress in Polymer Science*, 39(5): 921–958, 2014.

[45] R Seguela, S Elkoun, and V Gaucher-Miri. Plastic deformation of polyethylene and ethylene copolymers: Part II Heterogeneous crystal slip and strain-induced phase change. *Journal of Materials Science*, 33(7):1801–1807, apr 1998.

[46] Shijie Song, Jiachun Feng, and Peiyi Wu. Annealing of melt-crystallized polyethylene and its influence on microstructure and mechanical properties: A comparative study on branched and linear polyethylenes. *Journal of Polymer Science Part B: Polymer Physics*, 49(19):1347–1359, oct 2011.

[47] Artur Rozanski and Andrzej Galeski. Plastic yielding of semicrystalline polymers affected by amorphous phase. *International Journal of Plasticity*, 41:14–29, feb 2013.

[48] Martina Podivinska, Klara Jindrova, Josef Chmelar, and Juraj Kosek. Swelling of polyethylene particles and its relation to sorption equilibria under gas-phase polymerization conditions. *Journal of Applied Polymer Science*, 134:45035, 2017.

[49] Maila N. Cardoso and Adriano G. Fisch. Bimodal High-Density Polyethylene: Influence of the Stereoregularity of the Copolymer Fraction on the Environmental

Stress Crack Resistance. *Industrial & Engineering Chemistry Research*, 55(22): 6405–6412, jun 2016.

[50] Amin Sedighiamiri, Leon E. Govaert, Marc J W Kanters, and Johannes A W Van Dommelen. Micromechanics of semicrystalline polymers: Yield kinetics and long-term failure. *Journal of Polymer Science, Part B: Polymer Physics*, 50(24): 1664–1679, 2012.

[51] J. A W van Dommelen, M. Poluektov, A. Sedighiamiri, and L. E. Govaert. Micromechanics of semicrystalline polymers: Towards quantitative predictions. *Mechanics Research Communications*, 80:4–9, 2017.

Part II

Multivariate Analysis for Process Monitoring

Chapter 5

Nondestructive evaluation of sintering and degradation for rotational molded polyethylene

Nondestructive evaluation of sintering and degradation for rotational molded polyethylene

F.P.C. Gomes[1], M.R. Thompson[1]

[1]Department of Chemical Engineering, CAPPA-D/MMRI

McMaster University, Hamilton, Ontario, Canada

Published manuscript at Polymer Degradation and Stability

DOI: 10.1016/j.polymer.2017.10.041

Author contributions:

The first author, F.P.C. Gomes, was responsible for experimental design and execution; data processing and analysis; and writing the manuscript that was accepted by the scientific journal after peer-review process. The author M.R.Thompson contributed with supervision in all stages of experimental executions and analysis; and with the revision of the written document.

Main scientific contributions of the paper:

- Application of nonlinear ultrasonic test for nondestructive quality assessment of rotational molded parts (bulk structural qualification).
- Monitoring of two distinctive processes that have effects on product quality of rotational molded parts (sintering and degradation) using one characterization test.
- Presentation of multivariate calibration for ultrasonic spectra and destructive test results (prediction tool).

ABSTRACT

Developments in new sensor technologies and data processing are helping to increase the number of applications of nondestructive characterization methods. In this study, two major physiochemical phenomena affecting product quality of rotationally molded polyethylene parts, namely sintering and degradation, were evaluated using both traditional characterization techniques and a newer alternative ultrasonic-based method. Oven temperature and heating cycle time were controlled to produce six different process conditions for rotomolding. Increasing peak internal air temperature (PIAT) inside the mold produced a reduction in surface voids (pitting) and increased the impact strength for produced parts, which can be related to greater densification during sintering. Contrary to these characterizations denoting improved part quality, degradation was detected for PIAT above 220 ^{o}C by an increase in surface carbonyl groups by Fourier-transform infrared spectroscopy (FT-IR) and an increase in zero-shear viscosity, both relatable to thermo-oxidative free radical reactions. The newly proposed monitoring technique applying propagating ultrasonic guided waves showed that its data-rich spectral features based on harmonic frequencies were positively correlated to the same sintering and degradation properties observed above. Coupled with multivariate statistical analysis, the nondestructive ultrasonic technique shows great promise for combining multiple analyses in a single sensor technology, making it well suited to the implementation of advanced manufacturing methodologies in polymer processing practices.

Key-words: nondestructive evaluation, ultrasonic, impact, degradation, polyethylene

5.1 Introduction

Industry has been changing in recent years with the introduction of digital informatics and the growing efforts towards advanced manufacturing. The focus in manufacturing is moving towards the development of tools that will allow more reliability, flexibility and capacity for optimizing processes. These tools are not simply hardware but rather process information collection with improved data processing, new control strategies and faster communications[1]. Examples of these advancements in polymer processing have been gradually presented[2–5]. Those studies have shown how sensor signals conveying single variable descriptive data can improve a process; however, the challenge becomes how to incorporate more complex data-heavy techniques and sensors that can expand the possibility of the envisaged framework for advance manufacturing in polymer processes.

The production of hollow parts using rotational molding involves the melting then densification of polymer powders without the aid of external compression or shear forces; these steps are referred to as sintering and are similarly seen in the newer 3-D printing technology known as selective laser sintering (SLS)[6]. This method is widely used for production of large shapes such as storage tanks, marine shells and other diverse components. Final quality of rotational molded parts is highly dependent on the extent of two contrasting phenomena: sintering and thermo-oxidative degradation[7]. During the melting stage of the process, liquid bridges form among the particles trapping air bubbles that need to vanish during the subsequent densification stage, all occurring under moderate temperatures above the polymer melting point for a moderate period of time[8]. If these bubbles are not removed, the produced parts will have poor mechanical properties[9]. Due to the nature of the hollow mold, the polymer melt will be constantly exposed to oxygen and maintained at high temperatures, which

will promote thermo-oxidative degradation and also alter mechanical properties[10]. Polyethylene degradation leads to discoloration, poor long term mechanical properties and possibly embrittlement due to chain crosslinking[11]. Process reliability depends on monitoring features of the produced part related with these two processes, and thus the selection of characterization methods plays a key role in ensuring production quality.

Currently, the manufacturing industry relies on destructive tests to assess the quality of these parts. Impact strength is the most heavily relied upon property for rotational molding, being easily affected by process conditions and readily highlighting issues related to incomplete sintering[7,12]. Other similar options are to evaluate elastic modulus, hardness[13] and fracture toughness[14]. Chain branching and cross-linking during thermo-oxidative degradation will increase the viscosity of polyethylenes typically used in rotational molding, which can be seen by measurements like melt flow index[15] or parallel plate rheometry[16]. However, none of these tests are applicable to quality assurance of each part produced, instead requiring a small number of parts from each production run to be diverted for testing and where those tests can take hours before the processor is informed whether the process conditions were acceptable. Therefore, in order to adopt practices of increased process reliability and flexibility, applications of nondestructive techniques are desirable.

Spectroscopic methods are examples of nondestructive techniques that have seen limited use in manufacturing, mostly because of the large amounts of data collected and expertise required by the user for their interpretation, but there have been rare examples of their use for rotational molding albeit not for quality assurance. Fourier-transform infrared spectroscopy (FT-IR) was used to identify oxidation products at the surface of rotomolded parts[17]. Additionally, X-ray diffraction[18] and Raman spectroscopy[19] were used to evaluate changes in crystal morphology for evidence of

degradation. Neither technique is readily integrated into a manufacturing process and these instruments are expensive. Linear ultrasonic measurements have been demonstrated for processed polyethylene comparing acoustic properties with different materials, at different temperatures and different stresses[20,21]. On the other hand, no reports have been made of ultrasonic spectroscopic testing in rotational molding of polyethylene. Traditional single variable ultrasonic methods are very efficient for density measurement by relating this property to changes in velocity or attenuation of a sound wave propagating through a sample, with noted examples for different polyolefins[22,23] and polymer foams[24]. However, recent developments in the field of ultrasonics have turned the focus towards the generated spectrum from a propagated signal as means to interpret structural features of polyethylene samples[25]. Specifically, a new approach analyzing the amplitude of spectral harmonics has been successfully applied to evaluate changes in crystal morphology using ultrasonic guided waves[26]. This advancement in ultrasonic methods relies upon small out-of-plane mechanical strain to correlate structural features of a material to resonant frequencies in the collected signal; the method did not permanently damage a part but not all shapes molded can be easily distorted and hence a better training method is needed to extract the information from these complex signals and correlate with quality properties. The challenge of any new spectroscopic techniques, however, is how to correlate the large quantity of spectral data with one or multiple quality properties currently of interest to the industry, and consequently their incorporation in the production line for improved process operations.

This study compares the effectiveness of a ultrasonic nondestructive spectroscopic technique to replace multiple traditional destructive and nondestructive tests needed to evaluate both sintering and degradation processes for rotational molded polyethylene samples. An important goal of the work was to better highlight the benefits of ultrasonic

spectroscopic techniques in polymer processing.

5.2 Methods

5.2.1 Material

For this study, a high density polyethylene (ExxonMobilTM HD 8660.29) powder of 35 Mesh size was provided by Imperial Oil Ltd. The resin has a melt index of 2 g/10 min (ASTM D1238, with a standard load of 2.16 kg) and stated crystal melting temperature of 129 ^{o}C, according to the vendor.

5.2.2 Rotational molding

Samples were prepared using a laboratory-scale uniaxial rotational molding device coupled with a data acquisition system for monitoring of the internal mold air temperature as well as controlling the oven temperature. A shot of 100 g was loaded to a Teflon-coated steel mold. The oven was pre-heated to the designated temperature and the batch run was started when the mold was moved inside. Each batch run followed a specific heating cycle time, and after a designated period of time the mold was removed from the oven to be cooled by forced air applied at approximately 2.5 m/s (measured by a digital anemometer). The time between start of the batch and the removal from the oven is considered the heating or oven time. The mold was cooled to 80 ^{o}C before removal of the sample. The final samples resembled a cube missing its front and back panels, with each molded wall panel being approximately 85 mm x 85 mm by 3 mm thick cut from the sample using a band saw. Each chosen heating cycle condition was used to prepare at least three replicate samples.

5.2.3 Surface analysis

A square area of 40 mm x 40 mm was isolated on the outer facing surface of a wall panel using adhesive tape. A low viscosity lubricant containing a mixture of micron-sized copper and graphite particles (Permatex) was brushed over the designated area, with the excess wiped away. By this procedure, surface holes were filled with the dark colored lubricant so they would be more clearly seen. Images were taken with a digital camera and processed with image analysis software to estimate the surface area coverage of voids per sample.

5.2.4 Fourier-transform infrared spectroscopy

Infrared vibrational spectroscopy (FT-IR) was performed with a Thermo Scientific Nicolet 6700 in attenuated total reflection (ATR) mode. Both internal and external surfaces of the panels were analyzed by FT-IR. Mid-range wavenumbers between 700 to 4000 cm^{-1} were scanned at a resolution of 0.4 cm^{-1} and an average of 32 scans was reported. After baseline correction, peaks were identified using a Voigt window search and normalized based on the reference peak at 2915 cm^{-1}.

5.2.5 Ultrasonic spectroscopy

Panel wall specimens were tested using an ultrasonic guided waves test apparatus, as previously reported[26]. The distance between ultrasonic transducers was kept at 55 mm. Each resultant spectrum per specimen was produced from the combined averaging of 31 different signals corresponding to a stepwise frequency sweep from 135 to 165 kHz, incremented by steps of 1 kHz. Three panels were tested per sample.

5.2.6 Impact test

After samples were tested using the non-destructive methods of FT-IR and ultrasonic, each wall panel was characterized for impact behavior using a dart impact test. Samples were grouped based on the processing conditions, thus totaling 12 tests per group. Test samples were pre-conditioned in a freezer at -40 ^{o}C for 24 h. For each group, an initial height was selected and moved using the staircase method based on the resultant failure or non-failure. A standard 6.804 kg dart was used with varying height steps of 0.1524 m (0.5 ft) based on minimum scale unit of the equipment used for this study. A resultant average failure height was converted to impact energy in Joules (J) and reported for each group. Standard deviation of mean energy value was calculated following ASTM D5420.

5.2.7 Rheology

Specimens from the molded samples were evaluated for their viscosity with a Discovery HR-2 TA Instruments configured to operate with 25 mm parallel plates. A small square was cut from the wall panel of a sample and melted in the plates at 190 oC. Polymer melt was compressed to a gap between plates of 1.5 mm, residual air bubbles were reduced and the excess polymer was removed. A frequency sweep spanning 0.1 to 200 s^{-1} was performed at a strain of 0.15. Zero-shear viscosity was estimated using the Cross model after transformation of the oscillatory data to steady shear considering Cox-Merz relationship. Additional information related to rheology tests and model used can be seen in Appendix A.

5.2.8 Multivariate statistical analysis

Spectral data collected from the ultrasonic tests was used to construct a statistical model to differentiate molded samples in relation to both sintering and degradation processes. Two projections to latent structures (PLS) models were built using measurements from traditional tests as training references. The statistical software R was used with the library 'pls'. Ultrasonic spectra matrix data was pre-processed with a baseline correction for the sintering model and additional normalization for the degradation model. The number of components chosen were based on the minimum root-mean square of prediction error (RMSEP) for an internal cross-validation using the leave-one-out method.

5.3 Results and Discussion

5.3.1 Process exploration

Two factors were considered for the experimental design: oven temperature, that influenced the heating rate; and heating time, considered to be the duration that the mold stayed inside the oven. It was expected that both would influence the profile of the mold temperature. Longer oven time and higher heating rates leading to a higher maximum temperature reached. A two level factorial with center point was designed, with lower and upper limits of 300 and 340 ^{o}C for the oven temperature, and 12 minutes and 18 minutes for heating time. A sixth point was added to further explore the upper limits of heating rate at the center point oven time of 15 minutes. Experiments were monitored using a thermocouple installed in the rotational arm that measured the internal mold air temperature. Resulting internal temperature profiles, shown in Figure 5.1, demonstrate the positive effect of the two factors towards

reaching the highest possible maximum temperature inside the mold. A common way of interpreting variations between rotational molding batches is to refer to the maximum temperature inside the mold as the peak internal air temperature (PIAT). Although this measurement does not reflect the complete history of the heating and cooling cycle, it can be used as a single variable descriptor for the effectiveness of sintering. Thus, for the next sections, experimental results will be referenced based on their values of PIAT.

From the results presented in Table 5.1 it was observed that operating at the lower factor levels, samples produced lower impact strength and higher surface voids in the molded parts, due to incomplete sintering. Conversely, for the higher factor levels, a significant increase in zero-shear viscosity was observed, indicating crosslinking due to thermo-oxidative degradation. Longer heating cycles at a low heating rate produced a slight improvement in impact strength compared to shorter heating cycles at higher heating rates, even though both approaches reached similar PIAT.

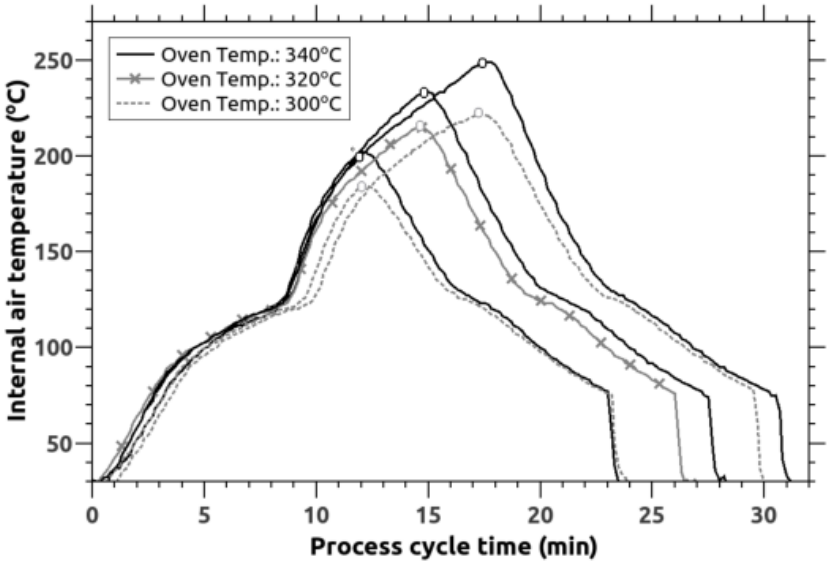

Figure 5.1: Rotational molding temperature profiles (marked dots indicate the removal of the mold from the oven and the end of the heating cycle)

Table 5.1: Results from experimental design

Process conditions			Product characterization		
Oven Temperature – ^oC	Heating time - min	Peak internal air temperature (PIAT) – ^oC	Impact Energy – J	Surface voids area coverage – %	Zero-shear viscosity – Pa.s
300(−1)	12(−1)	181 ± 5	0.31 ± 0.18	6.6 ± 1.1	6403 ± 212
340(+1)	12(−1)	200 ± 2	0.37 ± 0.13	4.5 ± 0.9	6496 ± 44
300(−1)	18(+1)	218 ± 5	0.50 ± 0.16	1.8 ± 0.8	7242 ± 741
340(+1)	18(+1)	250 ± 3	0.65 ± 0.16	0.4 ± 0.2	12689 ± 714
320(0)	15(0)	215 ± 6	0.43 ± 0.18	3.6 ± 1.9	6868 ± 893
340(+1)	15(0)	238 ± 4	0.65 ± 0.16	0.6 ± 0.2	12033 ± 84

5.3.2 Sintering

Based on changes in the temperature profiles shown in Figure 5.1, the powder cohesion and melting phase took between 8 minutes to 10 minutes. After this point, the additional heat energy was directed to the densification or melt coalescence process by removal of the air bubbles formed during initial melting. Observations from the surface of the samples provided a direct estimation of the residual concentration of bubbles at the end of a batch trial. Figure 5.2 presents a comparison of images and calculated coverage area of surface voids (i.e. pitting) from the samples with different PIAT and a control sample (compression molded for 10 minutes at 175 ^{o}C and 2 kPa, then quenched using water-cooled plates); surface coverage area is being considered as a two dimensional representation of the void content or porosity of the overall sample in this work. Results from control group can be interpreted as baseline for testing methods, however, their values cannot be practically achieved from the rotational molding method due to the different nature of the process without variation in pressure. A high PIAT produces molded parts with lower value of residual bubbles. A maximum of 5 % to 7 % was observed for the surface coverage area with low PIAT whereas

near-negligible values below 1 % (still higher than the control) were reported for samples with PIAT above 230 ^{o} C. From Figure 5.2c is possible to visually observe large residual bubbles at the end of the sintering process, those will take a longer time to disappear even at high mold temperatures, as the removal rate of bubbles will be proportional to the porosity of the part (which is related to bubble size and the number of bubbles present) [24].

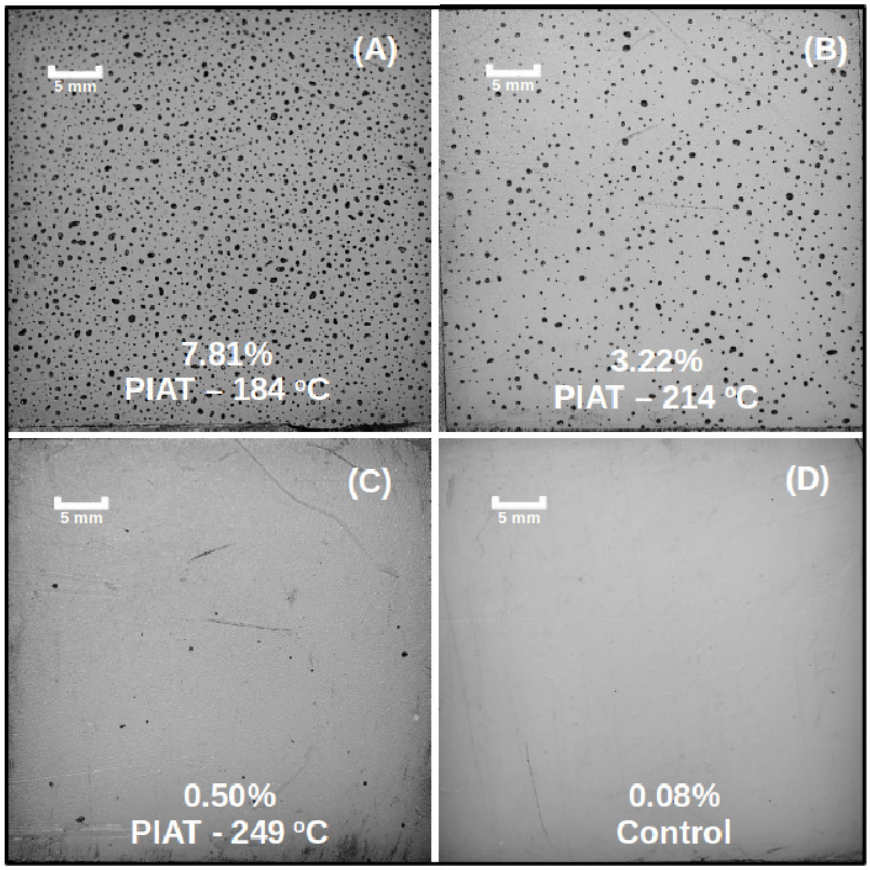

Figure 5.2: Rotational molding temperature profiles (marked dots indicate the removal of the mold from the oven and the end of the heating cycle)

The extent of bubble removal is inversly related to impact properties. As shown in Figure 5.3, samples with higher coverage area of surface voids showed a lower value of impact energy. Those samples at the low end of the range of impact properties often demonstrated a brittle failure during testing with easy crack propagation found

between voids. A progressive increase in impact strength was observed with reducing porosity, which correspondingly denoted a transition between brittle to ductile failure with increased fibrillation observed at the point of impact. No significant increase in impact energy was observed for samples above 230 ^{o}C, which corresponded to the lower observed range for the surface voids coverage area. The maximum impact values observed were lower than obtained by the control samples, prepared by compression molding.

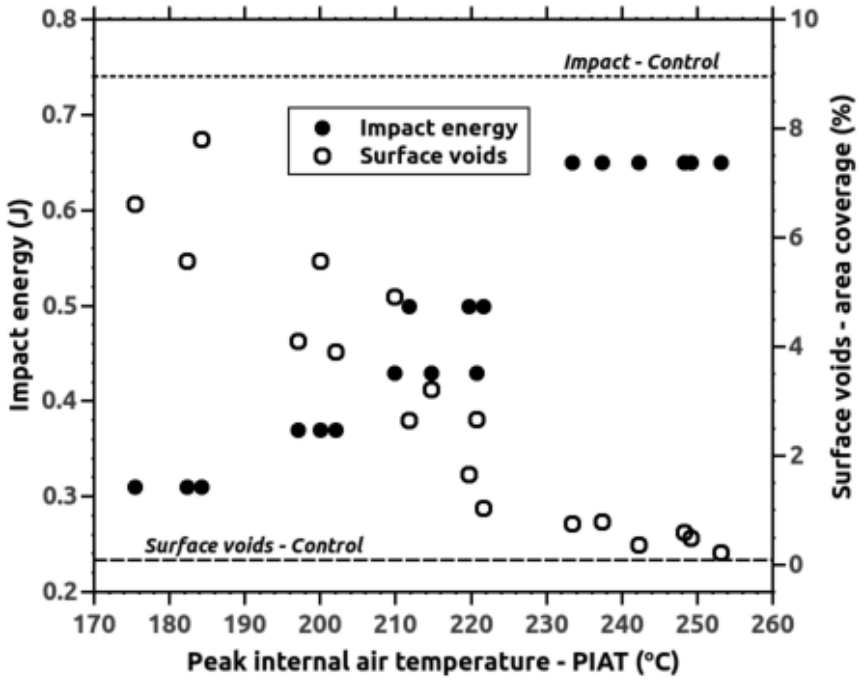

Figure 5.3: Surface voids area coverage and impact energy for rotational molded samples with different peak internal air temperatures (horizontal dashed lines indicate reference values for the control samples)

The multiple methods of analysis mentioned above are standards for the industry to provide a good estimation for the degree of sintering, but do not reflect the overall concentration of voids internally and at least in the case of the surface analysis, might not be practical for all mold profiles or different types of product finishes. An alternative

yet still traditional nondestructive test method for porosity is to use ultrasonics to infer density based on the propagation of sound waves through the part; while this approach is not what is ultimately to be disclosed in this paper regarding the perceived strength of ultrasonic analysis, it provides a context to build towards that discussion. Using the same propagation distance for samples of similar dimensions, variations in the maximum signal amplitude of a propagating sound waves (on a time domain) may be connected with the attenuation caused by the presence of bubbles in the part. Figure 5.4 shows the increased ultrasound amplitude found with increasing PIAT, thus presenting a good correlation with the impact energy of this group of samples. Samples with PIAT above 230 ^{o}C showed amplitude values comparable to the control sample. A lower limit for the application of this method is the detection of signals for samples with high value of attenuation.

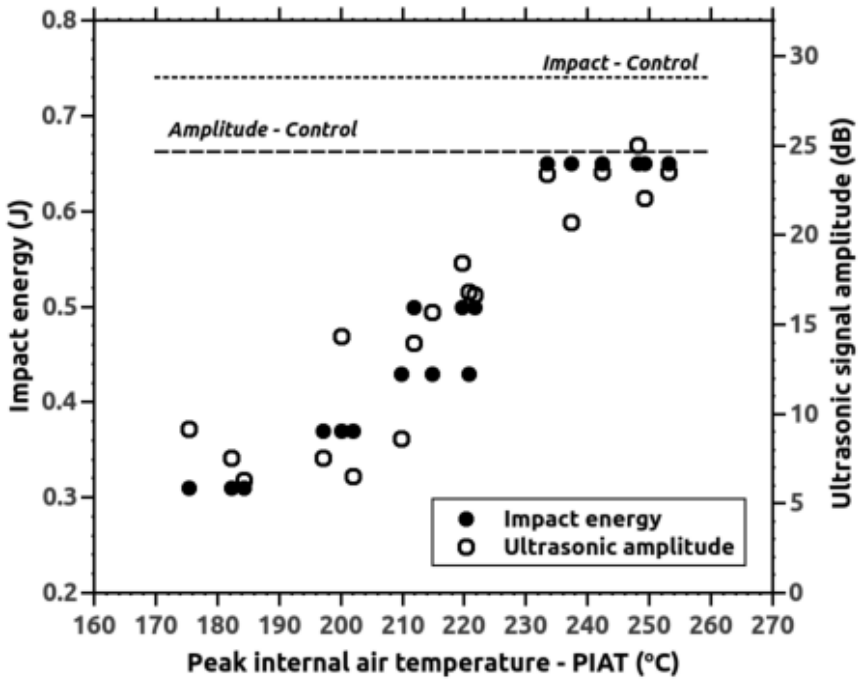

Figure 5.4: Ultrasonic signal amplitude and impact energy for rotational molded samples with different peak internal air temperatures (horizontal dashed lines indicate reference values for the control samples)

5.3.3 Degradation

Effects of degradation were investigated using FT-IR spectroscopy to monitor for oxidation products at the surface of the molded samples. Both surfaces of panel cut from a sample were tested ; however, only the internal surfaces showed any development of carbonyl compounds which were detected at 1715 cm-1; thermo-oxidative degradation is expected to be predominantly on inner surfaces of a part due to their continuous exposure to trapped air at high temperatures during rotational molding, while outer layers are effectively shielded by their contact with the mold surface that prevents direct contact with hot air and reduces the consumption rate of antioxidants[7]. Figure 5.5 gives FT-IR spectra showing the appearance of the oxidation product for inner

surfaces of samples with PIAT above 230 ^{o}C. For samples molded with PIAT lower than this threshold it can be expected that antioxidants were not depleted.

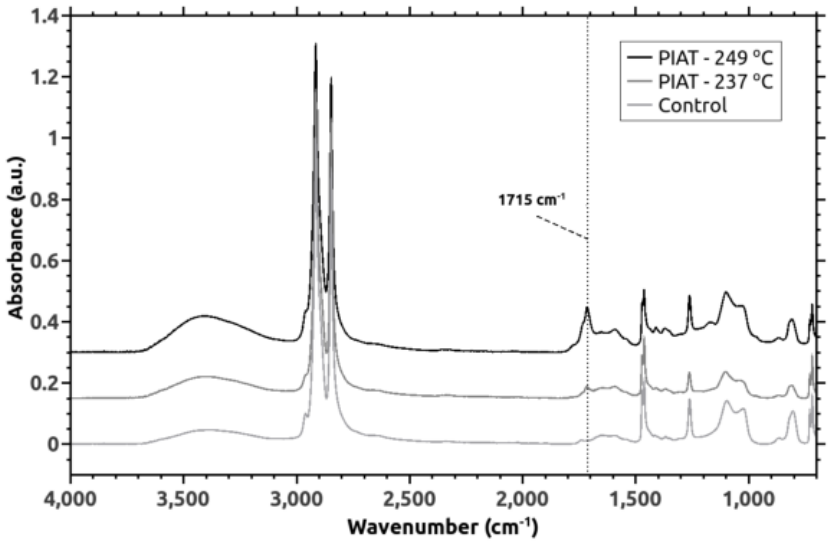

Figure 5.5: FT-IR spectra from the internal surface of samples with different PIAT highlighting the appearance of subproducts of thermo-oxidative degradation (vertical dashed line indicates the wavenumber of the carbonyl peak)

Alternatively, rheology can be used as an indirect method to evaluate degradation. During thermo-oxidative degradation, free radicals are formed increasing the chances of chain cross-linking for polyethylene. This will have a significant effect on the molecular weight distribution, thus affecting the viscosity[16]. A marked increase in degradation is seen by the significant rise in zero-shear viscosity for samples with PIAT higher than 220 ^{o}C, observable in Figure 5.6. Comparing the trends between the rheological and infrared analysis, the viscosity measurements seemed to provide better sensitivity to degradative changes, because of their bulk nature of assessment rather than being limited to only the top several microns of polymer species near the surface of the panel by FT-IR. Although, other references have mentioned an effect of crosslinking on impact strength, which could be initially beneficial but ultimately reduce the quality

at very high PIAT values (above 250 ^{o}C)[11], none of the mechanical detrimental effects were observed for the process conditions investigated in this study.

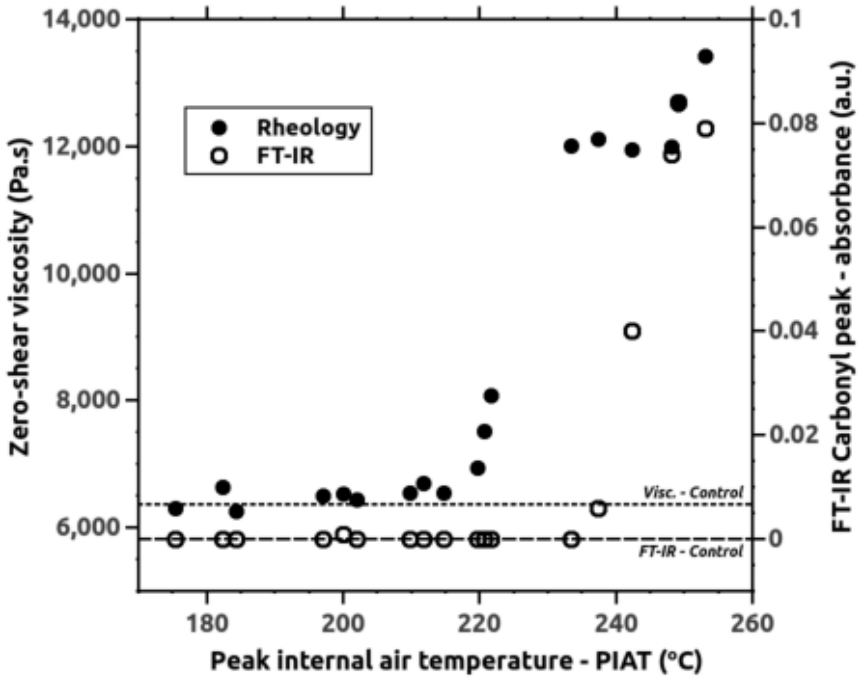

Figure 5.6: Zero-shear viscosity and absorbance level of carbonyl peak from FT-IR for samples with different PIAT (horizontal dashed lines indicate reference values for control sample)

5.3.4 Ultrasonic spectrum with multivariate statistical analysis

Results from the methods previously described in this study presented good but limited response to either sintering or degradation quality related features. With the objective to evaluate the quality of samples related to both phenomena simultaneously, a new approach was tested using spectroscopic analysis of the ultrasonic wave propagation. Figures 5.7 and 5.8 show examples of ultrasonic spectra from parts with increasing PIAT. For the first case, looking at samples selected for showing little or no level

of degradation, an increase was observed in Figure 5.7 for the peak corresponding to the frequency range of the excitation signal (between 135 and 165 kHz) reflecting a decrease in attenuation of the propagated wave due to fewer voids for a higher PIAT. This behavior is similar to what was found from the time domain analysis, as demonstrated in Figure 5.4, but now identified as being localized to specific resonant frequencies. In Figure 5.8, a second group of samples was selected with similar extent of sintering but differing degrees of thermo-oxidative degradation. The resultant spectra were normalized before plotting and show an increase in the third harmonic range (frequencies from 405 to 495 kHz) related to the excitation frequencies with increasing PIAT. This variation in the ratio between the peak amplitude of higher harmonics was highlighted in a previous publication being a as descriptor of morphological changes within semi-crystalline structures after applied plastic deformation or solvent absorption[26]. Although, so far, results presented in this section have demonstrated that features of the ultrasonic spectrum can be correlated with sintering and degradation phenomena, interpretation of this spectroscopic data for different molded parts is not trivial and cannot be compared to the descriptors used in previous study that observed the progression of modifications for the same sample. In order to make definitive correlations based on the variance contained in the ultrasonic spectral dataset of several molded parts with traditional characterization methods, an inferential model using latent variables statistical methods was developed.

Two PLS models were constructed using the full spectral dataset from the ultrasonic measurements of the molded samples. Table 5.2 presents a summary of conditions used as some general descriptors to develop these models. Data from the coverage area of surface voids was used as reference information for calibrating the sintering model, while results from zero-shear viscosity were applied for the degradation estimation. An internal cross-validation, based on the leave-one-out method, estimated a root-mean

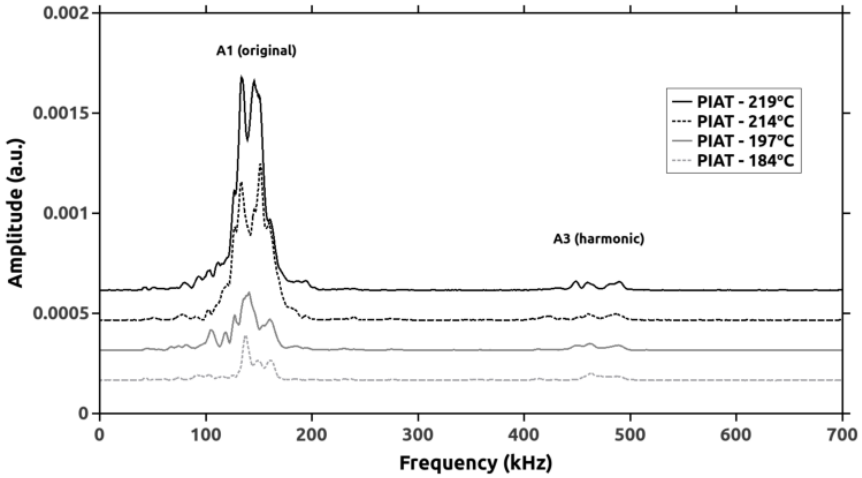

Figure 5.7: Ultrasonic spectra for samples with different PIAT presenting different levels of sintering (A1 indicates the peaks at original excited frequencies and A3 indicates the peaks at third harmonic range)

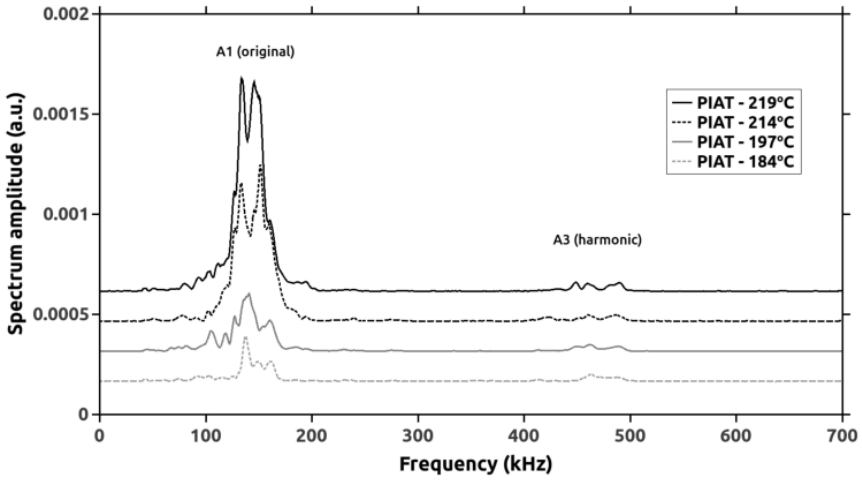

Figure 5.8: Ultrasonic spectra for samples with different PIAT presenting different levels of degradation (A1 indicates the peaks at original excited frequencies and A3 indicates the peaks at third harmonic range)

squared error of prediction (RMSEP) for several number of components. The ultimate number of four components was chosen to fit the model based on the case with lower value of error, 1.37 % for the sintering model and 2524 Pa.s for the degradation model. A higher number of components could have been selected to increase the variability

Table 5.2: Summary of PLS models

Number of experimental samples for training		15
Number of ultrasonic spectra per sample		3
Points per spectra (frequencies)		2500
Total number of points for data matrix		112500
Model	Sintering	Degradation
Variable used for training	Surface voids area coverage	Zero-shear viscosity
PLS - Number of components	4	4
Internal cross-validation error- RMSEP	1.37 %	2524 Pa.s
Variance explained of the training variable	80.9 %	73.0 %
Variance explained of the data matrix	83.5 %	58.6 %

explained, however the selection based on the RMSEP value helped to avoid over fitting and still was able to explain the correlation between the matrices introduced for calibration. Additional information on the design of the model can be found in Appendix B. The value of RMSEP showed in Table 2 demonstrates the error for the model to predict an internal value. Moderate values of explained variance were observed for both models, which shows how much of the variance from the original data was used in the correlation between the training variable and the calibration matrix.

Figures 5.9 and 5.10 present the model predictions superimposed with the observed values. Errors in prediction were higher for the sintering model at high concentration of voids (values of coverage area of surface voids higher than 5 %), mostly due to limitations imposed on the method by the high attenuation of the propagated signal. A classification of the inferred properties was proposed by comparing the estimated value with two control groups, formed by samples selected from the training group that had complete sintering (coverage area of surface voids <1.0 %) and no degradation

(zero-shear viscosity <7000 Pa.s), with six and nine samples per group, respectively. The model predictions were statistically compared with the reference groups and if the value exceeded a 98 % confidence interval threshold, they would be classified as incomplete sintering or degraded samples. This classification criteria represents the capacity of the model constructed with the ultrasonic spectroscopic data to distinguish a sample with unsatisfactory properties. Results of this classification are shown in Figures 9 and 10 highlighted as solid or hollow circles, and a group separation is observed around a PIAT of 220 oC, marking the point of end of the sintering process and acceleration of degradation process.

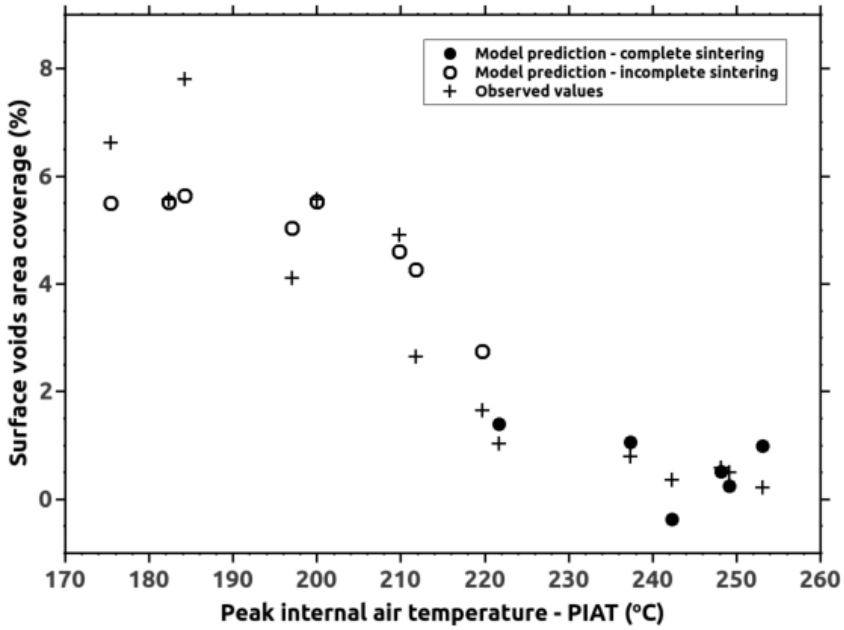

Figure 5.9: Prediction results for surface voids area coverage of samples with different PIAT using a PLS model (classification of incomplete sintering based on statistical comparison with reference group, for a p-value<0.02)

Analysis of the PLS model parameters can help to explain the success of its predictions and to understand elements of the multivariate spectrum ultrasonic signal[27,28]. Higher values of model loadings were attributed to two groups of frequencies located

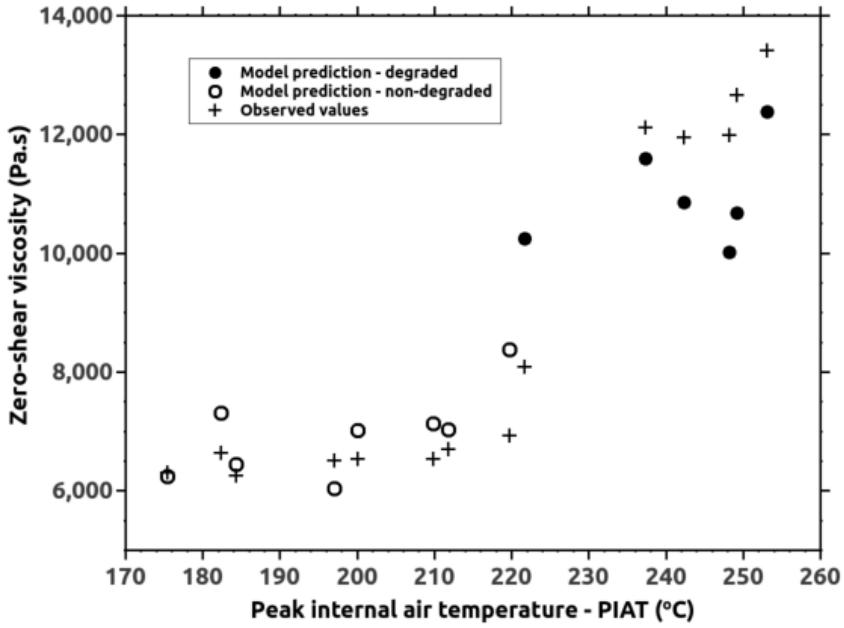

Figure 5.10: Prediction results for zero-shear viscosity of samples with different PIAT using a PLS model (classification of degraded based on statistical comparison with reference group, for a p-value<0.02)

close to the primary signal (between 135 and 165 kHz) and the third harmonic (between 430 and 480 kHz). An interesting aspect for the viscosity PLS model is an inverse relationship between harmonic areas for components 3 and 4, in agreement with the previous observation of the importance of the amplitude ratio to prediction of degradation.

A group of four samples was randomly chosen from the original batch runs and was not introduced in the model during its training to serve as a validation group. Table 5.3 shows both the prediction values and the classification of these samples for sintering and degradation. These results support our assertion that the model is capable of predicting major changes for both phenomena correctly, recognizing for increasing PIAT values that the prediction should be for coverage area of surface voids to decrease while zero-shear viscosity increases accordingly.

Table 5.3: Comparison of PLS model prediction using ultrasonic spectra data for validation group

Sample	Sintering – surface voids area coverage				Degradation – zero-shear viscosity			
PIAT (^oC)	Predicted value (%)	Observed value (%)	p-value	Incomplete sintering? (p<0.02)	Predicted value (Pa.s)	Observed value (Pa.s)	p-value	Degraded? (p<0.02)
201	5.4	3.9	$< 10^{-3}$	Yes	6843	6447	0.36	No
214	2.6	3.2	0.006	Yes	8228	6541	0.001	Yes
220	3.1	2.6	0.006	Yes	10011	7622	0.0008	Yes
233	1.1	0.8	0.69	No	11187	12019	0.0001	Yes

5.4 Conclusions

A new nondestructive evaluation method was demonstrated to simultaneously evaluate both sintering and degradation phenomena in polyethylene rotational molded samples. Spectral amplitude at excitation frequencies can be used to evaluate the degree of sintering, with increase amplitude showing a reduction in attenuation caused by void concentration. This is a standard density evaluation. However, at the same time the amplitude of higher harmonics in the ultrasonic spectrum increased with increasing degradation. When compared to more traditional degradation characterization methods, the harmonic amplitude showed good correlation with the rheological data and higher sensitivity than FT-IR. A key point in favor of this new method for monitoring degradation is that greater damage has been shown to occur to the internal surfaces of the rotomolded parts, which are not accessible to nondestructive testing using FT-IR. PLS models showed their potential to estimate the values from the traditional methods and classify samples based on sintering and degradation properties, decoupling this spectroscopic approach from its earlier reliance on mechanical deformation to train the method to identify structural changes. Overall, this study demonstrates a new characterization method for rotational molded parts that not only can provide an

alternative to current destructive techniques but also combines the observation of two distinctive phenomena in one single technique. The development of this method can represent a valuable additional tool for the polymer processing industry to tackle the challenge towards advanced manufacturing, improving on process reliability and flexibility.

Acknowledgements

The authors would like to acknowledge the importance for this study of Ron Cooke for the resin supply and Conselho Nacional de Desenvolvimento Científico e Tecnológico (CNPq)/Brazil for the financial support with the Science Without Borders Scholarship.

Bibliography

[1] Behzad Esmaeilian, Sara Behdad, and Ben Wang. The evolution and future of manufacturing: A review. *Journal of Manufacturing Systems*, 39:79–100, apr 2016.

[2] D. I. Abu-Al-Nadi, D. I. Abu-Fara, I. Rawabdeh, and R. J. Crawford. Control of rotational molding using adaptive fuzzy systems. *Advances in Polymer Technology*, 24(4):266–277, 2005.

[3] Wen-Chin Chen, Pei-Hao Tai, Min-Wen Wang, Wei-Jaw Deng, and Chen-Tai Chen. A neural network-based approach for dynamic quality prediction in a plastic injection molding process. *Expert Systems with Applications*, 35(3):843–849, oct 2008.

[4] Zhijun Jiang, Yi Yang, Shengyong Mo, Ke Yao, and Furong Gao. Polymer Extrusion: From Control System Design to Product Quality. *Industrial & Engineering Chemistry Research*, 51(45):14759–14770, nov 2012.

[5] K. Mitra. Genetic algorithms in polymeric material production, design, processing and other applications: a review. *International Materials Reviews*, 53(5):275–297, sep 2008.

[6] Ian Gibson and Dongping Shi. Material properties and fabrication parameters in selective laser sintering process. *Rapid Prototyping Journal*, 3(4):129–136, dec 1997.

[7] M. J. Oliveira, M. C. Cramez, and R. J. Crawford. Structure-properties relationships in rotationally moulded polyethylene. *Journal of Materials Science*, 31(9):2227–2240, 1996.

[8] M. Kontopoulou and J. Vlachopoulos. Bubble dissolution in molten polymers and its role in rotational molding. *Polymer Engineering & Science*, 39(7):1189–1198, jul 1999.

[9] A. G. Spence and R. J. Crawford. The effect of processing variables on the formation and removal of bubbles in rotationally molded products. *Polymer Engineering & Science*, 36(7):993–1009, apr 1996.

[10] E Epacher. Processing stability of high density polyethylene: effect of adsorbed and dissolved oxygen. *Polymer*, 41(23):8401–8408, nov 2000.

[11] M.C Cramez, M.J Oliveira, and R.J Crawford. Optimisation of rotational moulding of polyethylene by predicting antioxidant consumption. *Polymer Degradation and Stability*, 75(2):321–327, jan 2002.

[12] Bharat Indu Chaudhary, Elizabeth Takács, and John Vlachopoulos. Processing enhancers for rotational molding of polyethylene. *Polymer Engineering & Science*, 41(10):1731–1742, oct 2001.

[13] Andreia C. Tavares, Joseane V. Gulmine, Carlos M. Lepienski, and Leni Akcelrud. The effect of accelerated aging on the surface mechanical properties of polyethylene. *Polymer Degradation and Stability*, 81(2):367–373, jan 2003.

[14] Abu Saifullah, Ben Thomas, Robert Cripps, Kamran Tabeshfar, Lei Wang, and Christopher Muryn. Fracture toughness of rotationally molded polyethylene and polypropylene. *Polymer Engineering & Science*, 58(1):63–73, jan 2018.

[15] A.A. Mendes, A.M. Cunha, and C.A. Bernardo. Study of the degradation mechanisms of polyethylene during reprocessing. *Polymer Degradation and Stability*, 96(6):1125–1133, jun 2011.

[16] A.A. Cuadri and J.E. Martín-Alfonso. The effect of thermal and thermo-oxidative degradation conditions on rheological, chemical and thermal properties of HDPE. *Polymer Degradation and Stability*, 141:11–18, jul 2017.

[17] J. V. Gulmine, P. R. Janissek, H. M. Heise, and L. Akcelrud. Degradation profile of polyethylene after artificial accelerated weathering. *Polymer Degradation and Stability*, 79(3):385–397, 2003.

[18] Maria Clara Cramez, Maria Jovita Oliveira, Stoyko Fakirov, Robert James Crawford, Anton Atanassov Apostolov, and Marina Krumova. Rotationally molded polyethylene: Structural characterization by x-ray and microhardness measurements. *Advances in Polymer Technology*, 20(2):116–124, 2001.

[19] Yusuke Hiejima, Takumitsu Kida, Kento Takeda, Toshio Igarashi, and Koh-hei Nitta. Microscopic structural changes during photodegradation of low-density polyethylene detected by Raman spectroscopy. *Polymer Degradation and Stability*, 150:67–72, apr 2018.

[20] Don E Bray, John Vela, and Raed S Al-Zubi. Stress and Temperature Effects on Ultrasonic Properties in Cross-Linked and High Density Polyethylene. *Journal of Pressure Vessel Technology*, 127(3):220, 2005.

[21] Dawei Jia, G. Bourse, S. Chaki, M. F. Lacrampe, C. Robin, and H. Demouveau. Investigation of Stress and Temperature Effect on the Longitudinal Ultrasonic Waves in Polymers. *Research in Nondestructive Evaluation*, 25(1):20–29, jan 2014.

[22] Keiichiro Adachi, Gilroy Harrison, John Lamb, Alastair M. North, and Richard A. Pethrick. High frequency ultrasonic studies of polyethylene. *Polymer*, 22(8): 1032–1039, 1981.

[23] Akira Tanaka, K Nitta, and S Onogi. Ultrasonic velocity and attenuation of polymeric solids under oscillatory deformation: Apparatus and preliminary results. *Polymer Engineering and Science*, 29(16):1124–1130, aug 1989.

[24] Abdelhadi Sahnoune, Jacques Tatibouet, Richard Gendron, André Hamel, and Luc Piché. Application of Ultrasonic Sensors in the Study of Physical Foaming Agents for Foam Extrusion. *Journal of Cellular Plastics*, 37(5):429–454, sep 2001.

[25] F.P.C. Gomes, W.T.J. West, and M.R. Thompson. Effects of annealing and swelling to initial plastic deformation of polyethylene probed by nonlinear ultrasonic guided waves. *Polymer*, 131:160–168, nov 2017.

[26] F.P.C. Gomes and M.R. Thompson. Analysis of Mullins effect in polyethylene using ultrasonic guided waves. *Polymer Testing*, 60:351–356, jul 2017.

[27] Dieter Fischer, Jan Müller, Sven Kummer, and Bernd Kretzschmar. Real Time Monitoring of Morphologic and Mechanical Properties of Polymer Nanocomposites

During Extrusion by near Infrared and Ultrasonic Spectroscopy. *Macromolecular Symposia*, 305(1):10–17, jul 2011.

[28] Edward V. Thomas. A primer on multivariate calibration. *Analytical Chemistry*, 66(15):795A–804A, aug 1994.

Chapter 6

Data-driven smart manufacturing for batch polymer processing using a multivariate nondestructive evaluation

Data-driven smart manufacturing for batch polymer processing using a multivariate nondestructive monitoring

Authors: F.P.C.Gomes[1], A. Garg[2], P. Mhaskar[2], M.R. Thompson[1]

[1]Centre for Advanced Polymer Processing and Design (CAPPA-D) [2]McMaster Advanced Control Consortium (MACC)

Department of Chemical Engineering, McMaster University, Canada

Manuscript submitted to Industrial and Engineering Chemistry Research journal

Authors contribution: The first author, F.P.C. Gomes, was responsible for experimental design and execution of the experiments; data processing and analysis of the ultrasonic data for the in-line monitoring and correlation of the ultrasic data and process dynamics for the on-line monitoring; and writing the manuscript. The second author, A. Garg, contributed with the model calibration and analysis of the dynamic process model and with revision of the manuscript. The authors P. Mhaskar and M.R.Thompson contributed with supervision in all stages of experimental tests and data analyis; and with the revision of the written document.

Main scientific contributions of the paper:

- Validation of the information contained on the nonlinear ultrasonics for quality classification of rotational molded polyethylene parts.
- Proposed in-line monitoring approach for quality control based on nondestructive test data from historical batches.
- Presentation of a novel approach for on-line projection of final quality part based on the correlation of a dynamic process model and ultrasonic spectrum in a reduced space.

ABSTRACT

Incorporation of advanced manufacturing practices into polymer processing depends on efficient strategies that can use new sensor technologies to improve quality monitoring and process understanding. Nonlinear ultrasonics have been proposed a multivariate nondestructive method for the characterization of produced plastic parts to observe changes in polymer's mesostructure. To enable efficient use of this technique, two approaches are proposed that analyze and integrate ultrasonic spectroscopic data for in-line quality classification and on-line monitoring and prediction. Data processing with principal component analysis (PCA) and a soft class analogy classification method are used for cluster identification of products with differing quality based on information contained in the multivariate ultrasonic signal. A state-space dynamic model using subspace identification is applied to historical process data and correlated with the ultrasonic-based quality data for on-line quality prediction. Results were validated with experimental data from the sintering phase of a polyethylene uniaxial rotational molding process.

Keywords: Advanced manufacturing, Quality monitoring, Nonlinear ultrasonics, Batch dynamic modeling.

6.1 Introduction

Manufacturing has progressively changed from a manual to machine-dependent environment over the last century. Based on recent trends, the next decades will be focused on wide utilization of advanced manufacturing concepts, such as big data, cyber-physical systems and cloud computing[1]. Although these cyber resources are gradually becoming known and adopted for use, broad application of these techniques is still years away from being realized.

In polymer manufacturing, which is the focus of the present application, much

emphasis has been on additive manufacturing[2], with too little discussion yet on intelligent, data-driven smart manufacturing strategies for traditional processes. The concept of data-driven smart manufacturing refers to the collection and use of larger amounts of process and quality data to make decisions based on a more intimate understanding of the process[3]. The concept of smart manufacturing is becoming increasingly relevant due to the increase in the amount of digital data being recorded and stored, which in turn arises from the adoption of new sensors to monitor processes and characterize produced parts, moving beyond traditional univariate descriptors, such as temperature, pressure and flow. Spectral sensors, for example, generate multivariate datasets that can provide multiple quality parameters for individual produced parts. On the molecular-level, structural modification has been demonstrated with the use of spectroscopic techniques, such as Raman spectroscopy to monitor changes in morphological amorphous and crystalline structures[4]; fast-Fourier transform infrared (FTIR) spectroscopy was used for observing chemical modification[5]; and, nuclear magnetic resonance (NMR) can be used to to differentiate molecular level chain dynamics[6].

When considering bulk nondestructive characterization methods, a study[7] recently demonstrated the use of multivariate nonlinear ultrasonics to identify differences in the structural morphology of polyethylene (PE). Linear ultrasonic characterization based on sound velocity and attenuation through the media has been traditionally applied[8–10]; however, this approach is limited by the viscoelastic nature of industrial polymers, like PE, creating a high signal attenuation that is dependent on frequency[11]. Although the adoption of new testing methods focused on multivariate analysis is suggested, a high level of expertise and high cost are the technological and economic barriers that have prevented implementation of these sensors for in-line manufacturing quality monitoring; in-line monitoring refers to the quality assessment after the product

has been produced.

Addressing the technological barrier, intelligent systems[12] have been proposed as an alternative. These decision tools are sought that can incorporate new groups of data, and improve their assessment and prediction performance of current quality control systems. Development of these techniques has been largely investigated in areas such as chemometrics[13] and image processing[14]. Orthogonal projections techniques, such as principal component analysis (PCA), have been a foundation for several multivariate data analysis tools. It can be used to simplify and quickly understand complex databases with an algorithm that is simple to implement and easy to compute[15]. PCA has been widely used for analysis of in-line spectroscopic sensors to monitor chemical changes[16] and to detect tracer elements[17] in continuous compounding. In the area of polymer processing, infra-red and Raman spectroscopy sensors and univariate ultrasonic in-line measurements were applied to monitoring an extrusion process[18]. A hyperspectral imaging sensor was also applied to continuous extrusion and correlated with the final quality using multivariate statistical analysis[19]. Another studied process is the injection molding, where temperature and pressure sensors were used to monitor the process dynamics and predict and control final quality[20,21]. A new multivariate sensor technology was also introduced to improve monitoring ability[22]. Although these relevant studies have demonstrated the potential use of some nondestructive sensors, the application of multivariate spectral analysis of ultrasonic sensors for in-line polymer quality classification and further on-line (during the manufacturing of the product) monitoring for batch manufacturing process correlated with the final product quality measurement has not been explored.

Motivated by the above considerations, this study proposes an analytical and statistical framework that can efficiently use multivariate ultrasonic spectroscopic data (nonlinear ultrasonics) combined with process modeling to provide an in-line monitoring

tool for nondestructive assessment of produced parts and an on-line process modeling tool to improve understanding of the process variables and allow final quality prediction. The proposed methods were applied to a batch rotational molding manufacturing system to evaluate the ability of the monitoring tool to classify different product qualities related to structural properties captured by the ultrasonic multivariate signals and demonstrates the ability to predict final quality on-line. The manuscript is organized as follows: Section 2 shows the experimental methods used for practical application and validation of the technique. Section 3 describes the statistical approaches used for multivariate data processing and process modeling. Section 4 demonstrates the application of the monitoring tools, with historical batch data being used to build the models and demonstration of the prediction capability. Section 5 presents the concluding remarks.

6.2 Process Description and Quality Measurements

In this section, we describe the specific polymer manufacturing process and the destructive and nondestructive techniques utilized for characterization of the manufactured part quality.

6.2.1 Batch Manufacturing Process

A laboratory-scaled uniaxial rotational molding system was operated to prepare cubic samples using a high density polyethylene powder (Exxon MobilTM HD 8660.29, supplied by Imperial Oil Ltd.). Rotation speed was kept constant at 4 RPM. Two heated panels and a compressed air supply were manipulated variables, used to control

the heaters to a constant temperature using PI controllers. Temperature data for the heated panels and internal mold air was measured using K-type thermocouples and collected using a custom-written data acquisition system in Labview (National Instruments). After the powder was charged into the 90 mm cubic mold, each sample was subjected first to a heating cycle to a selected maximum temperature. In the subsequent cooling cycle, external forced air was applied to the mold to solidify the part, while all manipulated variables were turned off.

It is well understood that the final product quality is largely influenced by the temperature trajectory of the mold[23] The mold undergoes the following four phases over the course of the processing (see Figure 6.1 for a representative profile of the internal mold temperature)- the first is the adhesion phase, where the powder heats up and adheres to the surface, followed by the melting phase, and then the sintering phase. At the point where the heating is turned off, the mold first begins to cool down and then the molded part solidifies. Of the constituent phases, the sintering phase is the most critical component that dictates product quality[24]. Depending on the duration and temperature trajectory during the sintering phase, one can achieve a product with incomplete sintering (residual internal air bubbles present), or it could be degraded, with extensive thermo-oxidative degradation due to long exposure to heat; and, if the temperature trajectory is just right, meeting target quality, optimal mechanical properties and no significant degradation are observed. The determination of the temperature trajectory, and a quantitative understanding of how it influences the final product quality, remains an incredibly challenging problem. Traditionally, a univariate selection of batch time or maximum internal air temperature is used as decision for the end of the heating cycle. The changes in process operation (i.e. raw material variability) can be very frequent, requiring several adjustments in process variables to achieve desired quality. Monitoring approaches, that enable inexpensive

and quick quantification of the product quality in-line or on-line, are therefore highly valuable.

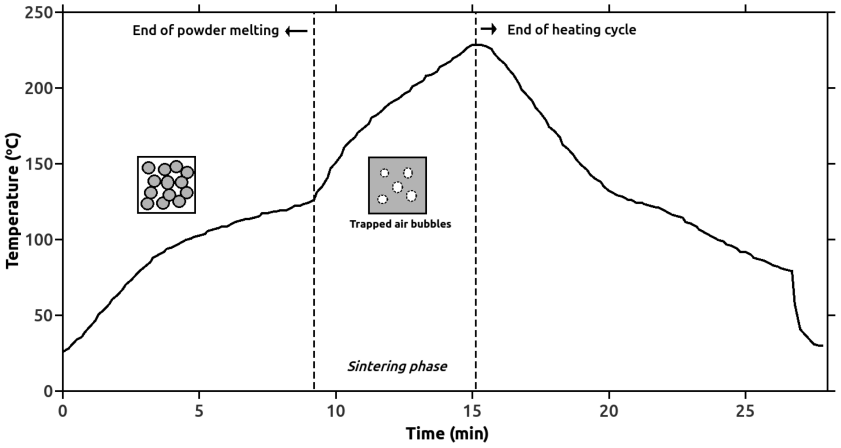

Figure 6.1: Rotational molding batch internal air mold temperature profile

6.2.2 Destructive characterization

In order to validate the quality of each sample, two traditional destructive tests were performed to evaluate the mechanical properties of produced parts. The extent of melt consolidation from sintering (i.e. removal of trapped air bubbles during the process) was evaluated using a standard falling weight dart impact test (ASTM D5420). The impact data was used for classification purposes in this study where a sample was considered fully sintered if its impact value was above 0.41 Joules (J); this threshold was determined as 80% of the maximum impact energy measured from historical batches available (0.51 J). To evaluate the thermo-oxidative degradation occurring for the polyethylene due to prolonged exposure to high temperatures, an oscillatory rheology test was performed on a square cut, 30 mm, from the wall edge of a part in a DHR 2 parallel plate rheometer (TA Instruments). Complex viscosity estimation was obtained with a frequency sweep from 0.1-100 rad/s at a temperature of 190 ^{o}C. Data

was converted using Cox-Merz transformation and approximate using the Cross model to estimate the value of zero-shear viscosity. Samples were classified as degraded if the zero-shear viscosity was above 8160 Pa.s, or 20% higher than the material before processing (approximately 6800 Pa.s).

The current industrial practice of the described characterization methods is limited to a small set of samples from a series of produced parts. Information obtained from a sampled group might not portray the real quality of all batch runs. Total cost of the quality assessment procedure is increased by the use of specific equipment and specialized procedures for different quality tests that need to be executed separately (sintering and degradation). This motivates the use of alternative, less expensive, quick and non-destructive test methods.

6.2.3 Ultrasonic characterization

Nonlinear ultrasonics was shown in a recent work[24] as an effective tool that can be correlated with traditional quality tests to evaluate both sintering and degradation aspects of a rotational molded polyethylene part. The ultrasonic measurements were carried out as follows: after the sample was removed from the mold and cooled to room temperature, two ultrasonic transducers (F30a - broadband and R15 - resonant at 150 kHz, Physical Acoustics Corp.) were positioned on one of the external surfaces at a distance of 35 mm apart (using a high vacuum grease, Dow Corning) to perform the nondestructive characterization. 10 cycles-burst of pulses with controlled frequencies from 135 to 165 kHz, in 1 kHz ascending frequency steps, were introduced to an uncut molded sample by the R15 resonant transducer acting as an emitter and captured by the F30a broadband transducer acting as a receiver. The signal was sampled at an acquisition rate of 4 MHz (using a National Instruments data acquisition board). The

spectrum used in the analyses was from all 31 captured signals for the same sample after Fourier transformation.

6.3 Data-driven classification and modeling approaches

We address the monitoring problem for the general scenario where a nondestructive multivariate sensor is available at the end of a batch process for product characterization, with specific application to the rotomolding process. To this end, two approaches are proposed, one for in-line quality classification and the second for on-line quality prediction and process visualization. The first approach focuses on the ultrasonic data evaluated from a produced part at the end of every batch run for an in-line classification. Strategies described in Section 6.3.1 and 6.3.2 demonstrate a data processing methodology to reduce the complexity of the signal and how to improve classification between qualitative classes. This nondestructive classification tool can be applied to situations where traditional characterization tests are ideally minimized since there is too much in every part to justify its sacrifice. The second approach combines process modeling and non-parametric evaluation, explained in Section 6.3.3 and 6.3.4, for on-line prediction of the final part quality. Correlation between a dynamic model with the ultrasonic reduced space allows, at the current state of the process, to predict the final product quality, which can be validated using the ultrasonic sensor once the process is concluded and the part is formed. This model as a decision support tool can help the user to understand causes of process variability and be a foundation for quality control strategies.

6.3.1 Principal component analysis (PCA)

Nonlinear ultrasonic analysis implies the interpretation of harmonic signals, thus requiring that the captured signal must be converted from the time to frequency domain. Instead of traditional ultrasonic analysis that focuses on amplitude and sound velocity calculations, in nonlinear ultrasonic analysis, changes in peak amplitude from different frequencies are correlated with structural characteristics[24]. To achieve this, Principal component analysis (PCA) was applied to first reduce the dimensionality of the ultrasonic multivariate data without losing important information, using Equation 1 below:

$$\mathbf{U} = \mathbf{T}\mathbf{P}^t + \mathbf{e} \tag{6.1}$$

where $\mathbf{U}$ is the matrix with ultrasonic spectra organized in rows from different batches; $\mathbf{T}$ is the concatenated scores vectors, $\mathbf{P}$ is a matrix with loading vectors, and $\mathbf{e}$ is the matrix of residuals. The reduced score space is able to capture the essence of the information available in the ultrasonic measurement, and can be interpreted using the loadings vector to understand the importance of frequencies. The PCA then forms the basis of the classification strategy described next.

6.3.2 Soft independent modeling of class analogy (SIMCA)

Ultrasonic spectroscopic data from rotational molded parts was correlated with traditional destructive tests to evaluate both sintering and degradation problems[24]. However, in the previous results, in order to create a calibration model for predicting product quality, controlled conditions based on a design of experiments and results from destructive tests are required. In practical industrial applications, this type of

data might not be available. Thus, a flexible and efficient method is proposed for quality classification based only on nondestructive data of historical samples, that can later be validated with secondary (destructive) tests. The soft independent modeling of class analogy (SIMCA) tool was utilized. The method utilizes the square prediction error (SPE) values calculated from PCA models to achieve classifcation[25].

Algorithm 1 describes in detail the steps required to create and update a classification model for different quality classes. Specifically, for the rotational molding process, three classes are used as a starting point for the SIMCA algorithm, in order to utilize the ultrasonic measurements alone to identify the presence of these different quality products. Any new sample is determined to belong to a particular class based on the SPE values, and the PCA models updated at the end of one set of new measurements to enable subsequent classification.

Algorithm 1 SIMCA algorithm

1. Create base PCA model with all available data.
2. Identify initial cluster points from the scores space, separate data into defined classes
   (a) Calculate separate PCA models for each class.
3. Classification of a new element
   (a) Calculate standard prediction error (SPE) for each PCA model.
   (b) Compare calculated values and locate in similar class using SPE limit values.
4. Model improvement: If a classification to a specific group meets the criteria, incorporate new sample to classified group; Repeat step 2 with the new dataset built. If newly introduced sample does not fit in to any previous groups, consider the creation of a new class.

This approach only requires data from the ultrasonic test and can be applied to any classification that allows differentiation by physical characteristics that reflect on

the ultrasonic spectrum, such as conditions covered by nonlinear ultrasonics, allowing a simple interpretation from a complex data set. As indicated earlier, supplementary destructive tests can be conducted to give meaningful physical labels after the fact. In the present examples, these could include, for instance, categories of target quality (on-spec equivalent), incomplete sintering and degraded.

6.3.3 Subspace identification for dynamic batch process modeling

The development of the on-line monitoring tool is based on a dynamic model that is able to predict the trajectories of the process variables (the internal mold temperature for the present application), for a candidate future manipulated input trajectory. Furthermore, the prediction from the dynamic model can then be utilized as the basis to predict the ultrasonic spectrum (described in the Section 6.3.4).

Batch manufacturing processes have traditionally been treated with a rigid recipe approach, requiring a design that would fit for each material and equipment. A flexible tool to model and understand variability in these processes is proposed with the application of subspace identification[27]. The model identification procedure outlined in[27,28] yields a linear time-invariant dynamic model that enables prediction of process outputs (based on candidate future inputs trajectories), and generalizes the subspace identification procedure[29] for batch process operation[30]. In contrast to previous PLS based modeling approaches[31] no batch time alignment is required. The identified model takes the form of Eqs.6.2-6.3 below:

$$\mathbf{x}_{k+1}^{d} = \mathbf{A}\mathbf{x}_{k}^{d} + \mathbf{B}\mathbf{u}_{k} \tag{6.2}$$

$$\mathbf{y}_k = \mathbf{C}\mathbf{x}_k^d + \mathbf{D}\mathbf{u}_k \tag{6.3}$$

where $\mathbf{x}_k \in \mathbb{R}^n$ represents the process state at different sampling instants, k; $\mathbf{u}_k \in \mathbb{R}^m$ and $\mathbf{y}_k \in \mathbb{R}^l$ denote the input and output values at sampling instant k, respectively; and matrices $\mathbf{A} \in \mathbb{R}^{n\times n}$, $\mathbf{B} \in \mathbb{R}^{n\times m}$, $\mathbf{C} \in \mathbb{R}^{l\times n}$, $\mathbf{D} \in \mathbb{R}^{l\times m}$, m input variables, and l measured variables. The model relies on subspace states to appropriately capture the process dynamics over the training data. For the purpose of prediction for a new batch, the subspace states need to be first estimated, and in the present work, this is done using a Luengberg observer, as shown in Eq. 6.4 (see,[32] for more details).

$$\hat{\mathbf{x}}[k+1] = \mathbf{A}\hat{\mathbf{x}}[k] + \mathbf{B}\hat{\mathbf{u}}[k] + \mathbf{L}(\mathbf{y}[k] - \hat{\mathbf{y}}[k]) \tag{6.4}$$

where the hat mark denotes the observer prediction and $\mathbf{L}$ is the observer gain determined by ensuring that the matrix $(\mathbf{A} - \mathbf{LC})$ is stable. From any point in time for a new batch (after the state estimator has converged), this model can be used to predict the process outputs for any candidate input trajectory, and can thus be utilized as a on-line monitoring tool. One of the contributions of the present work is to utilize the underlying dynamic model to build an associated quality model that is able to predict, and visualize the final quality, enabling its use as a quality monitoring tool.

6.3.4 On-line final quality projection

A combination of the ultrasonic data processing, described in Section 6.3.1, and the dynamic modeling, presented in Section 6.3.3, was used to develop an on-line monitoring tool to correlate process state and the final product quality.

The proposed new approach connects the subspace state variables with the reduced variables related to the final quality (ultrasonic frequency data after PCA) using the

historical batch data available for training. More specifically, multiple linear regression was utilized to build a model (see Eq. 6.5).

$$\mathbf{T} = \mathbf{R_a}\hat{\mathbf{x}}_\mathbf{f} + \mathbf{R_b} \tag{6.5}$$

where $\mathbf{R_a}$ and $\mathbf{R_b}$ are the multiple linear regression matrices that correlate the final state variable, $\hat{\mathbf{x}}_\mathbf{f}$, from the subspace models of Section 3.3 with the scores, $\mathbf{T}$, from the PCA of ultrasonic spectra.

This relationship is not built on a mechanistic understanding, but relies on the assumption that all of the information about the process is captured in the state vector. Thus, the final quality must also depend on the final state vector. This is also the basis of how the states are determined in the subspace identification approach.

Important advantages can be stated with the combination of the two techniques for on-line monitoring. The use of a subspace based time invariant model allows the quality model to be applied for all batches regardless of the batch length, without the need for an alignment variable. Any nonlinearities in the process dynamics are captured (as best as they are expressed in the available data) through the choice of the number of states and the resultant subspace model. The use of the reduced space (instead of the full spectrum) for the ultrasonic multivariate signal, on the other hand captures the essence of the information contained in the spectrum, and thus a linear relationship between these two sets of variables ends up being sufficient to predict the final quality.

One important contribution of the present work is the development of the visualization tool (that goes beyond the framework developed in[27]) In other words, while the subspace states are important in capturing the process dynamics, evolution of the subspace states by themselves does not lend itself readily to physical interpretation

(beyond the outputs they predict). In the present work, therefore, a visualization tool is developed aimed at predicting the ultrasonic spectrum at batch termination. Note that the ultrasonic spectrum, with its correlation to the final part quality, is much easier to interpret and be read by practitioners (see[33] for another instance of off-line process visualization tool).

Another tool that utilizes the proposed correlation between subspace states and the reduced space of the ultrasonics is demonstrated as an alternative to the classification steps in Section 3.2. A univariate non-parametric classification approach is utilized next to classify final quality based on the on-line reduced space projection of the ultrasonic signal. The task is then, for a new batch, to identify in the known samples which ones are most similar to the new produced part. This approach does not require an extensive calibration based on previous data points. In order to execute this search and recognition, the use of the k nearest neighbors (k-NN) algorithm is proposed. The objective is to find closest, or most similar, cases for a certain number of observations, k, thus minimizing the value of the Euclidean distance, d defined as follows:

$$d = \sqrt{\sum_{a=1}^{k} \sum_{b=1}^{p} (\hat{t}_b - t_b^a)^2} \tag{6.6}$$

where p is the number of components of the reduced space, $\hat{t}$ is the projected score from the current state variable from Eq. 6.5, and t^a is the score from the a-th closest sample from the database of historical batches.

With this non-parametric evaluation, the process data extracted from the subspace identification can be used to explore all the previous batch data available for prediction of product quality. Therefore, with new data being available, the prediction can be improved. However, bigger available datasets also require more computing power for the search, thus justifying the work being done in a reduced spaced (i.e. data

processing using PCA).

6.4 Results

6.4.1 In-line quality monitoring

Recall that univariate analysis of an ultrasonic signal, focused on time domain estimation of amplitude and sound velocity, is traditionally used for characterization or process monitoring. In order to demonstrate the effectiveness of the proposed approach, the traditional methodology is used as comparison. Figure 6.2 shows the ultrasonic amplitude for several batch runs with known final qualities separated into three different categories: incomplete sintering, with residual internal air bubbles present; degraded, with extensive thermo-oxidative degradation due to long exposure to heat; and, meeting target quality, optimal mechanical properties and no significant degradation. It is possible to observe a clear distinction between samples with incomplete sintering and the other groups, since the air bubbles present caused an increase in signal attenuation that reduced the final amplitude. However, no clear distinction is notable between the target and degraded groups. Also, even if a threshold value for amplitude was selected for differentiating each group, some samples would fall outside the defined groups due to natural variation in the amplitude that is related to the experimental procedure (for example, measurement sensitivity to the application of coupling the vacuum grease between transducer and surface of the sample). Thus, in the case of this study, relying only on the univariate analysis (i.e. signal amplitude) would not allow for a clear in-line classification between quality groups.

Using the same samples that were classified into the three categories previously mentioned, Figure 6.3 shows a score map of the first two components of a PCA model

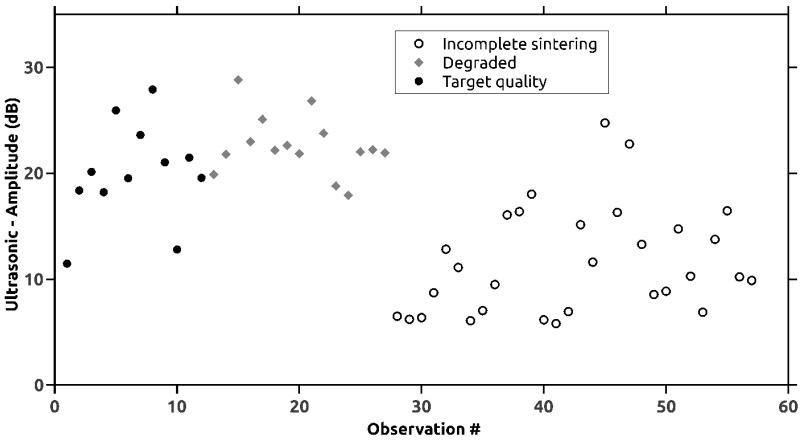

Figure 6.2: Ultrasonic amplitude of rotational molded polyethylene samples (symbols indicate different quality groups defined based on destructive tests)

constructed from the ultrasonic spectra for the group of molded samples. Of the available samples, 31 batch runs were used for training purposes. The number of components was determined by the minimum that would achieve a 90% variance explained for the selected group. A group of 7 samples was reserved for validation and not included in the calibration of the model. As can be seen from the projection, some clusters can be identified to help create the base groups, but do not elucidate all the differences between classes. Note that since the final class for each marked group is unknown, groups were numbered and not labeled. This first clustering using a general PCA model with the whole group of samples thus serves as the starting point for the classification. The SIMCA algorithm described in Section 3.2 was performed to create PCA projections from each individual group of samples (details on the performed calculation can be seen in Appendix A).

Although the selection of the samples contained in each group was based on the scores of the ultrasonic PCA, the experimental validation (see Table 6.1) demonstrates that each class is mainly populated by samples of different quality groups (incomplete sintering, target and degraded). In a practical scenario, only a small sample from each

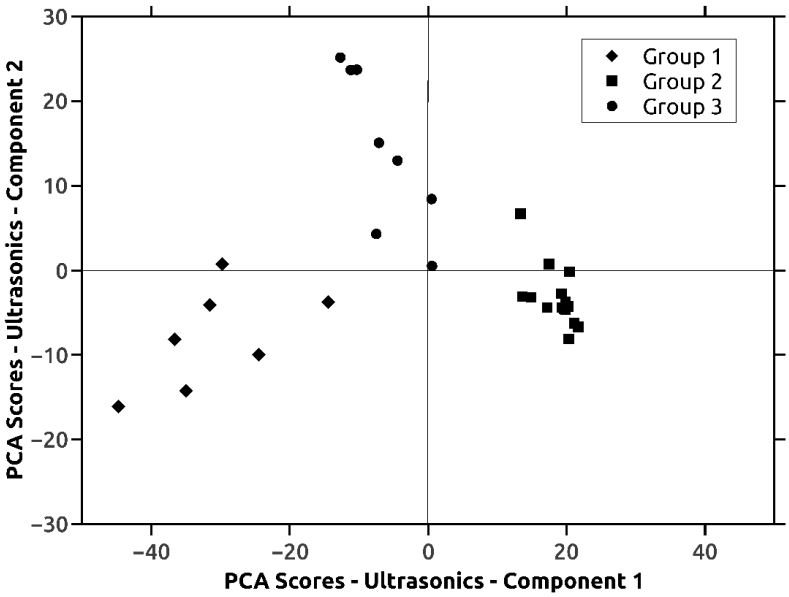

Figure 6.3: Projection of PCA scores from experimental batch samples using ultrasonic spectra data (different classes indicated by marker format)

Table 6.1: SIMCA groups label

	Experimental validation			
Group	Degraded	Target quality	Incomplete sintering	Label
1	58 %	20 %	0 %	Degraded
2	0 %	20 %	100 %	Incomplete sintering
3	42 %	50 %	0 %	Target
Total	100 % (n = 12)	100 % (n = 6)	100 % (n = 14)	

group is necessary to be tested in order to determine a quality label. For the clusters observed in Figure 6.3, Group 1 contained most of the degraded samples (58 %), Group 2 was populated with all parts characterized as incomplete sintering samples (100 %), and Group 3 had a combination of target (50 %) and degraded samples. These clear distinctions based only on the ultrasonic spectra differences represent significant evidence to support the proposed in-line classification method, that does not require extensive calibration with destructive methods, but only one or two samples from the respective groups can be tested for the purpose of labeling.

Another instructive analysis of each constructed PCA model is an evaluation of their loadings. Figure 6.4 shows the ultrasonic projection of the loadings considering all scores to be zero (center or average sample representation). Considering the areas of harmonic peaks, amplitude at the primary frequencies (same as the generated pulses) is lowest in the case of incomplete sintering, and increases for samples classified as target quality and degraded. This amplitude variation is expected from the increase in density with reduction of air bubbles. In the case of the third harmonic frequency range, there is also an increase in amplitude that follows the previous pattern between classes; however, another distinction was the increase in amplitude ratio value from target to degraded group. The variation in this nonlinear parameter, harmonics amplitude ratio, has been demonstrated as a sensitive indicator of morphological changes such as those related with thermo-oxidative degradation[24]. All of this analysis was observed considering only the clusters of groups based on given class attributes and data from ultrasonic spectra.

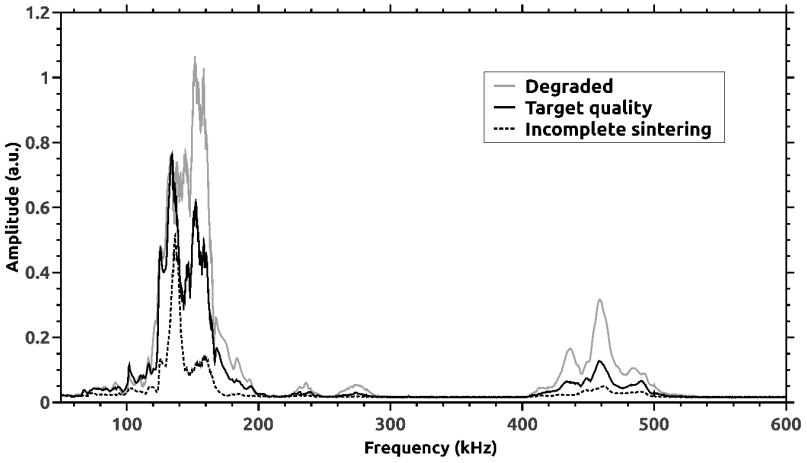

Figure 6.4: Ultrasonic spectra projected from loadings of PCA models of different quality groups

Validation of the classification approach using the SIMCA methodology is demonstrated in Table 6.2. Classification used the value of SPE as a reference for classification

Table 6.2: SIMCA groups classification

	SPE Values				
Sample	Group 1	Group 2	Group 3	Classification	Experimental validation
1	2590	4663	**1779**	Target	Target
2	**2568**	19665	13618	Degraded	Degraded
3	2877	**1932**	2486	Inc. Sintering	Inc. Sintering
4	2911	**2044**	2614	Inc. Sintering	Inc. Sintering
5	2670	**1567**	2386	Inc. Sintering	Inc. Sintering
6	3638	38187	**2062**	Target	Degraded
7	6351	40058	**3736**	Target	Target

into the labeled groups defined previously. All samples except one (Sample 6) were successfully classified based on the experimental validation test. It is possible to argue that classification in Group 3 accommodated samples with target quality and with some level of degradation, but did not represent the same structural change as observed in degraded samples classified in Group 1. A reclassification of the experimental limits or the separation of group 3 into two subgroups could be tried to improve classification. Recall that the traditional univariate descriptors simply did not allow any classification, and thus no attempt at validation was made. In contrast, the proposed approach was excellent in its ability to classify samples.

6.4.2 On-line quality monitoring and prediction

Process modeling and projection validation

The first step for the on-line approach is the process modeling using subspace identification. Following the approach described in Section 6.3.3, a third order state-space model was created using subspace identification for the process data available from historical rotational molding batches. In Figure 6.5, the fit using the dynamic model is shown for two representative batches.

Figure 6.6 shows the validation results using the identified model. In these results,

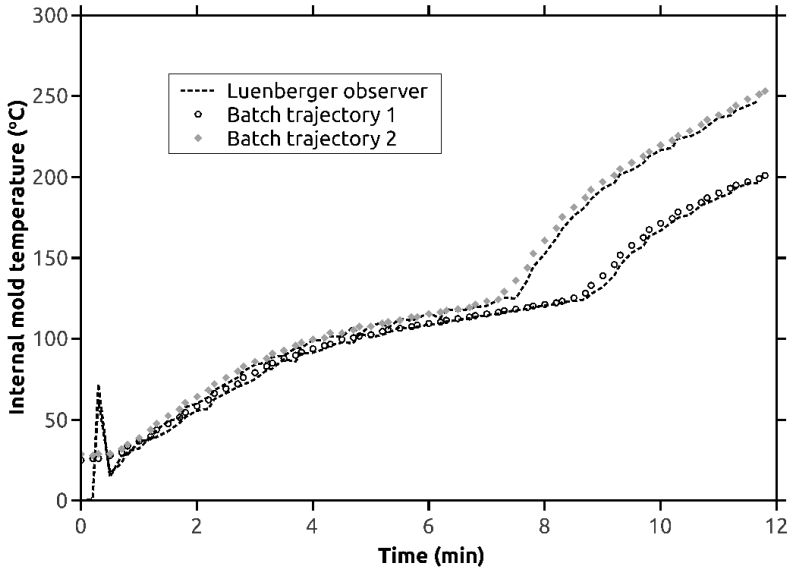

Figure 6.5: Batch internal air temperature profile for two validation batches until the instant of heating stage termination

the initial duration of a new batch is utilized by a Lungberger observer to estimate the state of the subspace model (thus imbuing the modeling approach with learning characteristics). After the states have converged (corroborated via the convergence of the estimated outputs to the measured outputs), the measured output trajectory is predicted for the remainder of the batch. The predictions are done starting from 3 different time points in the batch and demonstrate the improved ability of the model to predict the process evolution farther along in the batch.

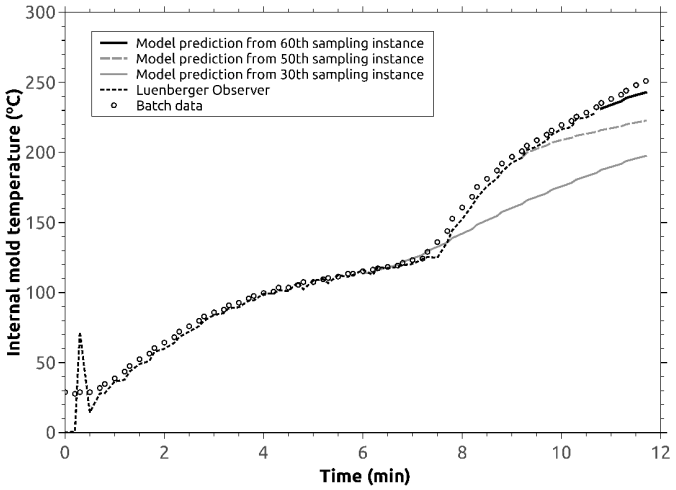

(a) Batch 1

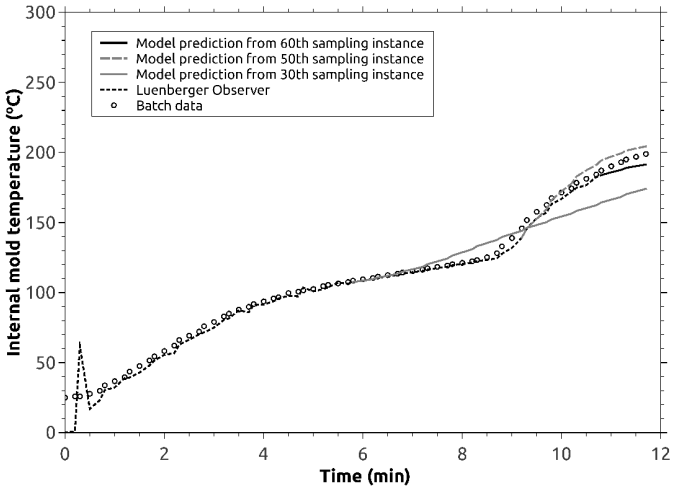

(b) Batch 2

Figure 6.6: Validation for dynamic model

On-line process visualization

Having illustrated the ability of the subspace model to capture the process dynamics, the objective of this section is to demonstrate the ability to predict the spectrum of the molded part. To this end, first, a model is built between the terminal subspace states, and the reduced ultrasonic spectrum for the training batches (as described in

Section 3.4). Thus, a multiple linear regression model was determined between the final state variables (dimension = 3) and the ultrasonic spectra data in a reduced dimension after PCA (number of components = 8). A total of 21 batch runs (with measured process variables and ultrasonic spectra from the molded part) were used to calibrate the model. A group of 7 samples, that were not included in the original model calculation, were separated for validation.

The results for this proposed correlation show excellent prediction capability. In particular, for validation purposes, two batches were chosen which corresponded to a incomplete sintering and degraded parts, respectively, exhibiting significantly different spectra. The model however, was able to predict very well the spectrum utilizing the final subspace states alone, as can be seen in Figures 6.7 and 6.8. The ability to predict the dynamic behavior (shown in section 4.2.1), along with the ability to predict the terminal spectrum based on the terminal states built confidence in the possibility of using the dynamic model together with the multiple regression model for the purpose of online monitoring, that is, for the purpose of predicting the terminal spectrum on-line.

Figure 6.9 shows the trajectory of a batch run for the first two components of the ultrasonic spectrum based on the process trajectory with batch time. In this figure, the states at any given point in time are used to compute the terminal scores. As the process evolves, the states get closer to the terminal states, and thus the ability to predict the terminal PCA scores keeps continually improving. In other words, with the progression of the sintering phase and increase in temperature during the heating phase, the process gets closer to the finished product, and thus closer to the region of model validity. This on-line process monitoring that combines measured process data with a projection of the product quality gives a useful visualization of the process state that goes beyond the collection of univariate measurements.

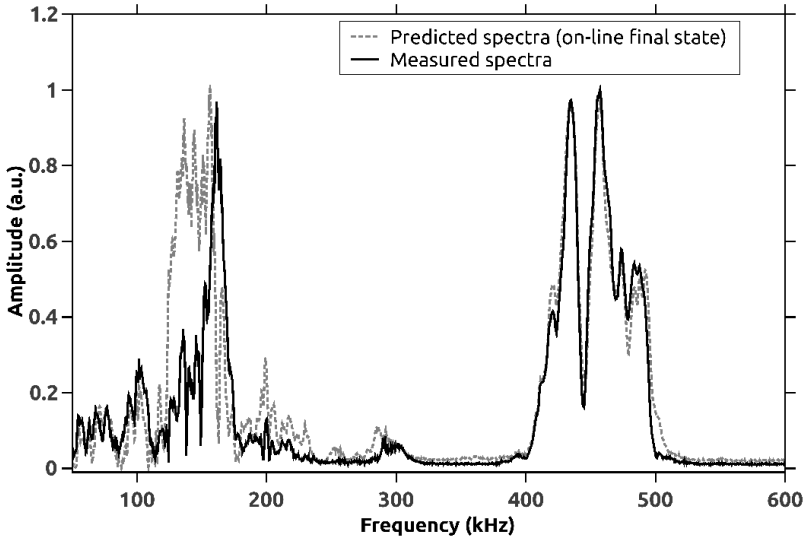

Figure 6.7: Experimental validation of the ultrasonic spectra projection from an incomplete sintering sample

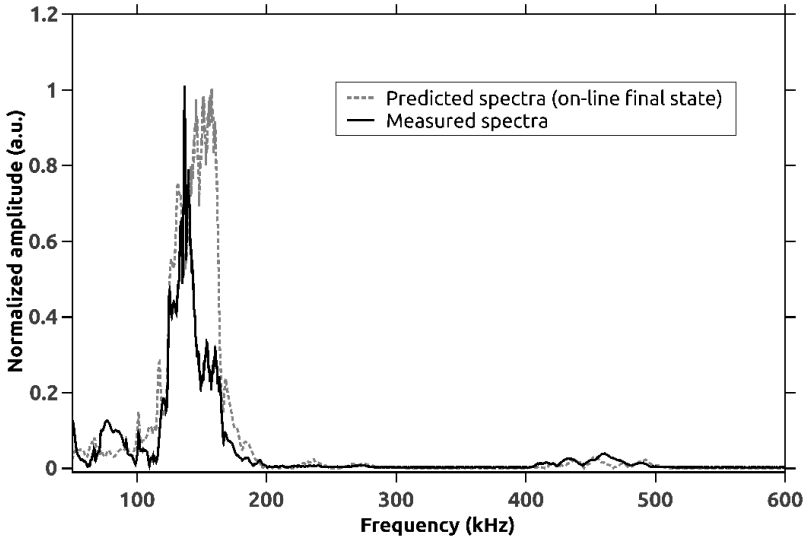

Figure 6.8: Experimental validation of the ultrasonic spectra projection from a degraded sample

The next set of figures shows another visualization tool. In particular, the tool captures the evolution of the mold through the various phases as the batch evolves. To build the tool, first the classification method using the k-NN algorithm described

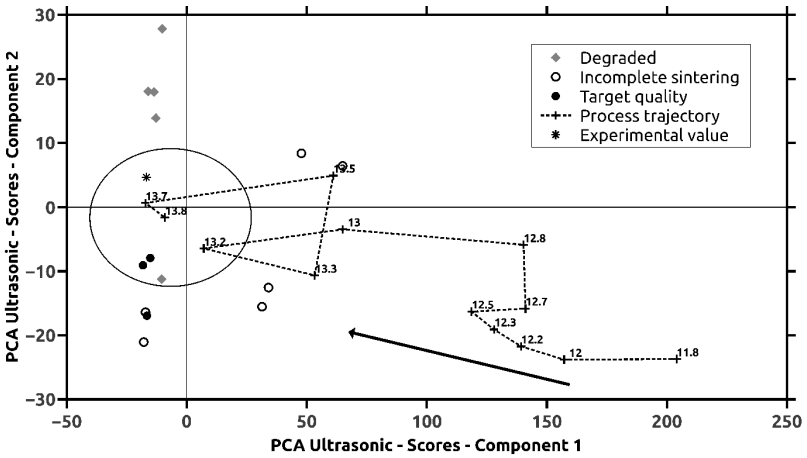

Figure 6.9: Process trajectory considering state-space variables at each sampling instant to project first two components of the reduced PCA ultrasonic spectra for a final degraded sample

in Section 3.4, with a k=3 was built. The predicted ultrasonic spectra were converted from the reduced space to the frequency domain using the PCA loadings, and the absolute values of the amplitudes were used (to avoid meaningless negative values). Figure 6.10 show the evolution of a particular batch. On the k-NN plot (top right corner), it is possible to see a gradual decrease in the calculated distance from the beginning of the sintering phase with prediction of incomplete sintering quality, when it shifts temporarily to degraded quality, but then consolidates as target quality in terms of a class prediction. From the projected ultrasonic spectra an increase in amplitude on the primary frequencies is first observed at early sampling instances, with a consequent reduction of the amplitude ratio based on the third harmonic peak amplitude. Note that there is no experimental validation of the spectrum predicted during this particular batch- i.e., the processing was not terminated at say 12 minutes into the batch. However, the training and, more importantly, validation samples did include batches that were terminated at different times into the batch, and that demonstrate the ability to predict the final spectrum at different times during the

batch.. Furthermore, the model-based classification also matches with the experimental classification.

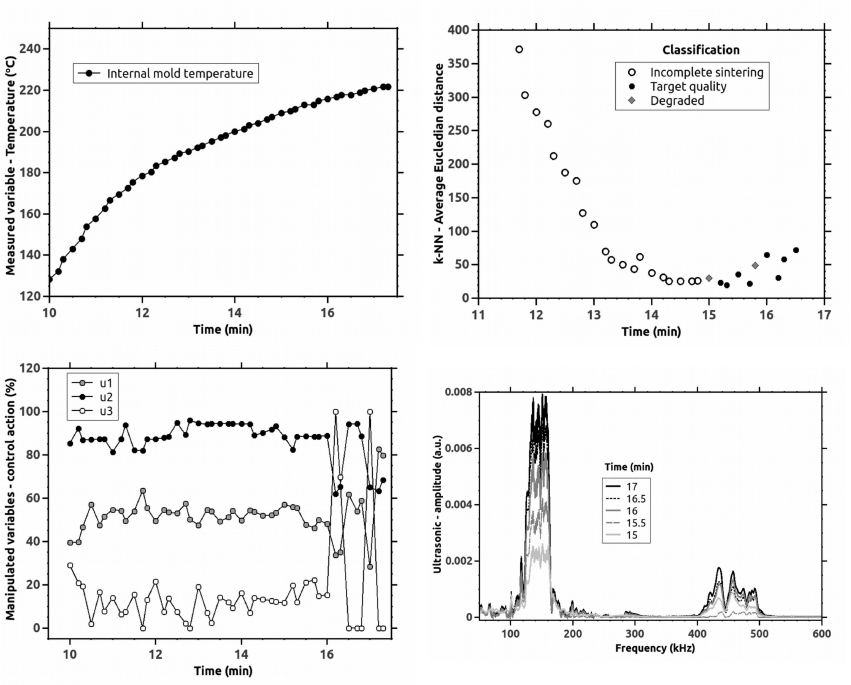

Figure 6.10: Process monitoring for a target quality sample with measured variables (top left), manipulated variables (bottom left), k-NN evaluation (top right) and ultrasonic spectrum projections (bottom right)

We next demonstrate the application of the proposed tool for the detection of process conditions and samples outside specifications, and explored with two extreme cases: an incomplete sintering and a degraded sample. For the first case, Figure 6.11 demonstrates the on-line measurements and projections during the sintering phase of the rotational molding process. Descriptor from the k-NN average distance shows a progression on the sintering process, however the terminal process conditions of low heating and internal temperature profile are not sufficient to remove the residual air bubbles. Thus, the predicted quality classification at the final instance indicates incomplete sintering. A different heating cycle is observed in Figure 6.12, with the process monitored presenting a higher heating rate that allows the internal mold

temperature to reach high values in a short time. The results represent a shift in classification with the k-NN search algorithm from incomplete sintering to a degraded projected final quality after 11 minutes of batch run, at which time the internal temperature was already above 220 ^oC. In both cases, the prediction of the final product quality class is a relevant tool. However, the proposed monitoring tools also allow for further process data interpretation. For the second profile, shown in Figure 6.12, it is noticeable that the heating conditions shifted the projections from incomplete sintering directly to a degraded sample. In contrast to the example shown in Figure 6.10, the sample did not go through a target quality condition. This questions the traditional view for the rotational molding process where the quality depends only on either the selection of the time to stop the heating cycle based on a fixed heating rate or based on the peak internal air temperature. In other words, a process operation run using the traditional understanding would not yield the target quality for either of these samples. It is understood that sintering and thermo-oxidative degradation in rotational molding are parallel processes influenced by a combination of time and temperature[34–36]. Thus, it is understandable that some heating profiles can accelerate or reduce these processes and might not be fully explained by the monitoring of individual variables. In summary, the proposed multivariate monitoring approach combines sufficient process knowledge without the need of mechanistic determination to provide an estimation of the progression of the final quality during the batch run.

In order to demonstrate the adaptability of the proposed statistical tools for quality monitoring, Table 6.3 groups the predictions and experimental verification for samples on the validation group, with all product classes being accurately predicted.

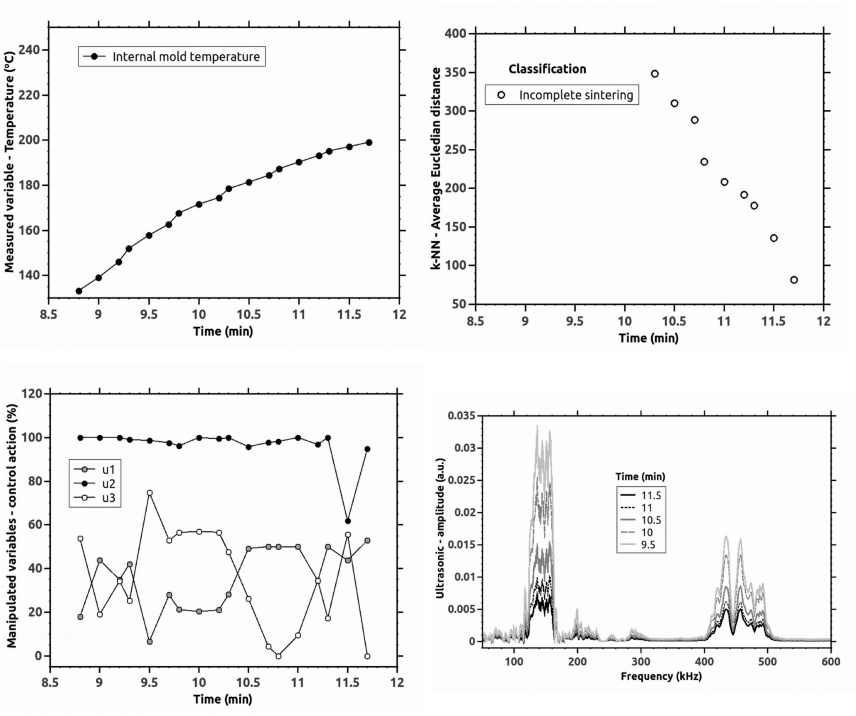

Figure 6.11: Process monitoring for an incomplete sintering quality sample with measured variables (top left), manipulated variables (bottom left), k-NN evaluation (top right) and ultrasonic spectrum projections (bottom right)

Table 6.3: Results for classification prediction and experimental measurements for validation group

	On-Line Prediction		Experimental validation				
Sample	k-NN	Prediction	Impact	Incomplete sintering?	Viscosity	Degraded?	Observed
1	95	Target	0.50	No	8088	No	Target
2	234	Incomplete	0.31	Yes	6645	No	Incomplete
3	62	Target	0.43	No	7522	No	Target
4	264	Degraded	0.65	No	13418	Yes	Degraded
5	52	Target	0.51	No	6966	No	Target
6	45	Degraded	0.51	No	11365	Yes	Degraded
7	82	Incomplete	0.37	Yes	6447	No	Incomplete

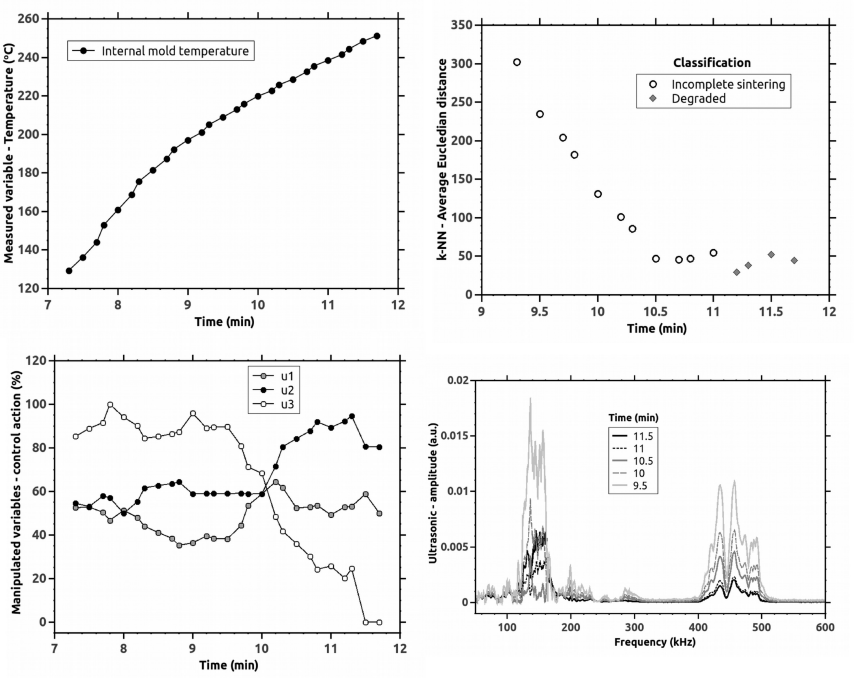

Figure 6.12: Process monitoring for a degraded quality sample with measured variables (top left), manipulated variables (bottom left), k-NN evaluation (top right) and ultrasonic spectrum projections (bottom right)

6.5 Conclusions

Data-driven approaches have been demonstrated for in-line classification and on-line monitoring and prediction of product quality based on the nonlinear ultrasonics data. Classification based on multivariate statistical analysis was efficient, even with minimal qualitative input, to confirm the validity of important structural properties contained on the multivariate ultrasonic spectrum measured from rotomolded polyethylene parts. The proposed correlation between the termination state-space from the end of the heating phase and the reduced space ultrasonic spectrum was applied for the on-line visualization and quality prediction. The data-driven tools described have strong potential to be used not only for quality evaluation but also to improve process understanding and to be used as basis for batch control strategies. The presented work also addresses the usefulness of nonlinear ultrasonics as a viable sensor technology for advanced manufacturing practices of batch processes in polymer industry.

Acknowledgement

The authors would like to acknowledge the financial support from Conselho Nacional de Desenvolvimento Cientifico e Tecnologico (CNPQ-Brazil).

Bibliography

[1] Behzad Esmaeilian, Sara Behdad, and Ben Wang. The evolution and future of manufacturing: A review. *Journal of Manufacturing Systems*, 39:79–100, apr 2016.

[2] Dazhong Wu, David W. Rosen, Lihui Wang, and Dirk Schaefer. Cloud-based design and manufacturing: A new paradigm in digital manufacturing and design innovation. *CAD Computer Aided Design*, 59:1–14, 2015.

[3] Fei Tao, Qinglin Qi, Ang Liu, and Andrew Kusiak. Data-driven smart manufacturing. *Journal of Manufacturing Systems*, 2018.

[4] Yusuke Hiejima, Takumitsu Kida, Kento Takeda, Toshio Igarashi, and Koh-hei Nitta. Microscopic structural changes during photodegradation of low-density polyethylene detected by Raman spectroscopy. *Polymer Degradation and Stability*, 150:67–72, apr 2018.

[5] Mintra Meemusaw, Joao Maia, Alexander Jamieson, and Rathanawan Magaraphan. Structural changes in HDPE produced by in-line plasma-pretreated reactive extrusion. *Materials Chemistry and Physics*, 199:34–42, sep 2017.

[6] Yadollah Teymouri, Alina Adams, and Bernhard Blümich. Impact of Exposure Conditions on the Morphology of Polyethylene by Compact NMR. *Macromolecular Symposia*, 378(1):1600156, apr 2018.

[7] F.P.C. Gomes, W.T.J. West, and M.R. Thompson. Effects of annealing and swelling to initial plastic deformation of polyethylene probed by nonlinear ultrasonic guided waves. *Polymer*, 131:160–168, nov 2017.

[8] Vikram K. Kinra and Vasudevan R. Iyer. Ultrasonic measurement of the thickness, phase velocity, density or attenuation of a thin-viscoelastic plate. Part II: the inverse problem. *Ultrasonics*, 33(2):111–122, 1995.

[9] Akira Tanaka, K Nitta, and S Onogi. Ultrasonic velocity and attenuation of polymeric solids under oscillatory deformation: Apparatus and preliminary results. *Polymer Engineering and Science*, 29(16):1124–1130, aug 1989.

[10] Yi Zhang, P.-Y. Ben Jar, Kim-Cuong T. Nguyen, and Lawrence H. Le. Char-

acterization of ductile damage in polyethylene plate using ultrasonic testing. *Polymer Testing*, 62:51–60, sep 2017.

[11] J. S. Egerton, M. J. S. Lowe, P. Huthwaite, and H. V. Halai. Ultrasonic attenuation and phase velocity of high-density polyethylene pipe material. *The Journal of the Acoustical Society of America*, 141(3):1535–1545, mar 2017.

[12] Farid Meziane, Sunil Vadera, Khairy Kobbacy, and Nathan Proudlove. Intelligent systems in manufacturing: current developments and future prospects. *Integrated Manufacturing Systems*, 11(4):218–238, jul 2000.

[13] Richard G. Brereton. Pattern recognition in chemometrics. *Chemometrics and Intelligent Laboratory Systems*, 149:90–96, dec 2015.

[14] C. Duchesne, J.J. Liu, and J.F. MacGregor. Multivariate image analysis in the process industries: A review. *Chemometrics and Intelligent Laboratory Systems*, 117:116–128, aug 2012.

[15] Svante Wold, Kim Esbensen, and Paul Geladi. Principal component analysis. *Chemometrics and Intelligent Laboratory Systems*, 2(1-3):37–52, aug 1987.

[16] A. Almeida, L. Saerens, T. De Beer, J.P. Remon, and C. Vervaet. Upscaling and in-line process monitoring via spectroscopic techniques of ethylene vinyl acetate hot-melt extruded formulations. *International Journal of Pharmaceutics*, 439 (1-2):223–229, dec 2012.

[17] Walker Camacho and Sigbritt Karlsson. NIR, DSC, and FTIR as quantitative methods for compositional analysis of blends of polymers obtained from recycled mixed plastic waste. *Polymer Engineering and Science*, 41(9):1626–1635, 2001.

[18] P.D. Coates, S.E. Barnes, M.G. Sibley, E.C. Brown, H.G.M. Edwards, and I.J. Scowen. In-process vibrational spectroscopy and ultrasound measurements in polymer melt extrusion. *Polymer*, 44(19):5937–5949, sep 2003.

[19] Ryan Gosselin, Denis Rodrigue, and Carl Duchesne. A hyperspectral imaging sensor for on-line quality control of extruded polymer composite products. *Computers & Chemical Engineering*, 35(2):296–306, feb 2011.

[20] Songtao Zhang, Rickey Dubay, and Meaghan Charest. A principal component analysis model-based predictive controller for controlling part warpage in plastic injection molding. *Expert Systems with Applications*, 42(6):2919–2927, apr 2015.

[21] Xundao Zhou, Yun Zhang, Ting Mao, and Huamin Zhou. Monitoring and dynamic control of quality stability for injection molding process. *Journal of Materials Processing Technology*, 249(March):358–366, nov 2017.

[22] Guthrie Gordon, David O. Kazmer, Xinyao Tang, Zhoayan Fan, and Robert X. Gao. Quality control using a multivariate injection molding sensor. *The International Journal of Advanced Manufacturing Technology*, 78(9-12):1381–1391, jun 2015.

[23] M. J. Oliveira, M. C. Cramez, and R. J. Crawford. Structure-properties relationships in rotationally moulded polyethylene. *Journal of Materials Science*, 31(9):2227–2240, 1996.

[24] F.P.C. Gomes and M.R. Thompson. Nondestructive evaluation of sintering and degradation for rotational molded polyethylene. *Polymer Degradation and Stability*, 157:34–43, nov 2018.

[25] Yukio Tominaga. Comparative study of class data analysis with PCA-LDA, SIMCA, PLS, ANNs, and k-NN. *Chemometrics and Intelligent Laboratory Systems*, 49(1):105–115, sep 1999.

[26] R. De Maesschalck, A. Candolfi, D. L. Massart, and S. Heuerding. Decision criteria for soft independent modelling of class analogy applied to near infrared data. *Chemometrics and Intelligent Laboratory Systems*, 47(1):65–77, 1999.

[27] Brandon Corbett and Prashant Mhaskar. Subspace identification for data-driven modeling and quality control of batch processes. *AIChE Journal*, 62(5):1581–1601, may 2016.

[28] Abhinav Garg and Prashant Mhaskar. Subspace Identification-Based Modeling and Control of Batch Particulate Processes. *Industrial and Engineering Chemistry Research*, 56(26):7491–7502, 2017.

[29] S. Joe Qin. An overview of subspace identification. *Computers & Chemical Engineering*, 30(10-12):1502–1513, sep 2006.

[30] Lennart Ljung. System Identification. In *Signal Analysis and Prediction*, pages 163–173. 1998.

[31] Johan a Westerhuis, Theodora Kourti, and John F. MacGregor. Comparing alternative approaches for multivariate statistical analysis of batch process data. *Journal of Chemometrics*, 13(3-4):397–413, may 1999.

[32] Abhinav Garg, Brandon Corbett, Prashant Mhaskar, Gangshi Hu, and Jesus Flores-Cerrillo. Subspace-based model identification of a hydrogen plant startup dynamics. *Computers & Chemical Engineering*, 106:183–190, nov 2017.

[33] Ray Wang, Thomas F. Edgar, Michael Baldea, Mark Nixon, Willy Wojsznis, and Ricardo Dunia. A geometric method for batch data visualization, process monitoring and fault detection. *Journal of Process Control*, 67:197–205, jul 2018.

[34] M.C Cramez, M.J Oliveira, and R.J Crawford. Optimisation of rotational moulding of polyethylene by predicting antioxidant consumption. *Polymer Degradation and Stability*, 75(2):321–327, jan 2002.

[35] A. Hamidi, S. Farzaneh, F. Nony, Z. Ortega, S. Khelladi, M. Monzon, F. Bakir, and A. Tcharkhtchi. Modelling of sintering during rotational moulding of the thermoplastic polymers. *International Journal of Material Forming*, 9(4):519–530, sep 2016.

[36] M. Kontopoulou and J. Vlachopoulos. Bubble dissolution in molten polymers and its role in rotational molding. *Polymer Engineering & Science*, 39(7):1189–1198, jul 1999.

Chapter 7

Applications

The following chapter is a compiled collection of demonstrated uses of the developed testing methodology and process monitoring. Where the work has been published or in preparation to be published, the reference and all authors will be highlighted. The full published content shall not be included for brevity but a short presentation of the significant contributions and specific results related to the other chapters of this thesis will be given. Applications 1 and 2 show the use of the methodology described in Chapter 4 as nondestructive evidence for structural modification. Lastly, Application 3 demonstrates a control scheme based on the process modeling demonstrated in Chapter 6 for the rotational molding process.

7.1 Application 1: Plasticization of polyethylene

Plasticizing effect of oxidized biodiesel on polyethylene observed by nondestructive method

A.K. Saad[1], F.P.C. Gomes[1], M.R. Thompson[1]

[1]Department of Chemical Engineering, CAPPA-D/MMRI

McMaster University, Hamilton, Ontario, Canada

Manuscript draft under review

Author contribution:

The second author, F.P.C. Gomes, contributed with the supervision of the design of experiments, ultrasonic, mechanical and thermal characterization of the samples, and revision of the manuscript. The main author, A.K. Saad, was responsible for the design of the experiments, execution of the diffusion tests and other characterization techniques, and primarily contributed for the writing of the manuscript. The author M.R. Thompson was responsible for experiments supervision and revision of the manuscript.

Main scientific contributions of the paper:

- Demonstration of a nondestructive method to observe the effect of biodiesel as a plasticizer for polyethylene.
- Differentiation of the plasticizing effect between biodiesel and toluene.
- Analysis of the effect of biodiesel degradation on the diffusion and plasticizing effect.

ABSTRACT

This paper explores the compatibility of biodiesel with different grades of polyethylene, specifically examining their plasticization effect for better understanding of the interactions occurring after penetration. Initially, the influence on the polyethylene mesostructure was investigated by evaluated mass uptake, mechanical testing and the application of a novel nondestructive ultrasonic testing method. Diffusion and plasticization by biodiesel were directly compared with results obtained by toluene, a known plasticizer for polyethylene. Traditional tests confirmed that biodiesel acted as a plasticizer with reduced mechanical properties observed for the polyethylene proportional to the amount of fuel uptake; biodiesel uptake was inversely proportional to crystal content of the polymer and only 3% of toluene uptake. However, spectral analysis by ultrasonics showed that absorbed toluene and biodiesel influenced the microstructure of polyethylene differently. Notable differences in internal stresses were noted between the two fluids for the same amount absorbed. A subsequent study analyzed the impact that biodiesel degradation had on plasticization. Although, the trend showed a reduction in diffusion rate with increasing oxidation of the medium, the mechanical results did not show significant differences between fresh and degraded biodiesel test conditions within the span of the test. Combining the evidence observed

in this study, a mechanism is proposed for biodiesel plasticization that can help with failure prevention and material selection.

7.1.1 Highlighted results

Although biodiesel has been demonstrated as a plasticizer for polyethylene, some evidence indicates that the mode of interaction with the polymer semi-crystalline structure is completely different than a plasticizer like toluene. Results from the non-destructive ultrasonic testing help to support this hypothesis. Figures 7.1 and 7.2 show the different spectra attained from the samples before and after immersion in each fluid, Toluene and biodiesel, respectively, until it reached a saturation of around 3-4% of weight gain. Differences between samples are observed on the upper harmonics, more specifically at the third harmonic region (between 400-500 kHz). For the PE immersed in Toluene, this region presented a significant increase, while the samples in biodiesel had a minor reduction. When comparing the variation of the ultrasonic parameter for the different PE grades, it is clear that the opposite behavior on the propagated ultrasonic waves is evident for all and they all fall on the same variability, as observed in Figure 7.3.

The increase of this nonlinear ultrasonic parameter is known to be related to the swelling effect with a proportional increase in concentrated internal stress forces created by the penetrating molecules. Thus, it is noticeable that the biodiesel incorporation on PE did not show this effect, and can indicate that it might have helped to decrease internal stresses. This argument can be connected to the observation of the plastic deformation witnessed by these samples after immersion in the different plasticizers, as samples exposed to biodiesel had a significant decrease in fibrillation compared to toluene. A possible interpretation of the modes of plasticization is that while toluene

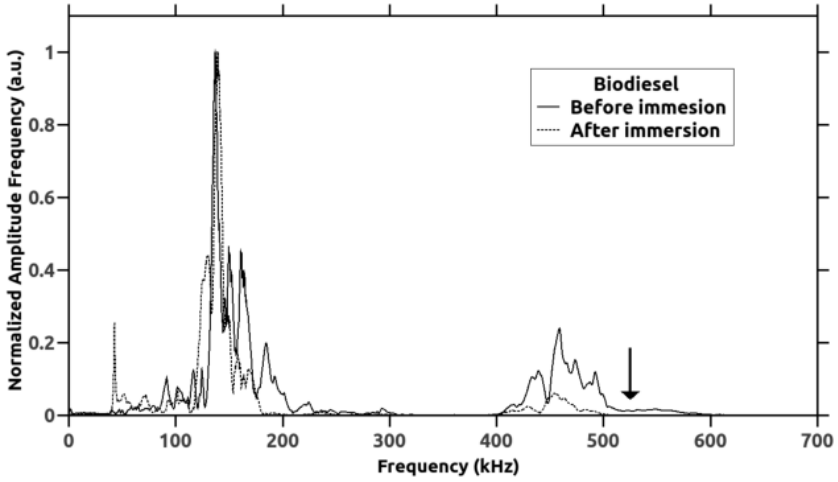

Figure 7.1: Ultrasonic spectra for the PE HD1 sample before and after biodiesel immersion (the arrow indicates the decrease of the third harmonic peak amplitude considering normalized signal based on primary frequency amplitude)

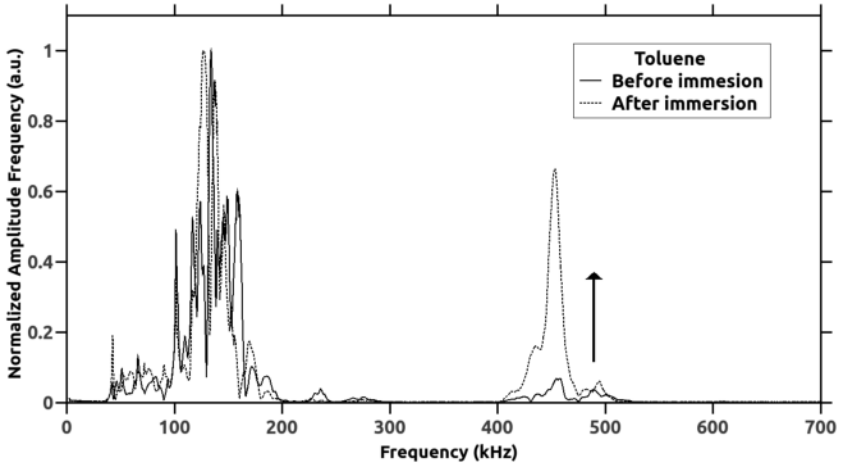

Figure 7.2: Ultrasonic spectra for the PE HD1 sample before and after Toluene immersion (the arrow indicates the increase of the third harmonic peak amplitude considering normalized signal based on primary frequency amplitude)

acts by penetrating the amorphous region, increasing the mobility of that phase and creating internal stresses, biodiesel is responsible for lubrication of the inter-crystalline chains, promoting more crystal slips during plastic deformation with no increase in internal stress.

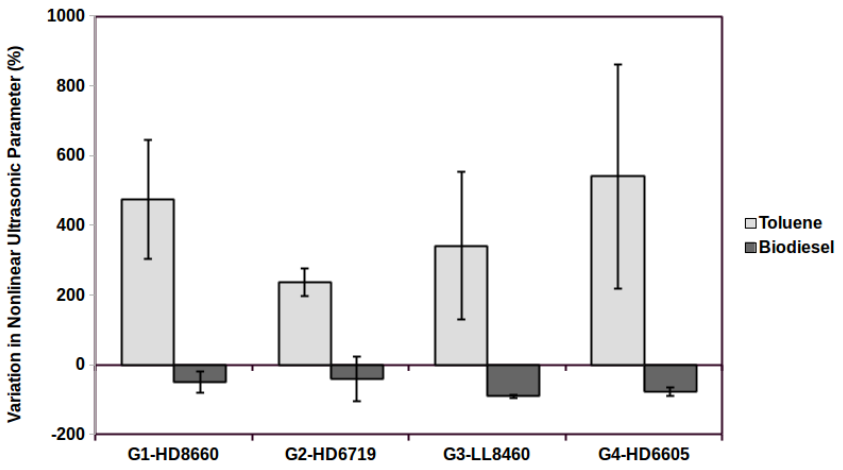

Figure 7.3: Nonlinear ultrasonic parameter variation for different PE grades with immersion in Toluene and biodiesel

7.2 Application 2: Plastic deformation of poly(lactic acid)

Physical aging as the driving force for brittle-ductile transition of polylactic acid

G. Zhao[1], F. P. C. Gomes[2], H. Marway[2], M. R. Thompson[2], Z. Zhu[1]

[1] Tongji University, China

[2] McMaster University, Canada

Manuscript draft under review

Author contribution:

The second author, F.P.C. Gomes, contributed with the ultrasonic testing and partially writing introduction, methodology and results sections. The main author, G. Zhao, was responsible for the design and execution of experiments, and writing of the manuscript. The authors H. Marway, M.R. Thompson and Z.Zhu were responsible for the project supervision and manuscript revision.

Main scientific contributions of the paper:

- Proposed treatment based on physical aging to improve toughness of PLA.
- Observation of the treatment effect on the initiation of plastic deformation using the proposed nonlinear ultrasonic parameter.

ABSTRACT

Polylactic acid (PLA) is inherently a brittle polymer in commercial uses, exhibiting a high modulus and elongation at break below 5%. To transition the failure mode of this polymer to one that is more ductile without loss in strength is challenging. To produce a more ductile PLA, a new strategy combining freezing and physical aging with ultraviolet (UV) radiation was carried out to improve the mechanical properties. A three-step method was used to control the plastic deformation nature of PLA: (a) low temperature treatment, applied to slow down the physical aging and transforming the sub-ordered structures into a more stable state; (b) introduction of a chain extender (CE) into PLA system to form branching structures and decrease the mobility of polymer chains for UV irradiation; and finally (c) UV treatment to increase the entanglement density of the amorphous phase and decrease the formation of undesired sub-ordered structures during physical aging. The elongation at break of PLA prepared with 0.75%CE was increased up to 18.25% by conditioning at -40℃ for 48 h followed by UV irradiation for 30 h. Results also demonstrated that tensile strength and Young's modulus remain statistically unchanged.

7.2.1 Highlighted results

Figure 7.4 shows the progression of the third harmonic peak for a treated sample with increasing flexural deformation. The harmonic generation is a reflection of the

initial plastic deformation, causing a nonlinear propagation of the ultrasonic signal. A variation of this parameter can be linked to the presence of connecting chains that accumulate internal stresses related to increased structural deformation. A small variation of the nonlinear ultrasonic parameter indicates that a secondary dislocation process has happened, i.e. crystal slip.

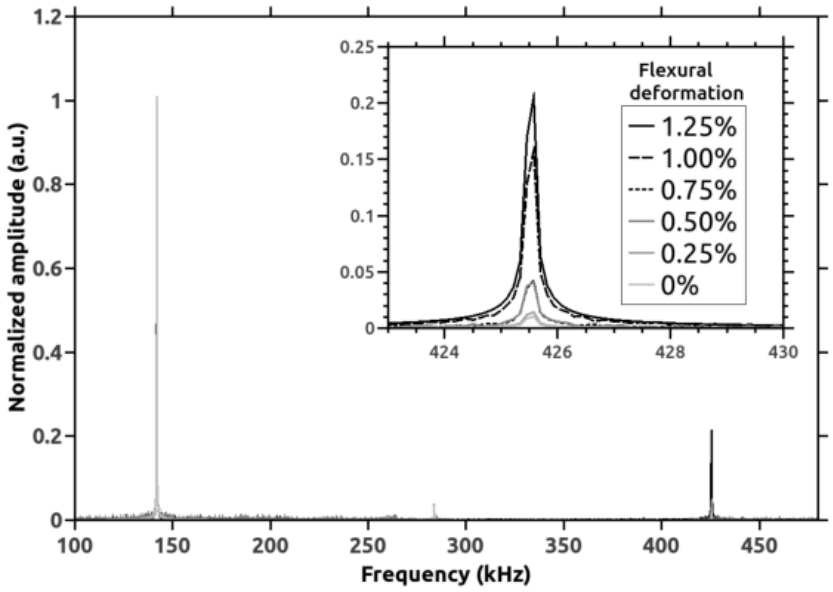

Figure 7.4: Ultrasonic spectrum of PLA+Joncryl+Thermal+UV sample with increasing flexural deformation (internal box highlights the third harmonic region)

Figure 7.5 shows that the addition of the chain extender, Joncryl, improves the plasticity of PLA, increasing the variation of the nonlinear ultrasonic parameter. In order to understand the effect of the thermal treatment on the plasticity of the treated PLA, samples were kept in freezing conditions after compression molded and equilibrated at room temperature for 5 minutes before test. Results showed a decrease in the nonlinear parameter that might be connected with a reduction in mobility of the chains. A similar reduction was observed in Figure 7.6 for samples after UV treatment, where the decrease in plasticity can be explained by an increase in the

degree of crosslinks. However, results for the complete treatment with the combination of thermal and UV subsequent stages, demonstrate a level of plasticity comparable to the original sample with Joncryl before the physical aging.

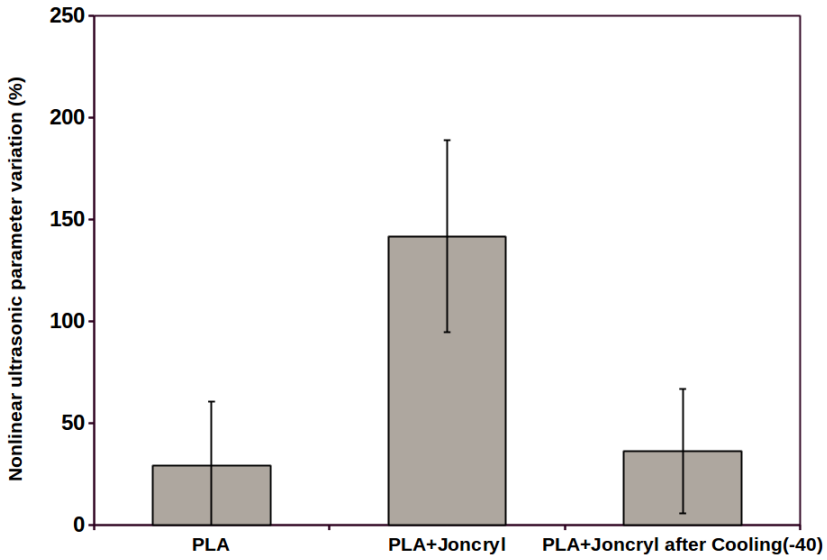

Figure 7.5: Maximum nonlinear ultrasonic parameter variation for PLA and PLA+Joncryl samples after flexural deformation (max. value of 1.25% strain)

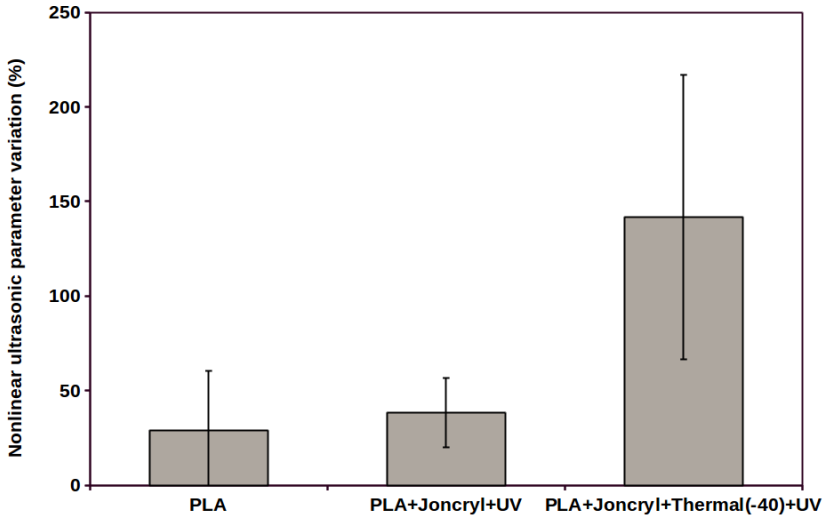

Figure 7.6: Maximum nonlinear ultrasonic parameter variation for PLA and PLA+Joncryl treated with UV or Thermal+UV samples after flexural deformation (max. value of 1.25% strain)

7.3 Application 3 : Process control for rotational molding

Model Predictive Control of Uni-Axial Rotational Molding Process

Authors: A. Garg[1], F. P .C. Gomes[2], P. Mhaskar[1], M. R. Thompson[1]

[1]Department of Chemical Engineering, MACC

[2]Department of Chemical Engineering, CAPPA-D/MMRI

McMaster University, Hamilton, Ontario, Canada

Published manuscript at Computers and Chemical Engineering

DOI: 10.1016/j.compchemeng.2018.11.005

Author contribution:

The second author, F.P.C. Gomes, adapted and executed the rotational molding experiments, tested the final quality of the produced parts and wrote partially the methods and results section. The main author A. Garg was responsible for the design of the experiments, coding of the application for modeling and control, supervision of the execution of the experiments and primarily writing of the manuscript. The authors P. Mhaskar and M.R. Thompson were responsible for supervision of the design of experiments and review of the manuscript.

Main scientific contributions of the paper:

- Application of subspace identification approach and model based predictive control for a rotational molding process.
- Proposed methodology for product quality optimization based on the operator selection from the historical batches available.

- Validation of the proposed method, demonstrating the effectiveness of the control scheme to achieve desired quality.

ABSTRACT

This paper addresses the problem of achieving tight product quality, and also enabling automated process changes to produce new product grade in a uni-axial rotational molding process. This is achieved by the implementation of a novel modeling and control formulation. In particular, a data driven state-space model of the process is first identified using experimental data. For a given trajectory of input moves (heater and cold air profiles), this dynamic model is able to predict the evolution of the measured variable (internal product temperature). The dynamic model is augmented with a quality model, which relates the terminal predictions from the dynamic model to the key quality variables (sinkhole area, ultrasonic spectra amplitude, impact test metric and viscosity). The dynamic and quality model are in turn utilized within a model predictive control (MPC) framework that enables specifying product quality requirements explicitly. Experimental results demonstrate the ability of the MPC not only in achieving tight quality control but also providing on-spec product for a new product grade.

7.3.1 Highlighted results

One of the key strengths of the proposed formulation is the ability to specify the control objective to reflect the product quality. In particular, to recognize the fact that the desired product quality reflects, in some sense, trading off some of the quality variables against others. This is quantified through the choice of the vector β. In this particular implementation, β is chosen in the following fashion: First, 'reasonable' values of the parameters are chosen based on the relative importance (and magnitudes)

of the quality variables. The objective function is then evaluated for the 21 batches in the training data and the batches ranked according to the objective function. The value of the parameters are then tweaked to ensure that the batches which are deemed, qualitatively, to be better are consistent with the objective function value (i.e., the best batches have the lowest objective function value). This is in line with industrial practice where an operator/quality controller could be asked to rank the product in terms of quality, which would then enable picking the parameters of β in a similar fashion. The above optimization problem is essentially a mixed integer linear program (MILP) but instead solved in a brute force fashion as three linear programs using linprog in MATLAB. To implement the control algorithm on the experimental setup, MATLAB is interfaced with LabView which inturn works as a data acquisition system.

The proposed modeling and control approach is next implemented on the experimental setups. Two sets of closed-loop implementations are carried out. Firstly, it is proposed to evaluate the ability of the controller to reject variability and meet product specifications (considering balanced importance given to all quality measurements). Secondly, the objetive is to evaluate the ability of the controller and achieve new product specifications. In the first implementation, the controller was implemented on five new batches. The feedback control algorithm achieves excellent quality results with the values obtained meeting the desired product specifications, and more importantly, the average value of the objective function obtained in the these MPC batches is 5.06. From these results, it can be noticed that the thermo-oxidative degradation was minimized with no significant change in viscosity (Q4) from the base material. However, values of Q1-Q3 (sinkhole area coverage, ultrasonic amplitude and impact energy) achieved an average quality. This formulation would be suitable for applications where effects from degradation should be minimized, such as formation of volatile components that can contaminate rotomolded water tanks.

In the second implementation, the efficacy of the proposed approach to obtain a different product quality (for instance, due to a client requirement), is evaluated. For some applications, a small degree of thermo-oxidative degradation can be acceptable with no drawbacks to mechanical stability. Thus, the objective function in the earlier formulation was modified such that the training batches with higher impact properties are the ones that result in the lowest values of the objective function. It should be noted that all the quality variables were still considered in this formulations as excessive heating and degradation should still be minimized. It can be seen that in this case, the product obtained at the end of the batches had lower sintering. It should be noted that the MPC resulted in a sharp increase in the internal mold temperature with reduced batch time (lf = tswitch + 300) compared to the previous case where MPC selected a safe heating profile with minimized degradation over a longer batch duration. This is to facilitate lower sintering in the product at the expense of some degradation. It demonstrates the capability of the proposed model in predicting the terminal quality effectively and thereby optimizing the process according to the desired quality requirements. Although not pursued in this work, the MPC formulation can readily be adapted to specify constraints on the value of individual quality variables.

To implement the proposed approach in an industrial setting, the model can be developed by utilizing the data from plant historian with a few identification experiments, if required. Once the proposed system is in place, the operator would not need any details on the identification or MPC algorithm and the desired product properties can be specified using a simplified interface. Further, for initial training the approach can be developed and provided to a operator in the form of a decision support tool which can aid in the decision making process with the flexibility to implement a safe the control action.

7.4 Conclusions

Results demonstrated in these applications help to validate the methodology proposed in previous chapters. In terms of the use of nonlinear ultrasonics for characterization of structural modifications, the study presented in Application 2 expands from the original paper (shown in Chapter 4) as it demonstrates how the method is capable to differentiate the effect from diffusion of biodiesel and toluene on polyethylene. Both fluids act as plasticizers but their extent and structural effect could be differentiated by the ultrasonic parameter from the harmonic amplitude ratio. Application 3 is a demonstration that proposed monitoring of the plastic deformation using nonlinear ultrasonic testing can be applied to a semi-crystalline polymer different from polyethylene. And, finally, Application 4 connects the data-driven framework approach demonstrated in Chapter 6 with the proposed process control strategy.

Chapter 8

Conclusions and future work

Under a limited scenario for quality control of polymer parts based on traditional destructive tests, we have presented a viable alternative for bulk structural characterization using a nondestructive methodology. With the use of a multivariate analysis of ultrasonic signal propagation in produced parts, relevant features of the internal micro-structure can be revealed. The validation of this sensor technology represents an important element to promote adoptions of advanced manufacturing strategies for the polymer manufacturing industry.

Barriers for application of ultrasonic testing to plastic characterization have been addressed with the adoption of new practices focused on the test format and signal processing. Advantages of guided waves over traditional pulse-echo tests have reduced the effects of signal attenuation in polymer parts and allowed characterization of a larger bulk area. Test efficiency was also improved with the selection of frequencies targeted for maximum signal amplitude specifically for polyethylene parts. In addition to the test format, a multivariate analysis of the propagated signal in the frequency domain helped to identify features of the signal that were not contained in the univariate analysis of amplitude and sound velocity. Based on variations of the harmonic peaks, considering the foundations of nonlinear ultrasonic propagation theory, changes in structural morphologies and damage progression were identified. The proposed ultrasonic characterization methodology was capable of identifying levels of plastic deformation and diffusion of solvents with a sensitivity that has not been report by other nondestructive tests.

Aside from a structural quality monitoring tool, the ultrasonic sensor technology applied for characterization of plastic parts has also been demonstrated as an important element for in-line process monitoring. Variations in process quality of a batch rotational molding process were connected with spectroscopic analysis of the propagated ultrasonic guided wave signals. Two different quality aspects, previously only characterized by

separate test methods, have been correlated to different ultrasonic frequency peaks using multivariate statistical analysis. As a result, we believe the application of an ultrasonic test on produced parts has sufficient information to provide quality classification of structural aspects in an in-line monitoring scenario. A novel approach was proposed as modeling tool that connects the process data from a dynamic modeling with the projection of the ultrasonic signal to a reduced space. This new approach can also be used for on-line visualization and can help improve process understanding. Thus, not only has the importance of the ultrasonic test have been demonstrated, but we have also examined through detailed studies which strategies to follow for incorporating this sensor technology into an advanced manufacturing framework for the polymer processing industry.

Contributions from this study only represent the starting point for application of this in-line monitoring technology for polymer processing. Other challenges have to be faced in test development, data processing and process understanding.

Some future research and development that will benefit the further development of this technology is the analysis of different ultrasonic sensors. In this study, contact piezoelectric transducers were applied with a coupling agent, however other alternatives have been investigated such as air-coupled and array sensors that can remove test barriers and improve performance.

Another important aspect to transfer this technology from laboratory to industrial conditions is consideration of the local-to-bulk properties in large parts. Investigation is required to determine how the spatial variability is reflected in the ultrasonic signal and how many tests from different areas are required to evaluate the part quality. A connection has to be estabilished between the information collected in the tested local area and the overall part quality and detection of process variability and defects. In addition, integration between different multivariate in-line sensors with the information

provided by the ultrasonic test can be developed. Combination of the structural quality from the ultrasonic with dimensional and/or chemical measurements by other sensors can provide a complete quality assessment of the produced part. Finally, the robustness of the proposed in-line monitoring tool can also be evaluated to quantify variability in feedstock or process variables, developing a more intelligent oversight system for the manufacturing process. Other polymer manufacturing processes can be explored by the technique now.

Appendix A

Supplementary material for Chapter 5

A.1 Rheology

The selection of oscillatory strain for frequency sweep tests was based on the viscoelastic limit observed from strain sweep curves of different polyethylene processed samples considering the linear limit for the storage modulus, as observed in Figure A.1. Rheology parameters from the frequency sweep tests were determined by fitting based on Cross model and comparison between tested samples was focused on the zero-shear viscosity representing the best fit to approximate initial plateau of curves, as seen in Figure A.2.

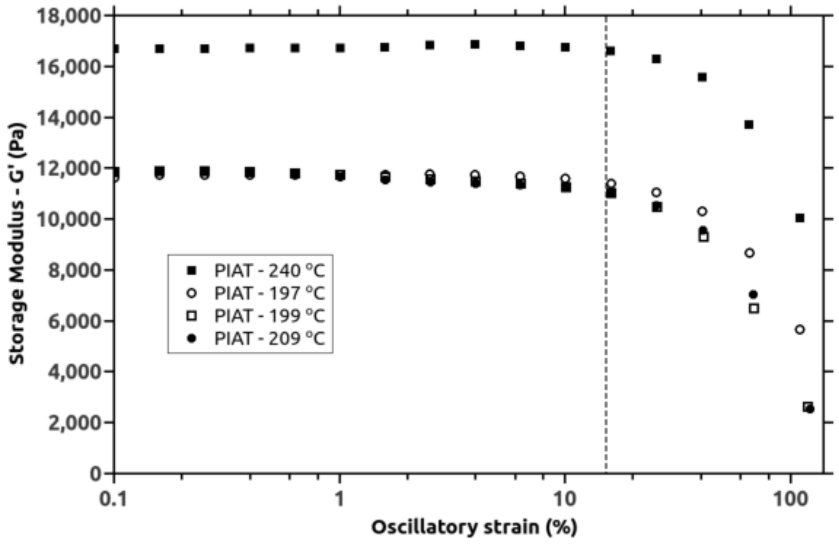

Figure A.1: Strain sweep curves for tested polyethylene samples after rotational molding processing at different peak internal air temperatures (PIAT) (vertical dashed line at 0.15 indicate the oscillatory strain selected for frequency sweep tests)

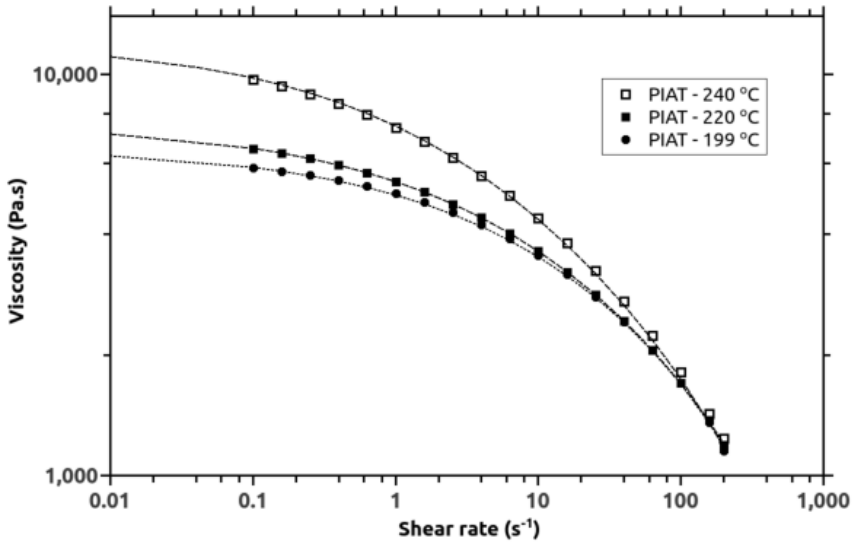

Figure A.2: Frequency sweep curves after Cox-Merz transformation for tested polyethylene samples after rotational molding processing at different peak internal air tempearatures (PIAT) (dashed lines indicate the projection of fitted Cross model values)

A.2 PLS Model

An important aspect of the design of a multivariate statistical analysis model using projection to latent spaces (PLS) is the selection of the number of components. Figure A.3 and A.4 show the progression of the variance explained and the root-mean square sum error of prediction (RMSEP) for both sintering and degradation models based on internal cross-validation with independent calculation between components.

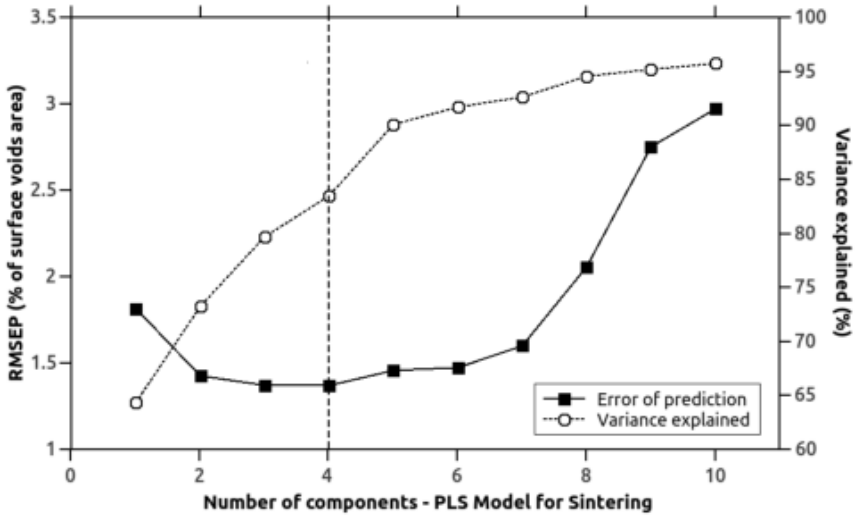

Figure A.3: Variance explained and error of prediction based on internal cross-validation for different components of PLS model correlating sintering quality and ultrasonic spectroscopic data (vertical dashed line indicated the selected optimal number of components)

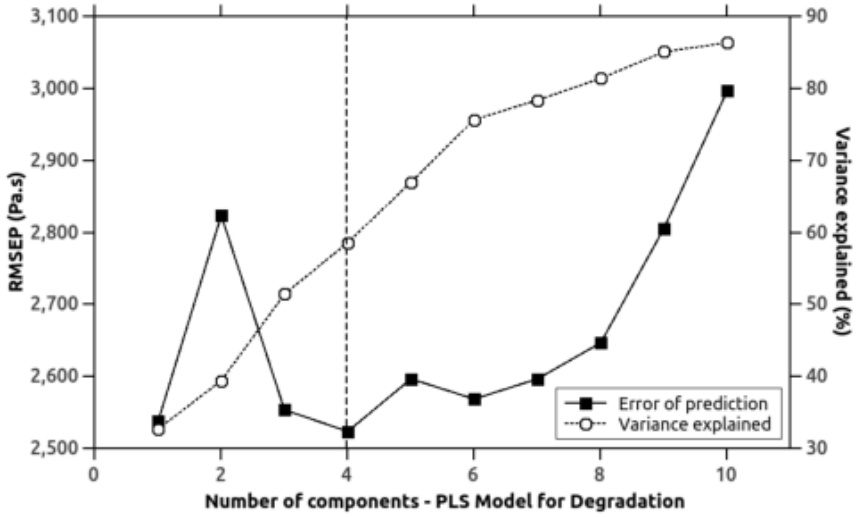

Figure A.4: Variance explained and error of prediction based on internal cross-validation for different components of PLS model correlating degradation quality and ultrasonic spectroscopic data (vertical dashed line indicated the selected optimal number of components)

Appendix B

Supplementary material for Chapter 6

B.1 SIMCA - PCA models

Figures A1, A2 and A3 and Table A1 demonstrate the details of PCA models constructed using samples with know product quality of three different classes (incomplete sintering, target quality and degraded) based on multivariate ultrasonic spectra data.

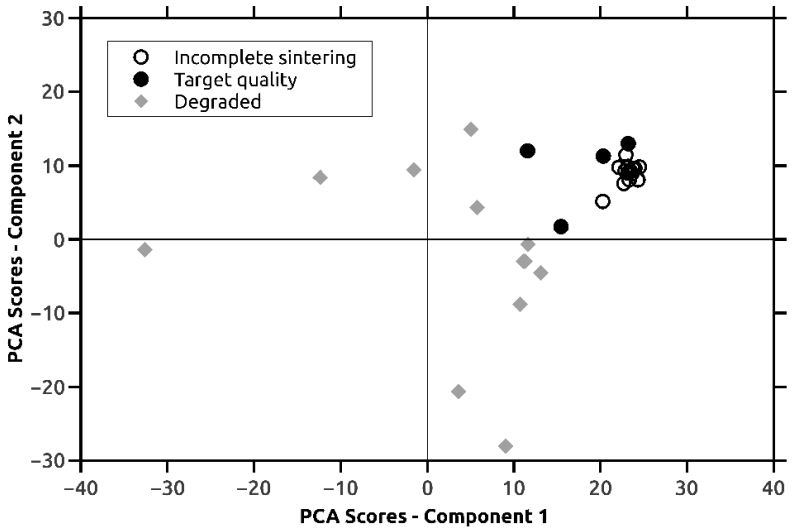

Figure B.1: Projection of PCA scores from experimental batch samples using ultrasonic spectra data of Group 1 (labelled as "Degraded")

Table B.1: Summary of PCA models for different quality groups

Model	Group 1	Group 2	Group 3
Label	Degraded	Incomplete sintering	Target quality
Number of components	5	12	5
Variance explained	90.6%	91.0%	91.2%
Number of samples on calibration data set	8	15	8
Number of variables on the original domain (ultrasonic frequencies)	1376		

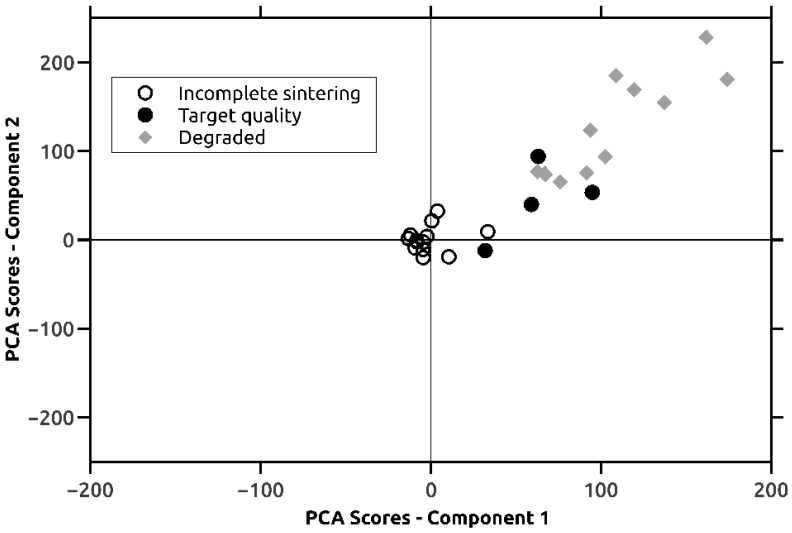

Figure B.2: Projection of PCA scores from experimental batch samples using ultrasonic spectra data of Group 2 (labelled as "Incomplete sintering")

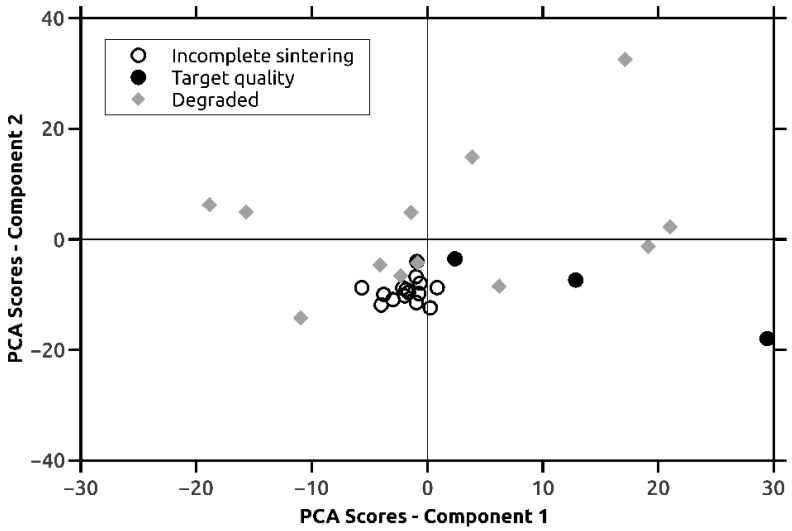

Figure B.3: Projection of PCA scores from experimental batch samples using ultrasonic spectra data of Group 3 (labelled as "Target quality")